

INFORMATION TO USERS

This manuscript has been reproduced from the microfilm master. UMI films the text directly from the original or copy submitted. Thus, some thesis and dissertation copies are in typewriter face, while others may be from any type of computer printer.

The quality of this reproduction is dependent upon the quality of the copy submitted. Broken or indistinct print, colored or poor quality illustrations and photographs, print bleedthrough, substandard margins, and improper alignment can adversely affect reproduction.

In the unlikely event that the author did not send UMI a complete manuscript and there are missing pages, these will be noted. Also, if unauthorized copyright material had to be removed, a note will indicate the deletion.

Oversize materials (e.g., maps, drawings, charts) are reproduced by sectioning the original, beginning at the upper left-hand corner and continuing from left to right in equal sections with small overlaps. Each original is also photographed in one exposure and is included in reduced form at the back of the book.

Photographs included in the original manuscript have been reproduced xerographically in this copy. Higher quality 6" x 9" black and white photographic prints are available for any photographs or illustrations appearing in this copy for an additional charge. Contact UMI directly to order.



Bell & Howell Information and Learning
300 North Zeeb Road, Ann Arbor, MI 48106-1346 USA
800-521-0600

University of Alberta

A GENETIC STUDY OF A P-ELEMENT LINE EXPRESSED IN
REGENERATING IMAGINAL DISCS OF
Drosophila melanogaster

by

Ariel Finkielsztein



A thesis submitted to the Faculty of Graduate Studies and Research in partial
fulfillment of the requirements for the degree of Master of Science

in

Molecular Biology and Genetics

Department of Biological Sciences

Edmonton, Alberta

Spring 1999



National Library
of Canada

Acquisitions and
Bibliographic Services

395 Wellington Street
Ottawa ON K1A 0N4
Canada

Bibliothèque nationale
du Canada

Acquisitions et
services bibliographiques

395, rue Wellington
Ottawa ON K1A 0N4
Canada

Your file Votre référence

Our file Notre référence

The author has granted a non-exclusive licence allowing the National Library of Canada to reproduce, loan, distribute or sell copies of this thesis in microform, paper or electronic formats.

The author retains ownership of the copyright in this thesis. Neither the thesis nor substantial extracts from it may be printed or otherwise reproduced without the author's permission.

L'auteur a accordé une licence non exclusive permettant à la Bibliothèque nationale du Canada de reproduire, prêter, distribuer ou vendre des copies de cette thèse sous la forme de microfiche/film, de reproduction sur papier ou sur format électronique.

L'auteur conserve la propriété du droit d'auteur qui protège cette thèse. Ni la thèse ni des extraits substantiels de celle-ci ne doivent être imprimés ou autrement reproduits sans son autorisation.

0-612-40046-8

University of Alberta

Library Release Form

Name of Author: Ariel Finkielsztejn

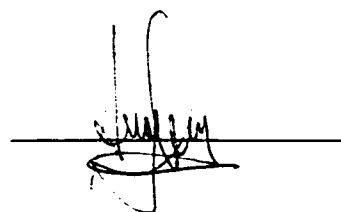
Title of Thesis: A GENETIC STUDY OF A P-ELEMENT LINE EXPRESSED IN
REGENERATING IMAGINAL DISCS OF *Drosophila*
melanogaster

Degree: Master of Science

Year this Degree Granted: 1999

Permission is hereby granted to the University of Alberta Library to reproduce single copies of this thesis and to lend or sell such copies for private, scholarly, or scientific research purposes only.

The author reserves all other publication and other rights in association with the copyright in the thesis, and except as hereinbefore provided, neither the thesis nor any substantial portion thereof may be printed or otherwise reproduced in any material form whatever without the author's prior written permission.

A handwritten signature in black ink, appearing to read 'Ariel Finkielsztejn', is written over a horizontal line.

1403 10883 Saskatchewan Dr.
Edmonton, Alberta,
Canada T6G 4S6

March 19, 1999

University of Alberta

Faculty of Graduate Studies and Research

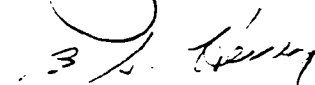
The undersigned certify that they have read, and recommend to the Faculty of Graduate Studies and Research for acceptance, a thesis entitled A GENETIC STUDY OF A P-ELEMENT LINE EXPRESSED IN REGENERATING IMAGINAL DISCS OF *Drosophila melanogaster* submitted by Ariel Finkielsztejn in partial fulfillment of the requirements for the degree of Master of Science in Molecular Biology and Genetics.



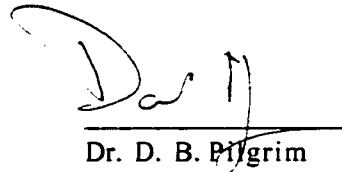
Dr. M. A. Russell



Dr. T. Gordon



Dr. B. S. Heming



Dr. D. B. Pilgrim

March 17, 1999

Abstract

Adult structures in the fruitfly *Drosophila melanogaster* are derived from the imaginal discs in larvae. Patterning of imaginal discs has been shown to involve several key growth factors like *wingless* and *decapentaplegic*. I report here a new locus involved in imaginal disc patterning isolated from a P-element enhancer-trap line, G45. G45 lacZ is ectopically expressed on one side of the wound heal in disc fragments. Clonal analysis experiments were done using $\Delta 53$, a small deficiency generated by imprecise excision of G45. Clones of $\Delta 53$ produced ectopic margin and outgrowths in the wing pouch, defective ocellus, duplicated bristles in the thorax and disorganized ommatidia. These effects showed remarkable similarity to those produced by clones that misexpress *wingless* product. A genomic probe flanking the G45 insert was used to isolate the putative gene reported by G45. Two putative transcripts were identified. Their combined expression in the embryo mimics the G45 lacZ pattern. However, genomic Southernns showed that neither of these two transcripts map to the insertion site at 100E.

Acknowledgement

I would like to in the first place my supervisor, Dr. Mike Russell for his encouragement, patience, and for giving me the freedom to choose my own research project and helping me with the interpretation of genetic experiments. I also would like to thank my committee members, Dr B. B. Heming, Tessa Gordon and Dr. Dave Pilgrim for their enthusiasm, advice and constructive criticism of my experiments.

I wish to thank Sam Scanga for his valuable help with techniques and ideas which help me take the right direction in my research. He also provided the lab with several *Drosophila* lines which were key to the success of the clonal analysis experiments.

Dr. Morris Maduro helped me solve many computer problems and encouraged me to continue my work in critical moments.

Many other students contributed to this study, among them I would like to thank John Higgins for technical assistance with the deficiency line used in this study and Dave Dansereau, who assisted in the characterization of the cosmids.

I would like to thank Lisa Ostafichuk and Don Price, who also contributed to make Mike's lab a very friendly and "stress-free" environment.

Finally, I would like express my gratitude to rest of those who, directly or indirectly, helped me in my research with material or useful advice. A probably incomplete list is provided below.

Ali Riazi, Bill Clark, Gary Ritzel, Dr. Bill Brook, Dave Hansen, Dr. John Locke, and Song Hu.

Table of contents

I	Introduction	1
I.1	Imaginal discs as a model for pattern formation in cellular systems	4
I.2	Regeneration and duplication of disc fragments in culture	6
I.3	Regeneration as a system to discover new patterning genes	15
I.4	G45 expression in the context of disc regeneration	17
II	Materials and Methods	19
II.1	<i>Drosophila</i> strains and culture conditions	19
II.2	Bacteria and Phage culture	19
II.3	Clonal analysis experiments	22
II.4	β -galactosidase staining	30
II.5	DNA work	30
II.6	Blot techniques	31
II.7	In situ hybridization to polytene salivary gland chromosome from larvae	31
II.8	Embryo and imaginal disc in situ hybridization	32
III	Results	34
III.A	A search of cDNAs using the G45 genomic flanking region obtained by plasmid rescue	34
III.B	Analysis of the cDNAs detected by the screen	34
III B.1	Cross hybridization experiment	34
III. B.2	Comparison between Embryonic and G45-lacZ expression	39
III. B.3	Comparison between imaginal disc cDNA hybridization pattern and G45-lacZ expression	39
III. B.4	A caveat	46
III.C.	Clonal analysis with a G-45 deletion line generated by imprecise excision of the P-element.	53
III.C.1	Results of the first clonal analysis experiment	53
III.C.1.1	Wing abnormalities	63

III.C.2 Second clonal analysis experiment.	78
III.C.3 Third clonal analysis experiment	90
III.C.4 Summary and conclusions from the clonal analysis experiments	90
III.D. Interaction between $\Delta 53$ and a <i>wingless</i> pathway gene, <i>kiwi</i> .	94
III.E. Genetically mapping G45 Δ 53	96
IV Discussion.	97
IV.A Genetic organization of the G45 region	96
IV B. Function of genes in G45 region	99
IV.B.1 Phenotypes seen in the clonal analysis experiments	104
IV B.2 Non-autonomy versus cell-autonomy	105
IV B.3 Growth effects	106
V Conclusion	108
VI Bibliography	109

List of Figures

Figure I.1 The polar coordinate model for positional information represented by a clock face	8
Figure I.2 Schematic representation of Meinhardt's model for the leg imaginal disc positional information system	13
Figure I.3 Pz enhancer trap construct used in the screen	16
Figure II.1 FRT/FLP system	24
Figure II.2 Construction of line 1	25
Figure II.3 Construction of line 2	26
Figure II.4 Construction of line 3	27
Figure II.5 Construction of line 4	28
Figure II.6 Construction of line 5	29
Figure III.1 Cross hybridization experiment I	37
Figure III.2 Cross hybridization experiment II	38
Figure III.3. G45 embryo lacZ expression	40
Figure III.4 Wild type late stage embryos stained by <i>in situ</i> hybridization with non-radioactively labeled cDNA G45-7 or G45-11	41
Figure III.5 cDNA G45-7 and G45-11 hybridization pattern in wild type and heat-treated su(f) ¹² imaginal discs	44
Figure III.6 Genomic lambda clones from a EMBL4 library isolated in a screen using the rescued genomic flanking region as a probe	45
Figure III.7 Schematic representation of sequence relationship between the STS from the Cosmid 65F1, the FLR and the cDNA G45-7	48
Figure III.8 The 2.3 kbp genomic flanking region (FLR) is chimeric	49

Figure III.9 cDNAs G45-5, 6, and 7 have homology to a Cosmid that maps to the chromosome X.	50
Figure III.10 cDNA G45-7 does not map to 100E.	51
Figure III.11 cDNA G45-11 does not map to 100E.	52
Figure III.12A Crossing scheme used to generate control clones for the first and second clonal analysis experiments	55
Figure III.12B Crossing scheme used to generate control clones for the first clonal analysis experiments	56
Figure III.13 Crossing scheme used to generate clones in the first clonal analysis experiment	57
Figure III.14 Eye abnormality in the first clonal analysis experiment	58
Figure III.15 Thorax abnormalities in the first clonal analysis experiment	61
Figure III.16 Ocellus abnormality	62
Figure III.17 Defective palp of an orange-eyed fly of the first clonal analysis experiment	64
Figure III.18 Dorsal view of thoraces of orange-eyed flies of the first clonal analysis experiment	65
Figure III.19 Frequency and position of ectopic patches of marginal bristles found in the first clonal analysis experiment	68
Figure III.20 Ectopic triple row bristles in the wing blade in the first clonal analysis experiment	69
Figure III.21 Ectopic medial and dorsal triple row wing abnormalities in the first clonal analysis experiment	70
Figure III.22 Ectopic double row bristles and outgrowths in the wing blade in the first clonal analysis experiment	71
Figure III.23 Clones in the normal margin do not affect bristle	

phenotype	77
Figure III.24 Crossing scheme used to generate clones in the second clonal analysis experiment	81
Figure III.25 Triple row abnormalities in the second clonal analysis experiment	82
Figure III.26 Double row abnormalities in wings of the second clonal analysis experiment	83
Figure III.27 Ventral outgrowth in a wing of a fly from the second clonal analysis experiment	84
Figure III.28 Crossing scheme used to generate clones in the third clonal analysis experiment	91
Figure III.29 Crossing scheme used to generate control clones for the third clonal analysis experiment	92
Figure III.30 Dorsal clone in a wing of a fly from the third clonal analysis experiment	93
Figure III.31 G45 Δ 53 interacts with an allele of <i>kiwi</i> , A64, showing a thorax and wing margin phenotype.	95
Figure IV.1 Components of the Dorsal/Ventral pathway	101

List of Tables

Table II.1 <i>Drosophila</i> strains used in this thesis.	20
Table II.2 Lines constructed for the clonal analysis experiments	21
Table III.1 cDNAs detected by the flanking region	36
Table III.2 Comparison between T ₃ , T ₇ , riboprobes, G45-7 and G45-11 cDNAs signals in heat-treated su(f) imaginal discs	43
Table III.3 Frequency of disorganized ommatidia in different genotypes	59
Table III.4 Distribution of marked and duplicated thoracic bristles of flies from the first clonal analysis experiment	66
Table III.5 Number of ectopic patches in 103 wings of the first clonal analysis experiment	73
Table III.6 Phenotypes of the medial triple row bristles in the ectopic dorsal anterior patches in wings of the first clonal analysis experiment	74
Table III.7 Percentage of bristles in normal margin in the first clonal analysis experiment	75
Table III.8 Statistical analysis of the first clonal analysis experiment (t-test)	76
Table III.9 Distribution of marked and duplicated bristles in thoraces of flies of the second clonal analysis experiment	79
Table III.10 Number of ectopic patches in 31 wings of the second clonal analysis experiment	86
Table III.11 Distribution of marked and unmarked medial triple row bristles in ectopic dorsal anterior patches and in the anterior margin of wings of the second clonal analysis	

experiment	87
Table III.12 t-Test of the second clonal analysis experiment	88
Table III.13 Comparison of the percentages of yellow medial triple row bristles in ectopic patches and normal margin in wings from the second clonal analysis experiment	89

Abbreviations

AP	Alkaline phosphatase
<i>ap</i>	<i>apterous</i>
<i>arm</i>	<i>armadillo</i>
<i>As-C</i>	<i>Achaete-scute complex</i>
b p	base pair
cDNA	complementary DNA
CNS	Central Nervous System
<i>DI</i>	<i>Delta</i>
DNA	Deoxyribonucleic acid
<i>dpp</i>	<i>decapentaplegic</i>
d r	double row
EDGP	European Drosophila Genome Project
EDTA	Ethylene-diamine-tetra-acetic acid
<i>e n</i>	<i>engrailed</i>
<i>fng</i>	<i>fringe</i>
FRT	Flip recombinase target
<i>h h</i>	<i>hedgehog</i>
k b	kilobase
kbp	kilobasepair
mtr	medial triple row
mtrb	medial triple row bristles
<i>N</i>	<i>Notch</i>
NBT	Nitroblue Tetrazolium chloride
PBS	Phosphate-buffered saline
PBT	0.1% Tween 20 in PBS
p fu	plaque forming units
PNS	Peripheral Nervous System
p r	posterior row
RNA	Ribonucleic acid
RT	Room temperature
<i>Ser</i>	<i>Serrate</i>
<i>sgg</i>	<i>shaggy</i>
STS	Sequence Tagged Site
TAE	Tris-Acetate EDTA

tr	triple row
wg	<i>wingless</i>
X-gal	5-Bromo, 4-chloro, 3-indolyl galactose
X-phosphate	5-Bromo, 4-chloro, 3-indolyl phosphate
ydtrb	yellow dorsal triple row bristles
ymtrb	yellow medial triple row bristles
yvtrb	yellow ventral triple row bristles
Zw3	<i>Zeste-white3</i>

I. INTRODUCTION

In development, a single cell, the zygote, transforms itself into an adult. This process involves growth, cell division and cell differentiation based on differential gene expression. These processes are coordinated to generate a repeatable pattern of cells with different developmental fates. The fate of a cell was shown by classical embryologists to depend on its position in the embryo. Early experiments performed with the amphibian embryo *Triturus* showed that transplantation of the dorsal blastopore lip could trigger ectopic gastrulation, thus producing a secondary body axis (Spemann and Mangold, 1924). These experiments showed that the dorsal blastopore lip had organizing activity that exerted a long-range influence on adjacent cells to specify a new axis, since the secondary axis was composed of cells coming from both the donor and recipient tissues. This long-range influence was explained by proposing that cells somehow sense and interpret their environment, perhaps responding to different concentrations of fate determinants produced by the organizer region. In formal terms, the cells acquire a positional value in response to a positional information system, established by a morphogen. This positional value was proposed as being instrumental in determining the fate of a cell (Wolpert, 1969). Whereas the specification of positional values is a global property of an entire morphogenetic unit referred to as a field, interpretation must be a local function of each cell of the field.

A model organism such as *Drosophila* is useful for the genetic study of developmental processes because of the large number of genetic mutants that are available (reviewed in Martinez-Arias and Bate, 1993). A combination of genetics and molecular biology approaches has made it possible to identify which genes are involved in early patterning in the embryo, and to deduce some of their roles in the process (Lewis, 1978; Nüsslein-Volhard and Wieschaus 1980; Anderson et al., 1985; Tautz, 1988). The idea of positional information established by a morphogen gradient was first validated by study of the *bicoid* (*bcd*) gene. Homozygous mutants of *bcd* exhibit a maternal-effect-lethal phenotype resulting from an effect on the anterior-posterior pattern. Strong alleles of this gene cause loss of anterior structures, which are replaced by posterior structures in reverse polarity. Weak alleles cause phenotypic effects only in the most anterior segments of the larvae (e.g. labral derivatives). In addition, transplantation of cytoplasm taken only from the anterior part of wild type embryos to the anterior tip of *bcd* embryos rescued the *bcd* phenotype. Molecular data showed that *bcd* maternal mRNA was localized to the anterior pole of the unfertilized egg. Later, during the syncytial early cleavage stages this localized mRNA is translated into the *bcd* product (BCD). This protein diffuses posteriorly forming a morphogenetic gradient that organizes the segmentation of the head and thoracic primordia (Driever and Nüsslein-Volhard, 1988). BCD is a homeodomain protein that acts as a DNA binding transcription factor driving the expression of downstream genes (Driever et al., 1989; Struhl et al., 1989). These genes are involved in the establishment of the pattern of segments and the different embryonic domains (reviewed in Ingham, 1988), constituting the zygotically expressed genetic program that interprets the maternally specified BCD positional information.

The first genes involved in interpreting BCD gradient concentration are the gap genes. When mutated, they cause deletions of different sets of contiguous segments, thus creating gaps in the anterior-posterior axis. Examples of gap genes are *hunchback* (*hb*) *Krüppel* (*Kr*) and *knirps* (*kni*) (Nüsslein-Volhard and Wieschaus, 1980). All three encode DNA-binding finger domain proteins. *hb* (Tautz et al., 1987) is activated in response to high levels of BCD, while *Kr* is only active at low levels of BCD. Also, *hb* and *Kr* repress each other, and *kni* acts as a negative regulator of *Kr* (Jäckle et al., 1986). These interactions establish the gap-gene expression domains that serve the purpose of regulating the expression of a second class of genes, the pair-rule class and of delimiting the expression domains of the homeotic genes.

The pair-rule class consists of genes that mutate to yield phenotypes characterized by a pattern of missing alternating segments. Thus, mutant embryos usually have half the normal number of segments. Under the control of different concentrations of gap gene products expressed along the length of the embryo, these genes are expressed in the trunk region in striped patterns of seven or eight bands. Because the stripes are offset, the overlapping pattern of expression of different pair rule genes can specify the cells that will express genes of the segment polarity class which finally subdivide the pair-rule repeats into 14 segmental repeats. Three pair-rule genes, *even skipped* (*eve*) (Harding et al., 1986), *fushi tarazu* (*ftz*) (Kuroiwa et al., 1984), and *paired* (*prd*) (Kilchherr et al., 1986) play a key role in that process. They all encode proteins that have DNA-binding domains. *ftz*, *prd*, and *eve* products, which are FTZ, PRD, and EVE respectively, act as transcriptional regulators of genes of the segment-polarity and homeotic classes. *ftz* and *eve*, in particular, are transcribed in a complementary pattern of bands that coincide with and define the parasegments, the earliest metameric subdivisions of the embryo. Parasegment boundaries also coincide with the expression domains of the homeotic genes that specify the identity of segments. The *prd* transcript is detected in seven bands at early stages (syncytial blastoderm) but evolves towards a pattern of 14 bands at the cellular blastoderm, which resembles a segment polarity pattern (Baumgartner and Noll, 1991).

The segment polarity class is composed of genes that when mutated yield phenotypes that have the normal number of segments. However, each segment has a fraction of the normal pattern deleted, and the remaining portion is duplicated in a mirror-image pattern. The expression patterns of these genes at the end of the cellularization stage (cellular blastoderm) has the form of 14 narrow stripes. Two members of this class, *engrailed* (*en*), a homeobox-containing transcription factor gene (Desplan et al., 1985), and *wingless* (*wg*), a gene encoding a secreted factor (WG) involved in signaling between cells (Baker, 1987; Rijsewijk et al., 1987) are key components in specifying the boundaries of the parasegments. The anterior limit of each parasegment is defined by *en* expression, which is initially only one cell wide (Carroll et al., 1988). The posterior limit of the parasegment is marked by the expression of *wg*. Later in embryonic development, after pair-rule gene expression has ceased, these two components are locked in a positive

feedback loop in which they sustain each other (Vincent and Lawrence, 1994). This may represent the first step in the process of storing the "analogue" positional information (initially contained in the gradients of the gap and early pair-rule gene products) in a heritable "digitized" form. Thus, positional information can then be passed on to the cells that originate the imaginal disc compartments (see below).

Another class of genes that plays an important role in the interpretation of the positional information is the homeotic class. Mutants of these genes cause the transformation of a segment into another one (Lewis, 1978). Their expression patterns are initiated at the blastoderm stage, before cellularization takes place, as a result of combinatorial activation by various gap and pair-rule genes (reviewed in Ingham, 1988). After cellularization when these genes are no longer transcribed, the expression patterns of the homeotic genes are nevertheless maintained and clonally transmitted. This requires the products of the *Polycomb* and *trithorax* group, some of which encode chromatin proteins. Clonal transmission of *en* expression in the imaginal discs also requires these genes.

The positional information provided by BCD in the syncytial egg cell is generated in the form of a diffusion gradient. In this form it is transient and could not be maintained as cells form, divide and the system grows. The role of the segmentation and homeotic genes is therefore to translate the analogue signal into a digital form, as heritable determined states of cells encoded by selector genes. Thus the gap, pair-rule, segment polarity segmentation gene hierarchy subdivides the BCD gradient into successively smaller gene expression domains that repeat along the length of the embryo (parasegments). In addition, the gap genes turn on different homeotic selector genes that are used later to distinguish among the repeats (to specify the identity of different segments).

Adult cuticular structures and appendages do not differentiate until metamorphosis, during the pupal period. These structures nevertheless originate in the embryo in each segment, as groups of cells or polyclones, already determined for different imaginal fates (Chan and Gehring, 1971; Crick and Lawrence, 1975; Simcox and Sang, 1983). Unlike the rest of larval tissues these cells proliferate mitotically during larval life to form ectodermal invaginations named imaginal discs. These are the larval precursors of the adult legs, wings, eyes, antennae, head capsule, halteres and genital organs (reviewed by Cohen, 1993).

Morphological studies using anti-fasciclin III antibody defined the position, size, segmental specificity, and behavior in different mutant backgrounds of the primordia of thoracic imaginal discs (Bate and Martinez-Arias, 1991). Imaginal disc primordia could first be identified as a local reduction in the antibody staining when they segregate from the larval epidermis in the 10-11 h embryo. When larval epidermis is examined in the 12-14 h embryo, imaginal disc primordia can be seen as small clusters of cells close to the segmental border. Thoracic discs are seen in wild type

embryos in segments T1, T2 and T3. However, mutants that transform abdominal segments into thoracic ones show the characteristic group of cells that give rise to the imaginal discs primordia in abdominal segments. These experiments show that the origin of imaginal discs is associated with the larval epidermis.

Clonal analysis experiments provided support for the idea that the origin and patterning of imaginal discs is linked to the embryonic patterning. Clones induced in blastoderm stage embryos showed the imaginal disc primordia were already divided into two groups of cells in the embryonic stage, one committed to form anterior adult structures and the other to form posterior ones (Wieschaus and Gehring, 1976; Lawrence and Morata, 1977).

Experiments using molecular markers to follow the development of imaginal disc primordia confirmed the association to the larval epidermis. Cohen (1990) showed that *Distal-less* (*Dll*) is expressed in the position where the disc primordia originate. This expression overlaps the expression domains of *en* and *wg* and thus spans the parasegmental boundary. The expression data for *Dll* and the fact that mutants for *en* or *wg* neither develop thoracic imaginal disc primordia (Simcox et al., 1989) nor show *Dll* expression demonstrates that *Dll* expressing cells mark imaginal disc primordia. In addition, *Dll* is most strongly expressed at the intersection point between the *en/wg* boundary and the row of cells expressing *decapentaplegic* (*dpp*), which encodes an embryonic dorsal-ventral (D/V) morphogen (DPP) (Cohen et al., 1993). Both *wg* and *dpp* are subsequently important in specifying disc positional values in the mature imaginal discs (see below).

These experiments therefore showed that the origin and patterning of imaginal discs is closely linked to the (para) segmental and dorso-ventral positional information generated in the embryo (Cohen, 1993; Couso and González-Gaitán, 1993). Thus, the position of an imaginal disc in the embryo may be established by the cooperation of two morphogens (i.e. WG and DPP); and the early subdivision into two groups of cells giving rise to anterior and posterior adult structures would be established by the embryonic expression pattern of *en* product (EN). The latter represents the first step in imaginal disc patterning.

I.1 Imaginal discs as a model for pattern formation in cellular systems

The interpretation of BCD positional information in the embryo takes place in a syncytial blastoderm. However, this is not the case in higher organisms such as vertebrates, where the developmental process is cellular from its inception. Unlike in the early *Drosophila* embryo, pattern specification in imaginal discs also takes place in a cellular system. Therefore, imaginal discs constitute a better model than the embryo to identify genes involved in pattern formation in cellular systems.

Early attempts to understand how pattern specification occurs in imaginal discs came from fate mapping experiments. Disc fragments cultured in larval hosts were only able to make a fraction of the adult structures that they normally differentiate during metamorphosis. This was used to construct fate maps, for example, of the male leg disc (Schubiger, 1968). These experiments showed that the leg disc is organized like a telescoped leg, with the distal parts of the adult leg cuticle derived from the center of the imaginal disc and the proximal segments from the periphery.

A different approach to the study of patterning in imaginal discs was carried out by García-Bellido et al. (1973). Clonal analysis was used to test for heritable commitments of cell lineages. Clones of cells were made homozygous for cell autonomous marker mutants that have no effect on pattern formation. These mitotic clones could be created at a specific time in development since they are induced in response to X-rays. This technique was enhanced by using Minute (M) mutant flies. Minute/+ heterozygous flies have a normal but delayed development. When a clone is produced carrying two copies of the M⁺ allele its cells divide faster than their neighbors and overgrow neighboring clones. Under these conditions a restriction in clonal competence indicates when a cell lineage becomes committed to a certain developmental fate.

The results of these experiments showed that clones of marked cells induced at specific times in development demarcated lines that separated different parts of the adult wing. These lines which appeared at different time points in development, were called compartment boundaries. Thus, clones produced early in development defined a compartment boundary that separated anterior from posterior parts of the wing. Clones induced in later developmental stages (from about the end of the first larval instar) were also restricted to the upper or lower parts of the wing. (García-Bellido et al., 1973; Crick and Lawrence, 1975) thus defining a new compartment boundary that separated dorsal from ventral compartments.

These experiments suggested that successive compartmentalization events progressively subdivided cell lineages, thus restricting their developmental potential to more and more specific cell fates. The subdivisions into new compartments were observed to be binary in nature (i.e. representable by a code of zeros and ones). Thus two successive divisions determined the four compartments (A/D, A/V, P/D, and P/V) of the wings. Because the disc cells grow by mitosis throughout all larval stages, cell determination states were observed to be heritably maintained. This model, referred to as the compartment model for imaginal disc development, was originally put forward as an alternative to gradients as the mechanism to explain patterning in imaginal discs.

Further evidence on the basis of compartmentalization came from analysis of *en* mutants. In *en/en* flies, structures that are normally found in the anterior compartment of the wing blade are also found in the

posterior part. In addition, *en/en* flies do not show phenotypic effects in the anterior compartment (Morata and Lawrence, 1975).

Minute⁺ clones did not define the A/P boundary if induced in *en* mutant background (Morata and Lawrence, 1975). When *en/en* clones were induced in the anterior compartment of the wing imaginal disc on an *en/+* background and reached the A/P boundary, they did not cross the boundary. However, if induced in the posterior compartment, mutant clones were able to cross the A/P boundary (García-Bellido, 1975; Morata and Lawrence, 1975). Clones of *en/en* cells induced in the posterior compartment caused transformations into structures normally seen in the anterior part. Clones of *en⁻* did not produce any phenotypic abnormalities when induced in the anterior compartment (Morata and Lawrence, 1975; Lawrence and Morata, 1976). This suggests *en* is turned on in all posterior compartments cells where it is required for posterior fate, but is turned off in all anterior cells where it is not required.

This data on the *en* mutant led García-Bellido (1975) to propose that *en* is an example of a selector-gene. According to this model, a different selector gene acting as a binary switch would control each compartmental subdivision. Expression of these genes would be maintained clonally in the compartments that they specify so that the combination of selector genes active would be a record of a cell's lineage history. The specification of compartment-specific cell fates could then be accomplished by each combination of selector genes activating a different set of specific downstream genes. The formation of compartment boundaries could be explained if selector-gene-expressing cells would not mix with cells not expressing the same selector gene. This model provided a possible explanation for the heritable commitment of cells from each compartment to differentiate compartment-specific structures. However, it did not explain how selector genes are switched on in a position-specific manner when compartments are formed; or how patterning within compartments is accomplished.

I.2 Regeneration and duplication of disc fragments in culture

Although cell determination states were cell heritable during normal imaginal disc development, imaginal disc fragments cultured in adult hosts for a prolonged period were able to form structures that transcended those expected from the fate map (Schubiger, 1971). For example, the upper medial quarter of the leg imaginal disc regenerated the entire leg pattern when cultured in an adult host for about seven days before transfer to a larval host for differentiation. The complementary 3/4 lateral disc fragment, duplicated itself. An important conclusion from these experiments was that regeneration of the entire pattern was possible even if a small fragment derived entirely from anterior compartment was used. Although duplication had been known from previous experiments, regeneration of the entire pattern from a fragment had not been shown. This became important because it implied that the normal heritable cell-fate-commitments represented by compartments could be respecified under

these experimental conditions. Therefore, paradoxically, cell determination states are normally fixed, but can nevertheless be changed.

Abbott et al., (1981), and Girton and Russell (1981) used marked clones of cells to study compartmental restriction in imaginal disc fragments undergoing regeneration or duplication. Fragments cultured *in vivo* initially heal by folding of the cut edge so that cells from different positions are confronted (Haynie and Bryant, 1976). This is followed by cell division to form the regenerate or duplicate. They were able to show that a small number of cells produced the new pattern, which came from a specific region located at the wound heal. These cells formed a regeneration blastema. In addition, clones of cells labeled before transplantation could cross the A/P compartment boundary, while clones induced later did not. Therefore, a clonal restriction was first lost and then reestablished during regeneration. This implies that under the conditions of these experiments, a respecification of cell fates takes place to generate cells of the posterior compartment, when committed cells from that compartment are not initially present. The possibility of respecification was not considered as part of the selector gene model, which also did not explain how a compartmental state originates in normal development. Therefore, these experiments provided an opportunity to approach this problem.

The idea of positional information was successfully used to predict where a new compartment boundary is specified in regeneration. The model was based on experimental results from different experimental systems. Results from grafting and other surgical operations in cockroach legs led French (1976) to propose the polar coordinate positional information model in which cells are assumed to have their positions specified by radial and circumferential values (Figure 1.1). In cockroach legs, removal of a longitudinal strip of epidermis and cuticle around the circumference of the femur creates a situation where cells from edges of the cut become juxtaposed. This causes the division of cells at the wound-heal producing a blastema that will differentiate the missing intermediate structures (intercalary regeneration). Thus, interpolation of circumferential positional values between the initial values of the cells at the two cut edges may instruct regeneration of the missing tissue.

Cell-cell interactions prior to regeneration were an obvious feature of these experiments involving cockroach legs. In imaginal discs, however, that was not the case because imaginal disc fragments were incubated inside the hosts, which prevented direct observation of the cells at the edges of the cut. Direct proof that the wound-heal brought together cells from different parts of the disc was shown by Reinhardt et al., (1977). Scanning electron microscopy of healing wing discs showed that regeneration or duplication started by bringing all the cells from opposite sides of the wound together. After two or three days of culture, a normal epithelium is re-established, and cell divisions are initiated at the wound-heal. Haynie and Bryant, (1976) showed that the fate of a duplicating fragment could be changed by interaction with another fragment from the

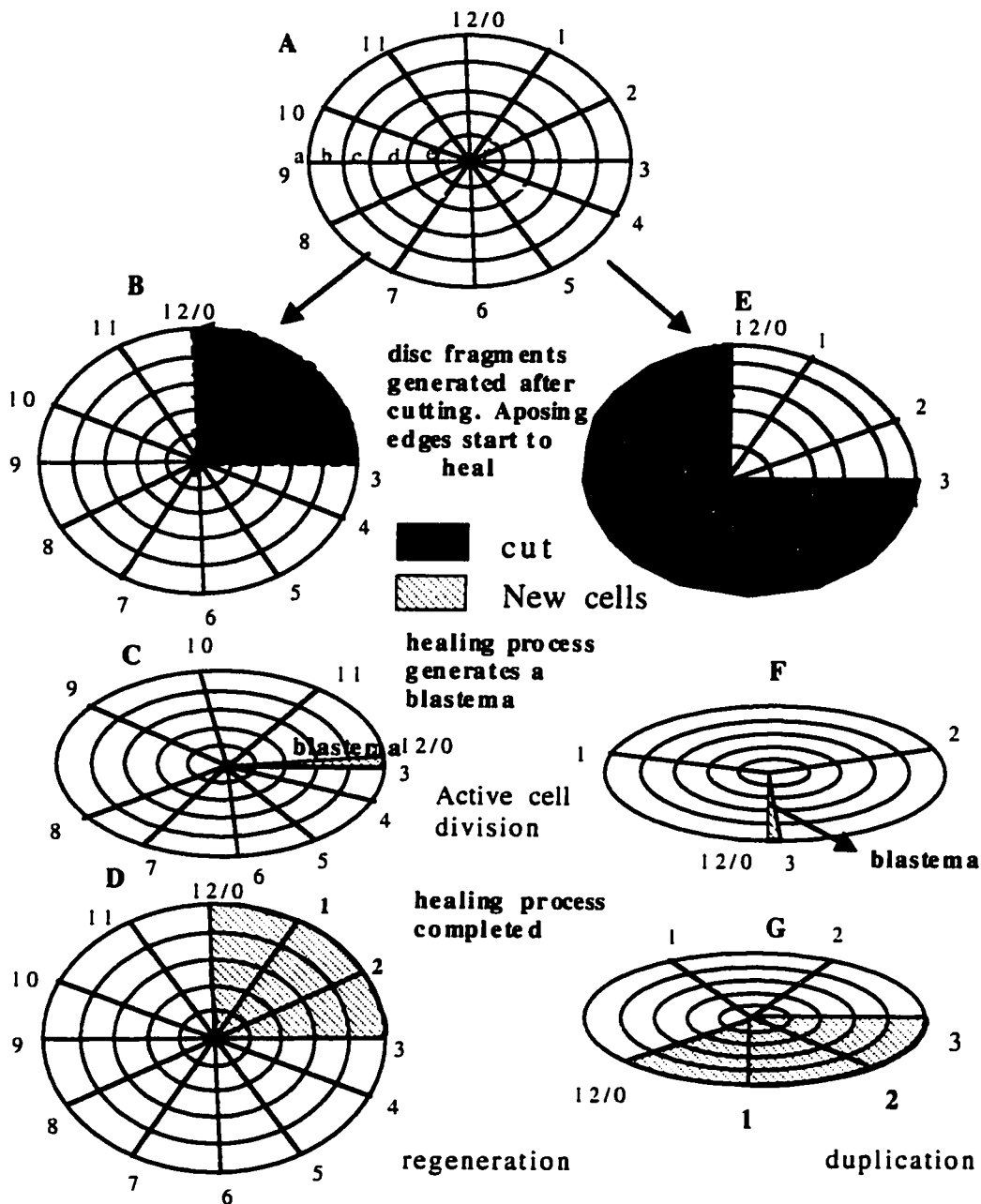


Figure 1.1. The polar coordinate model for positional information represented by a clock face (French et al., 1976). Schematic representation of the predictions of the shortest route intercalation rule when complementary disc fragments are cultured *in vivo*. A. Field map of the polar coordinate model in which radial coordinate values are indicated by the letters A through F and circumferential coordinate values by the numbers 1 through 12. Note that angular values are periodically continuous, so 12 and 0 represent the same value. B. Disc in which the upper medial quarter has been removed. C. Values 0 and 3 are confronted by healing followed by intercalation of the missing values 1 and 2, resulting in regeneration of the complete pattern (D). E. Quarter fragment, which is complementary to the fragment in B. F. Values 3 and 0 are confronted, G, the shortest route generates mirror-image duplication of the pattern seen in E.

opposite edge of the disc when these fragments were mixed and cultured *in vivo* for an extended period of time. These results showed that cell-cell interactions at the wound heal were instructive in determining the pattern regenerated by a disc fragment cultured *in vivo*. These experiments bridged the gap between cockroach legs and imaginal discs by showing that respecification of fate after injury depended on local cell-cell interactions. Thus, positional information could be specified in a homologous manner in different species.

French et al., (1976) and Bryant et al., (1981) showed in detail how the polar coordinate model can explain the behavior of a wide variety of duplicating and regenerating imaginal discs fragments and also grafts in cockroaches and amphibian legs. Positional values are represented in terms of polar coordinates in two dimensions. Thus, each positional value is specified by a radial and a circular coordinate value. On the fate map of a disc, the origin of the polar coordinate system specifies a distal fate and the outer edge represents the most proximal values (Figure 1.1). The model has two rules that were derived from the following experimental observations. If cells that are normally in non-adjacent positions in the disc epithelium are juxtaposed by grafting or wound healing, cell interactions will generate intercalation of intermediate positional values. There would be two ways of filling in the intermediate structures in the circumferential axis, but the observations imply only the shortest route is used. This first rule is called the shortest route intercalation rule; and it is the basis for duplication of a fragment that contains less than half the circumferential values and the regeneration of one that contains less than half (Figure 1.1).

Amputated cockroach legs regenerated the structures distal to the site of the amputation. This is explained in the model by proposing that cells at the cut, which have the most proximal values (highest radial values) regenerate the most distal values (lowest radial values). Also, when a longitudinal strip of integument is taken from the posterior face of the right femur and grafted into the anterior face; or when a left leg is grafted on a right stump, two supernumerary legs grew, which had all of the more distal parts of the leg. In all these situations, operation of the shortest intercalation rule value generates a complete circumference at the wound heal. These observations led to the proposal of the second rule of distalization (Schubiger and Schubiger, 1978; Bryant et al., 1981) which states that complete distal regeneration always occurs at a complete circle of circumferential values. This rule can also explain partial distalization using only strictly local cell-cell interactions. Cells at the base of the cut could become juxtaposed by folding of the edges, opposing different circumferential positional values. Intercalation would start by generating a cell that has an intermediate circumferential positional value. The radial value would be displaced one step more distal if a neighboring cell with the same positional value already exists. According to the model, new limbs form in these cases because cells with the highest discrepancy in positional values are juxtaposed at the cut. This causes intercalation of the complete circumferential values (shortest route) before regenerating all the more distal values (distal transformation). These two rules combined can explain supernumerary limb formation.

Despite its descriptive utility, the model did not suggest a cellular and molecular framework to explain how a positional information of this kind might be established at the genetic and molecular level. It did not integrate concepts of compartments and selector genes. Bryant (1993) attempted to bring molecular data into the polar coordinate model. He argued that the expression patterns of certain genes in concentric rings in the leg imaginal disc provides molecular evidence for positional information in the P-D axis. Similarly, expression of *wg* in a pie-shaped sector is suggestive of a circumferential coordinate. However, at least two genes, *disconnected* and *apterous* (*ap*), "in spite of showing expression at specific P-D level, are not required for leg development".

The arbitrarily assigned positional values constitute another weak point of the model. Angular values were assumed to be equally distributed around the wing imaginal disc. Since they all duplicate, according to the shortest route rule every 90° sector appears to have similar density of angular positional values as the three other 90° sectors. On the contrary, angular values around the leg imaginal disc had to be assigned in a different manner to explain the observations. Because the upper medial quarter of the leg imaginal disc regenerates, it would have to contain a higher density of positional values than any other 90° sector in the same disc. To explain its regulative behavior, French et al., (1976) proposed that the upper medial quarter has more than half the positional values of the entire imaginal disc. Finally, positional information was proposed to be two dimensional, while amphibian and insect limbs are three-dimensional structures.

In summary, the Polar coordinate model provided a good description of the outcome of a wide variety of surgical and grafting experiments. However, it did not account for the phenomenon of compartmentalization or integrate the selector gene model as a component of the positional information system.

A model for positional information in imaginal discs that includes the concept of morphogen gradients in three dimensions was proposed by Russell (1983). Since imaginal discs are three-dimensional structures (topologically like a sphere), Russell proposed that positional information would be more likely specified using a Cartesian Coordinate System in three orthogonal axes than a polar coordinate system using only two. Positional values along each axis would be established by a different molecule, which would be able to diffuse in the epithelium. Thus, every point in the imaginal disc surface would have a unique positional value (*x*, *y*, *z*) determined by a combination of three independent morphogen gradients. Thus, the disc positional field could be represented by spherical surface enclosing an origin, with a positional value 0,0,0. Positional values on the polar coordinate field are a projection of the cartesian system onto the *x-y* plane.

The advantage of this system is that a simple rule can account for regeneration and duplication of all complementary fragments. This rule states that "values in each coordinate are assigned by interpolation whenever normally non-adjacent cells are juxtaposed". By applying the mathematical transformation that converts values to the Polar-coordinate model, it was shown that this simple rule automatically generates the shortest route rule intercalation and distal regeneration values of the polar coordinate model. Thus apparently complex cell behavior could be explained by a physically simple process of diffusive smoothing of chemical gradients. Like the Polar-coordinate model, this model is also able to predict the outcome of all the grafting and regeneration-duplication experiments. In the polar-coordinate model, a fragment containing more than half of the positional values will regenerate the entire disc, while a one containing less than half will duplicate. In the Cartesian-coordinate model, a fragment containing the origin (0,0,0) will regenerate while one that does not will duplicate. This property of the model follows from the assumption that cell fate is determined by the relative values of the three variables x , y and z (expressed as a solid angle).

An important added feature of this model is its relationship to the phenomenon of compartmentalization. As shown by Garcia-Bellido et al., (1973) and Crick and Lawrence (1975), progressive compartmentalization events divide the wing imaginal disc orthogonally into the four A/D, A/V, P/D and P/V compartments, characterized by cells that have different states of determination. The compartment boundaries are geometrically related to a Cartesian coordinate system and might be established along threshold values of each variable of a Cartesian coordinate system of positional information. Thus, this model integrated the ideas of morphogen gradients, compartmentalization and positional values to explain regeneration and duplication in a relatively simple manner.

Meinhardt (1980, 1982, 1983), proposed a different model which also relates compartments and positional fields. In this model the positional information system in the form of morphogen gradients emanates from compartment boundaries. Thus this model placed compartmentalization upstream of positional information in the hierarchy of information flow. Meinhardt followed Turing (1952) in arguing that spontaneously organized patterning might be produced by coupling a short-range autocatalytic process with a long-range inhibitory process by diffusion of the morphogens involved (reaction-diffusion). Autocatalysis is one way to maintain a determined state and this could be the basis for compartments.

When the segment polarity genes are first activated, the action of long range signaling molecules like HH encoded by *hedgehog* (*hh*), and WG, stabilizes the two neighboring cell states. For example, EN activates *wg* expression in neighboring cells through HH, a diffusible factor. In turn, WG diffuses to stabilize *en* expression. This model also requires that *en* and *wg* exclude one another locally (at short range). The genetic evidence shows that *en* is initially activated by *wg* in the posterior part of the embryonic segments, but it becomes independent of *wg* later when its

expression becomes cell-heritable. This system could generate borders characterized by neighboring cells with different determination states.

To explain pattern formation in secondary fields, specifically in imaginal discs, Meinhardt's model combines several concepts. First, it includes Wolpert's ideas in which positional information is acquired by cellular interpretation of different concentrations of a morphogen. Second, it includes Garcia-Bellido, Lawrence and Morata's ideas of compartmentalization based on differential selector gene activation. Third, it introduced for the first time the concept of cooperation between gene expression domains at their borders to specify the source of a novel morphogen gradient. The initial requirement for the generation of positional information would be the formation of a boundary by means of an initial compartmentalization event (e.g. A-P by *en*). Cells at the boundary would generate a morphogen that would diffuse in opposite directions (to the anterior and posterior compartments). The distance from the border would determine the positional value of the cells. A similar mechanism could generate a D/V boundary and positional coordinates.

To generate positional information in the P-D axis, Meinhardt proposed that a third interaction between the A/P and D/V morphogens could create a local singularity at the point of intersection of the two compartment boundaries. This would generate a third morphogen with its highest concentration coinciding with the intersection of the compartment boundaries. Thus, the distalmost structures would be produced in the middle of the disc at the highest peak in morphogen gradient, and most proximal structures at the lowest concentration point at the edge (Figure I.2). Note the similarity to Russell's model. A prediction of the model is that distal transformation will occur if a new intersection of A/P and D/V boundaries is created. Recent evidence fully supports this prediction (see below). According to this model, distal transformation only needs the intersection of at least three compartments, not a complete circumference as in French et al. (1976).

Several experiments on signaling molecules support the boundary model. Supernumerary appendages in *Drosophila* produced as a result of ectopic expression of signaling molecules like HH and DPP, can be explained in terms of this model. In the leg imaginal disc, (reviewed in Campbell and Tomlinson, 1995) the homeobox transcription factor *en* is expressed in the posterior compartment. These cells also express the secreted factor HH in response to *en* expression (Tabata and Kornberg, 1994; Tabata et al., 1992; reviewed in Blair, 1992a). HH is a secreted protein that diffuses from posterior to anterior cells that lie at the A/P boundary. This causes a differential activation of genes in the anterior dorsal and anterior ventral compartments. Thus, *wg* is expressed in the anterior ventral compartment, and *dpp* is expressed mainly in the dorsal anterior compartment in a band close to the A/P compartment boundary (Capdevila et al., 1994). The conjunction of *dpp* and *wg* expression where the D/A, D/V and P compartments are juxtaposed creates a local singularity, marked by *Dll* expression that specifies the distalmost structures of the fate map and triggers the formation of the proximal-distal axis.

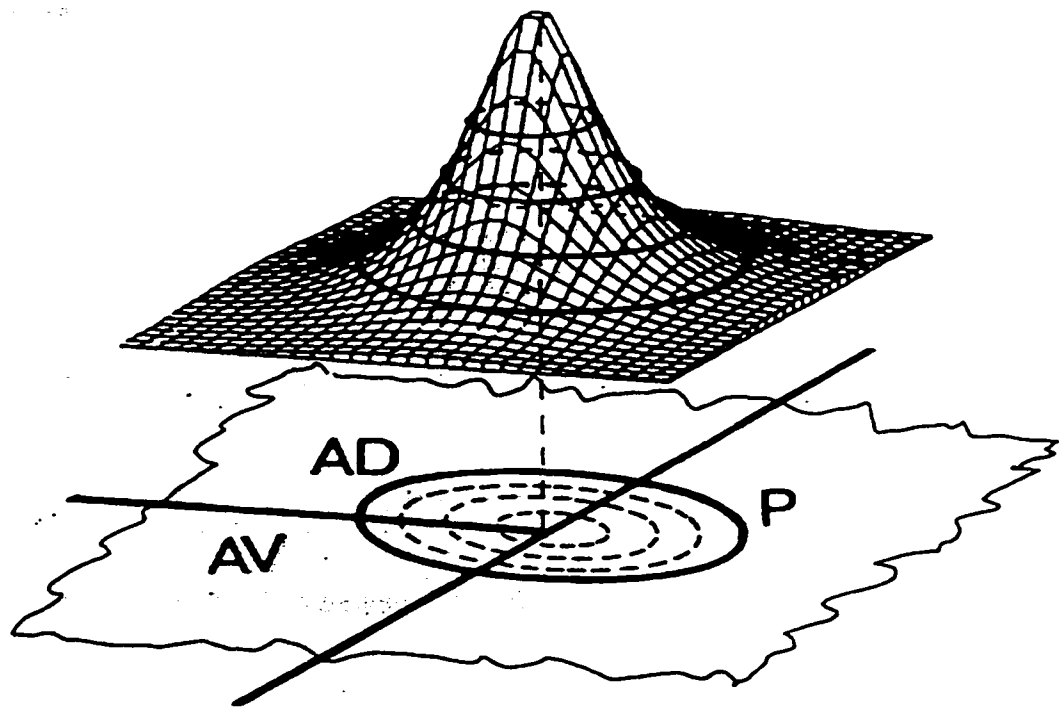


Figure I.2. Schematic representation of Meinhardt's model for the leg imaginal disc positional information system (Meinhardt, 1983). Meinhardt proposed that the point where the posterior, the anterior dorsal, and the anterior ventral compartments intersect is an "organizer", which acts as a morphogen source to specify position in the formation of the proximal-distal axis (after Meinhardt, 1983).

Misexpression experiments using *hh*, *dpp*, or *wg* flip-out cassettes (Basler and Struhl, 1994) can create new conjunctions of *dpp* and *wg* expression necessary for the formation of an ectopic distal outgrowth. This technique allows a chosen sequence to be expressed under the control of a constitutive promoter after a stop codon is removed by recombination. If *wg* is expressed ectopically in cells that are in close proximity to the cells that express *dpp* endogenously in the anterior-dorsal compartment, then an ectopic distal organizer is formed leading to the formation of supernumerary distal structures. In addition, if two clones of cells misexpressing *hh* are induced simultaneously near the anterior ventral and dorsal compartment border, a new P/D axis is also formed. This result is expected since anterior dorsal cells will produce DPP in response to *hh* and anterior ventral cells will express *wg*. Since WG and DPP are secreted molecules they are able to diffuse a few cell diameters, so the new P/D axis is formed at the intersection point of *wg* and *dpp* expression. Likewise, ectopic expression of *dpp* in the anterior or posterior compartments close to the D/V boundary where *wg* is expressed induces distal pattern duplications in the wing (Capdevila and Guerrero, 1994). This model is also able to explain the formation of supernumerary legs in cockroach leg grafts via the abnormal juxtaposition of compartments (Campbell and Tomlinson, 1995). Evidence for a lineage restriction corresponding to an A/P compartment boundary have been found in cockroaches (Bryant, 1980).

However, the boundary model is unable to explain several surgical results, (reviewed by Blair, 1995), for example, the upper medial quarter fragment of the leg disc that lacks all the cells from the posterior compartment, but which regenerates the entire pattern (including of course, distal structures). It does not explain either why there is duplication of the complementary fragment. As explained above, these results are predicted by applying the intercalation rule proposed by French (1976) using either the polar coordinate, or cartesian coordinate models. The boundary model does not consider what happens at wound healing, formation of blastema or propose any explanation for the observed intercalation of missing structures. To explain duplication of disc fragments in cell-lethal mutants, Meinhardt (1983) arbitrarily proposes that cell-death (Girton and Russell, 1981) may cause an unstable situation that results in the respecification of compartmental states so that some cells change from anterior to posterior.

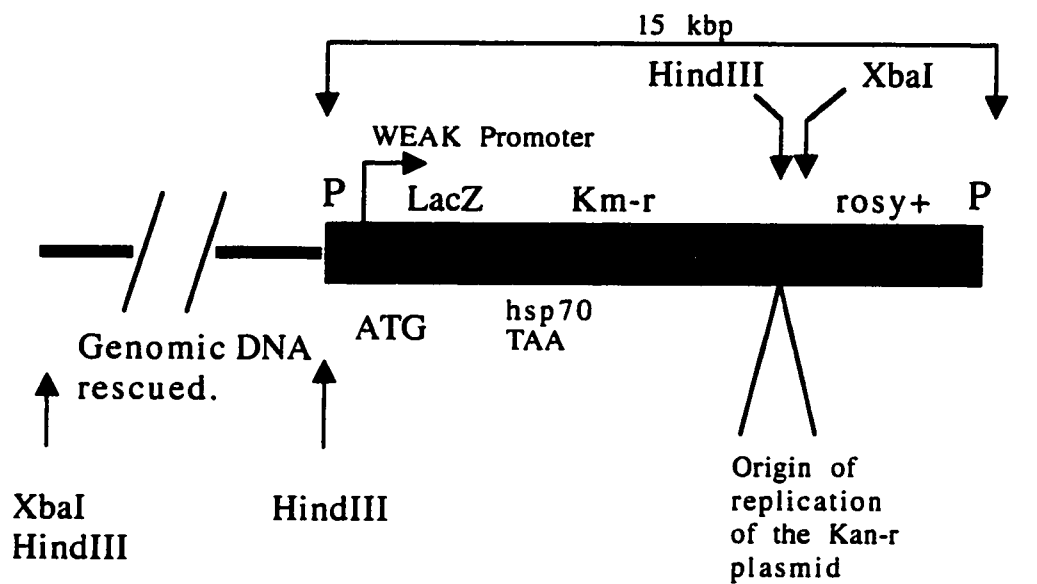
In summary, none of the models provides a complete and general description of all experimental results. It is known that the BCD-dependent gene hierarchy that generated the original pattern of compartmentalization is no longer active in repatterning. Therefore, different unknown genes may be responsible for respecification of fates and repositioning of compartment boundaries in regenerating discs fragments. These genes might be expected to be involved in positional signaling, and mediate some feedback between compartmental identity and positional specification.

1.3 Regeneration as a system to discover new patterning genes

The literature reviewed above indicates that the approaches used so far have been insufficient to fully understand insect imaginal disc pattern formation at the cellular and molecular level. There may be other genes involved in imaginal disc positional information that have not yet been identified. A way to study the genetic basis of positional signals in imaginal discs would be to identify genes involved in regeneration. However, until recently, in spite of many years of work on imaginal discs, no such genes had been identified because of the difficulties of selecting directly for the expected phenotype. A new approach, became possible, however, with the development of the enhancer-trap technique (reviewed by Spradling et al., 1995).

O'Kane and Gehring (1987) created a P-element construct that contains a lacZ reporter gene that encodes the β -galactosidase enzyme driven by the weak P-transposase promoter and a *rosy*⁺ gene marker (Figure 1.3). Because it carries the lacZ gene was named Pz. This P-element construct can be mobilized if complemented in trans with a P-insertion line carrying an active transposase gene. Transposition can be detected in the progeny of appropriate crosses using the *rosy*⁺ marker in the P-element. If the enhancer trap re-inserts near the regulatory sequences of an endogenous gene, lacZ expression may be induced. The β -galactosidase-staining pattern often corresponds to that of the endogenous gene (Wilson et al., 1989; Jacobs et al., 1989). This makes the system useful for identifying a desired class of genes on the basis of their expected expression patterns.

Pz also carries a plasmid origin of replication and the Kanamycin resistance gene to facilitate cloning in *E. Coli* of genomic sequence flanking an insertion. The genomic DNA from flies carrying the insert can be digested with XbaI, ligated, then used to transform a Kanamycin sensitive *E. coli* strain to rescue the plasmid. Plasmids isolated from these transformants usually carry genomic flanking DNA that should map to the region of insertion. Brook et al. (1993) used this system to screen for genes expressed ectopically in imaginal discs that were regenerating after cell death induced by a temperature-sensitive cell-lethal mutant (Russell, 1974). This screen was performed by mobilizing the P-element construct from the original insertion site on the X chromosome to one of the autosomes. A total of 826 independent insertion lines were generated and tested for altered expression in regenerating discs using *su(f)*¹², a temperature sensitive cell-lethal cell-autonomous allele of *suppressor of forked* (Russell, 1974), or for γ -ray treatment to induce cell-death. Several lines that showed differential lacZ expression were re-tested for the same behavior in regenerating disc fragments cultured *in vivo*. Expression was often seen specifically at the site of wound healing. G45 is an insertion of this kind.



P : inverted repeat of the transposon (P-element)

hsp70 TAA: hsp70 transcriptional termination sequences

Km-r: Kanamycin resistance gene

lacZ: Beta-galactosidase gene

rosy+: wild type copy of the *rosy* gene

Figure I.3 Pz enhancer-trap construct used in the screen.

I.4 G45 expression in the context of disc regeneration

The G45 P-lacZ insertion line was selected for further study because of its following properties. G45 reports expression only in regenerating discs after cell death or surgical fragmentation. In wing disc fragments of late third larval instar cultured *in vivo*, lacZ expression is detected only on one side of the wound heal by antibody staining (Brook 1993). This suggests that this line may report a gene with a significant role in a polarized cell-interaction across the wound heal, in a manner that might be expected of a signaling molecule, or a receptor activated by the regeneration process. The importance of genes expressed specifically at the wound heal stems from the fact that respecification of cell fates occurs via cell-cell interactions at this site (Haynie and Bryant, 1976, Reinhardt and Bryant, 1981). In addition, G45 reports expression in the embryonic nervous system, a feature seen in some other known patterning genes such as *en* and *wg*.

In earlier preliminary work with this line, genomic DNA flanking the G45 insertion was obtained by plasmid rescue and mapped to 100E (chromosome 3) by *in situ* hybridization to the polytene chromosomes. *Df(3R)faf^{pp}*, a deficiency line that deletes 100E-F was used to confirm by Southern hybridization that the flanking DNA was deleted in that location (Brook, 1994). Brook subcloned the flanking sequence in pBluescript SK⁺, placing it downstream of the T₃ and T₇ promoters. To see if the flanking DNA contained sequences of regeneration genes reported by G45, this plasmid was used to make single strand probes off opposite strands. One was made from the T₃ promoter and the other from the T₇ one. When hybridized to third instar imaginal discs these probes revealed different patterns of transcription. The T₇ single strand probe detected a signal behind the morphogenetic furrow in the eye antenna imaginal discs. This signal was the same in normal and regenerating discs. The T₃ single strand probe detected a signal from a putative transcript expressed generally in all discs under regeneration conditions but did not detect any signal under normal conditions. It was tentatively concluded that the flanking DNA contains a putative regeneration gene reported by G45. However, this result remained equivocal, as the region of insertion was not yet characterized.

For these reasons I decided to attempt cloning the gene or genes reported by G45 hoping to find one corresponding to the putative regeneration gene. My experimental design was based on the following line of reasoning. Since lacZ expression was not detectable above background in normal discs (lacZ is a very sensitive stain, capable of detecting transcription even at low levels), the likelihood of finding the desired transcript in a wild type imaginal disc library was very low. G45 did however, report expression in the embryonic nervous system.

I therefore used an embryonic cDNA library to screen for the putative cDNA possibly reported by G45 using the rescued fragment of DNA flanking the region of insertion. The cDNAs identified in this manner were

to be used for *in situ* hybridization experiments to embryos and to normal and regenerating imaginal discs. Then, by comparison to the expression patterns detected by the T₇ and T₃ probes, a putative transcript would be selected for further molecular characterizations such as sequencing, polytene chromosome *in situ* hybridization and Southern analysis, using overlapping cosmids spanning the region 100E-F to see if a full transcript could be found.

To test if a gene near the G45 insertion has any function in imaginal disc development I carried out a phenotypic analysis with one of the lethal-derivatives of G45. The G45 insertion is homozygous viable with no visible phenotype. In order to find clues as to the function of the gene or genes reported by the G45 lacZ expression, I made use of a lethal excision derivative of G45, obtained by W. Brook (1994). This derivative was obtained by crossing the original insertion line to a line that contained the PΔ2-3 constitutively expressed transposase gene cassette so that the P-lacZ element could be excised. Putative imprecise excisions were initially selected by the loss of the *rosy*⁺ marker and then as homozygous lethals which were then crossed to a *Df(3R)faf^{hp}* (Fischer-Vize, 1992), which uncovers the point of insertion of G45 (100E1-2). The ones that failed to complement were kept and analyzed at the cytological level. Some of them proved to contain cytologically visible deletions in the 100E region. The line G45Δ53 was chosen for this study because although it fails to complement *Df(3R)faf^{hp}* it shows no cytologically visible deletion (J. Higgins, personal communication), and so may delete fewer genes in the G45 region than the other larger deficiencies.

Since G45Δ53 is a homozygous embryonic lethal its effects on imaginal discs and adult structures could be best studied by inducing mitotic recombination in heterozygotes to produce clones of mutant cells. If a gene is needed in imaginal disc patterning, a phenotype will be seen in the adults because of the mutant clone. The FLP/FRT method was used because of the high frequency of clones that can be induced. Chromosomes were designed and constructed so that the clones would be marked to identify phenotypic abnormalities in different parts of the adult cuticle that were correlated with changes of clone genotype. Twin clones were used so as to be able to mark the position of the mutant clone even if it did not survive. Finally, controls were designed to rule out any non-specific effect due to markers.

This thesis reports two findings. Firstly, the 2.3 kbp flanking genomic region (FLR) is chimeric in origin but no exons were found that map to 100E. FLR includes instead a stretch of sequence that is 100% identical to a sequence tagged site (STS) that maps to the X chromosome. Secondly, Δ53 probably includes at least one gene involved in imaginal disc patterning and possibly another one regulating cell growth. Clonal analysis experiments showed phenotypic effects in the wing margin, notum, eye and ocelli in a manner that suggests Δ53 contains a gene that may cause ectopic activation of the *wg* pathway.

II. MATERIALS AND METHODS

II.1 *Drosophila* strains and culture conditions

Flies were grown on a medium prepared according to Nash and Bell, (1968). All the crosses were performed at RT on standard medium except in those cases where antibiotic was required for selection of the Neomycin gene. The antibiotic G418 (Geneticin, GIBCO laboratories) was used as described in Xu and Rubin, (1993). 300 μ l of a freshly made G418 solution (concentration: 25 mg/ml) was added per 10 ml of medium. This antibiotic is toxic to eukaryotic cells and only flies that carried the P[ry⁺; hs-neo; FRT] cassette could survive in this medium.

Fly stocks were usually kept at RT (19-20°C) or when necessary in an incubator at the indicated constant temperature. A list of the pre-existing strains used in this study is in Table II.1. Strains that I constructed for the clonal analysis experiments are described in Table II.2. For description of the markers and balancer chromosomes see Lindsley and Zimm (1992) and Flybase (<http://www.flybase.com>). Markers used in clonal analysis experiments are described below. The notation I used for the Pi M cassette (see below) was PiM pM or the greek symbol π M, the three are ways are equivalent in this thesis.

II.2 Bacteria and Phage culture

Escherichia coli strains were grown in LB or superbroth prepared according to Sambrook et al. (1989). Three bacterial strains were used. DH5 α (endA1 hsdR17 supE44 thi-1 recA1 gyrA96 relA1 D (argF-lacZYA) U169 ϕ 80dlacZ Δ M15), was used for growing plasmids and cosmids and for subcloning the cDNAs detected in the screen. Q358 (hsdR⁻K, hsdM⁻K supE ϕ 80⁺) (Karn et al., 1980), was used as a source of plating cells for phage λ gt10. LE 392 (supE supF hsdR) (Borck et al, 1976) was used as a source of plating cells for phage λ EMBL4. Phage λ gt10 (Huynh et al., 1985), was used to screen for cDNAs representing transcripts expressed in the embryo at 3-12 h and at 12-24 h. The original libraries were provided by Dr. T Kornberg. Phage EMBL4 (Karn et al., 1980), contained two previously isolated genomic clones from a *Drosophila* library λ 7 and λ 8 (Bill Brook, unpublished results). These phages had been previously isolated using a genomic fragment that mapped to 100E as a probe.

Table II.1 *Drosophila* strains used in this study

Line	Genotype	Name used in this thesis	Reference or source
A	G45 Δ 53 ry/TM3, Sb ry	G45 deficiency line	W. Brook (Ph. D. thesis)
B	P [lacZ ry ⁺] G45 ry/ P [lacZ; ry ⁺] G45 ry	G45, PZ line.	W. Brook (Ph. D. thesis)
C	y v f su(f) ¹²	suppressor of forked	M. A. Russell lab
D	Canton S		M. A. Russell lab
E	y w; TM3, Sb ry e/TM6B, Tb Hu e		M. A. Russell lab
F	w; TM3, Sb ry e/TM6B, Tb Hu e		M. A. Russell lab
G	w; TM3, Sb/Ly	white Lyra	S. Scanga
H	y w; TM3, Sb/Ly	yellow white Lyra	M. A. Russell lab
I	y w; P[ry ⁺ hs-neo FRT]82B P[mini-w ⁺ hs- π M]87E Sb ^{63b} P[ry ⁺ y ⁺]96E/TM6B, Hu ry ^a	2045	Xu and Rubin, 1993
J	y w P[ry ⁺ hs-FLP]1; TM3, Sb/Dr ^{M10}	Heat-shock Flip.	Xu and Rubin, 1993
K	P[ry ⁺ hs-neo FRT]82B/ry	2035	Xu and Rubin, 1993
L	y w; P[w+mC] l(3)j2A4/TM3, Sb ¹	P2167, (lethal insertion that maps to 100E01-02)	Y.N.Jan. (donor) Berkeley <i>Drosophila</i> Genome Project
M	PZ [lacZ ry ⁺] A64 ry/TM3, Sb ry	A64, Pz line	W. Brook (Ph. D. thesis)

^a The designation mini-w⁺ is used in this thesis instead of w⁺

Table II.2 Lines constructed for the clonal analysis experiments			
LINE	GENOTYPE	Use	PHENOTYPE of the line
1)	y w; P[ry ⁺ hs-neo FRT]82B P[mini-w ⁺ hs-πM]87E Sb ^{63b} /TM6B, Hu ry	To remove the P[ry ⁺ ; y ⁺]96E cassette from line I (Table II.1)	Orange eyes, yellow body, Stubble and Humeral.
2)	y w; P[ry ⁺ hs-neo FRT]82B P[ry ⁺ y ⁺]96E	To mark twin clones in the second clonal analysis experiment as yellow ⁺ , Sb ⁺ .	Yellow body, white eyes, Stubble ⁺ .
3)	y w; P[ry ⁺ hs-neo FRT]82B P[mini-w ⁺ hs-πM]87E Sb ^{63b} G45Δ53 /TM6B, Hu ry	To generate mutant clones marked with yellow in the first clonal analysis experiment.	Orange eyes, yellow body, Stubble and Humeral.
4)	y w; P[ry ⁺ hs-neo FRT]82B P[ry ⁺ y ⁺]96E G45Δ53 /TM6B, Hu ry	To generate mutant clones marked as Sb ⁺ in the second clonal analysis experiment.	yellow ⁺ body, white eyes, Stubble ⁺ and Humeral.
5)	y w; P[ry ⁺ hs-neo FRT]82B G45Δ53 /TM6B, Hu ry	To generate mutant clones marked as yellow in the third clonal analysis experiment.	White eyes, yellow body, Humeral, Stubble ⁺ .

II.3 Clonal analysis experiments

In order to generate marked clones the FRT/FLP-Recombinase system was used. The yeast flip recombinase (FLP) produces a high frequency of site-specific recombination when heat-shocked since the gene is under the control of a heat-shock promoter. Its target is called a flip recombinase target site, or FRT site. When a P element construct containing the FRT site is inserted at the base of a fly chromosome, heat-shock-induced expression of the flip recombinase gene carried in another P-element insertion, produces a high frequency of mitotic recombination. This recombination is detectable as somatic clones only between homologous chromosomes carrying these sites (Golic, 1991; Xu and Rubin, 1993) (Figure II.1). I used a FLP strain obtained by Xu and Rubin (1993) in which this P-element is inserted in the X chromosome and a FRT insertion at the base of the right arm of the chromosome III because the deletion G45 Δ 53 maps to 100E, at the tip of 3R.

Several lines developed by Xu and Rubin (1993) were useful for this study of the effect of G45 Δ 53 in imaginal discs and adult structures because they carry cell markers in the right arm of the chromosome III. These markers were used to mark clones in the adult. A marker for eye ommatidia is included in P[mini-w⁺ hs- π M], a cassette containing a derivative of the white gene. This mini-w⁺ gene gives a light orange color to the eyes when in single copy and a red-eyed color in two copies. Thus, when heterozygous in a white genetic background, the P[mini-w⁺ hs- π M] cassette gives an orange background color. This allows the identification of twin clones that carry either two copies of the mini-w⁺ gene (red color) or no copies (white color).

To mark macro and microchaeta in the head, thorax and legs, Sb and yellow⁺ markers were used. A wild type copy of the yellow⁺ gene was introduced via the P[ry⁺ y⁺] cassette, a construct inserted on the third chromosome at the cytological location 96E that expresses yellow⁺ constitutively in every cell of the adult cuticle (Xu and Rubin 1993). The flies display a wild type bristle color phenotype (dark bristles) in the head, thorax and legs. However, mitotic clones are produced in a yellow background so that clones that lose the P[ry⁺, y⁺] cassette show a yellow bristle phenotype.

Stubble (Sb) mutations are autosomal dominants that produce bristles that are shorter than the wild type ones. The gene maps to chromosome three at cytological position 89B9-10 (Lindsley and Zimm, 1992). Most Stubble alleles are cell-autonomous lethal. However, Sb^{63b} was used to mark clones in this study because it is a cell viable allele.

In order to perform the clonal analysis experiments it was necessary to construct several lines. Construction of lines 1, 2, 3, 4, and 5 is described in Figure II.2, Figure II.3, Figure II.4, Figure II.5, and Figure II.6,

respectively. Schematic representations of the crosses performed to generate clones in these three experiments are described in chapter III. In order to induce mitotic clones, six fertilized females were allowed to lay eggs for 24 h at 20°C in vials containing standard medium. The embryos were then incubated at 20°C for 24 h until the larvae reached first and second instar. Vials were then heat shocked for 1 h at 37°C in a water bath to induce expression of the FLP recombinase enzyme. Flies were screened for abnormalities in the eyes, head, maxillary palps and proboscis, legs, abdomen, and wings. Typically, more than 100 flies were scored. All flies were examined first with the dissecting microscope or the compound microscope after mounting parts on slides. Heads were observed under the dissecting microscope and photographed. Wings and thoraces were dissected and mounted on the slides using Gurr's medium, observed under the microscope and bristles were scored.

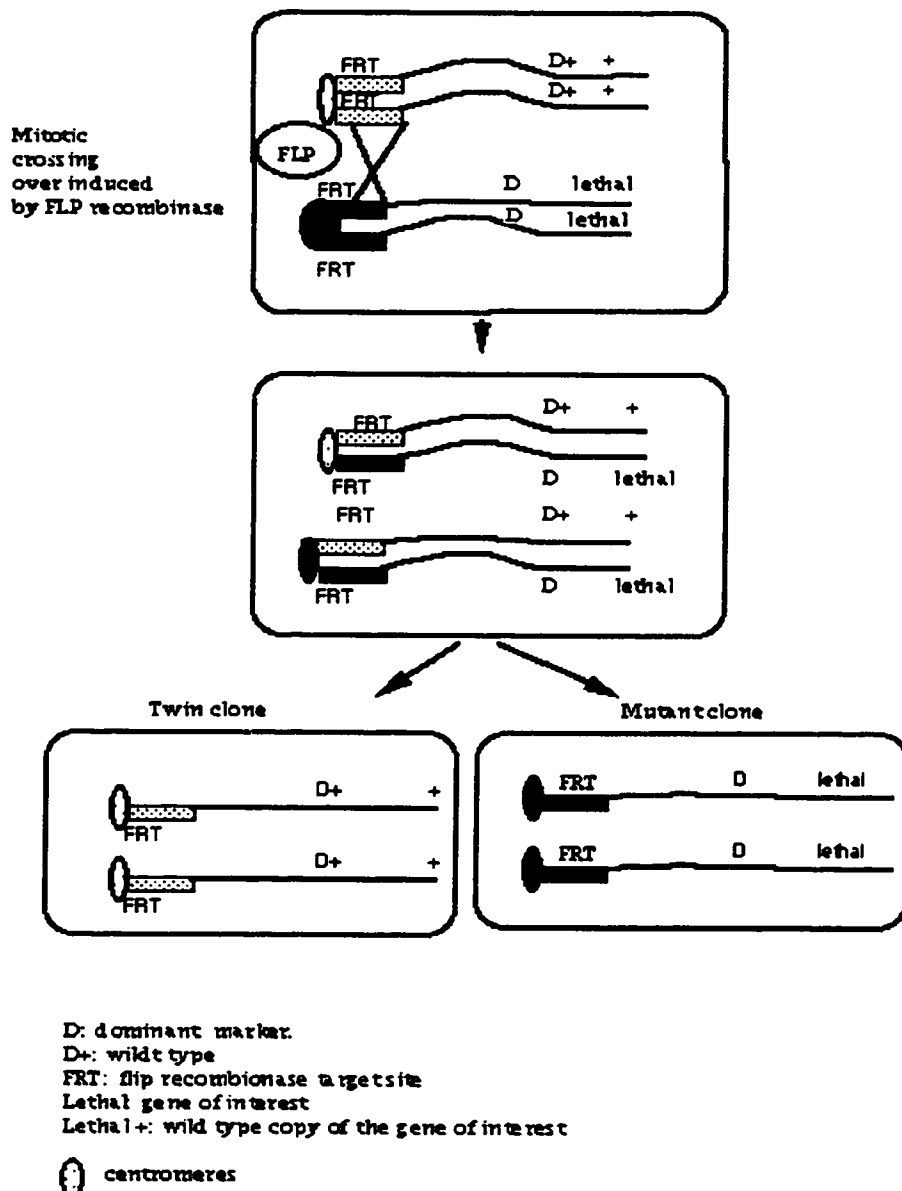


Figure II.1 FRT/FLP system. Schematic representation of the events leading to the generation of mutant clones using the FLP recombinase (FLP) from yeast and its target site (FRT). D: dominant marker such as Stubble (Sb) which causes a shorter bristle phenotype. The lethal can be any homozygous lethal, such as $\Delta 53$ in this study. After FLP generates a crossing-over event between the FRT sites, which are proximal to the dominant marker and the lethal locus, mitotic segregation of the chromatids produces cells that carry either two copies of the wild type allele of the dominant marker and two copies of the wild type allele of the lethal locus (twin clone), or two copies of the lethal mutant allele, and two copies of the dominant marker (Mutant clone). Mutant clones can be distinguished from the background because of the more severe phenotype caused by the dominant Sb allele in double copy. Alternatively, mutant clones carry a different dominant marker (see section on markers used in clonal analysis experiments). Twin clones are useful in marking the area where the crossover event occurred even if the mutant clone is inviable.

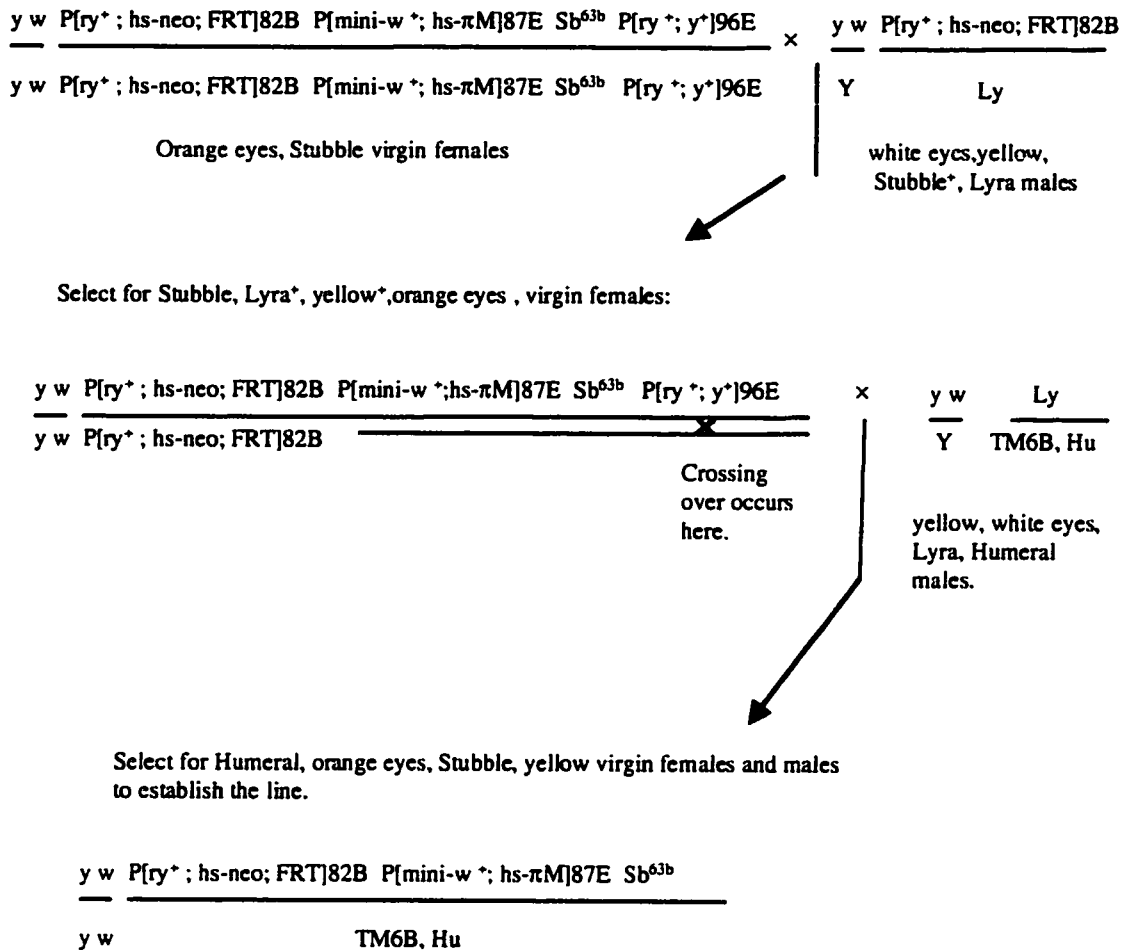


Figure II.2. Construction of line 1. Line 1 (Table II.2) was constructed by crossing homozygous females from the FRT line 2045 (Table II.1) to males carrying the $P[ry^+; hs-neo; FRT]$ cassette at the cytological position 82B (third chromosome) and a Lyra marker in its homologous chromosome. These females were phenotypically orange-eyed due to expression of the $P[mini-w^+; hs-\pi M]$ cassette and the males were phenotypically Lyra, white-eyed and Stubble⁺. The progeny selected was phenotypically Stubble, Lyra⁺, orange eyes, yellow⁺, females. These females carried the $P[ry^+; hs-neo; FRT]$ in homozygosis. They were heterozygous for the $P[mini-w^+; hs-\pi M]$ cassette, the Sb^{63b} allele and the $P[ry^+; y^+]$ cassette. These females were selected in order to recombine out the $P[ry^+; y^+]$ cassette. This was done by selecting the progeny from a cross between the females above and males phenotypically Lyra, yellow, white, Humeral. The progeny selected was Humeral, Lyra⁺, orange eyes, Stubble and yellow. These flies were crossed to one another to generate a stock.

$y\ w\ P[ry^+; hs-neo; FRT]82B\ P[mini-w^+; hs-\pi M]87E\ Sb^{63b}\ P[ry^+; y^+]96E$ \times $y\ w\ P[ry^+; hs-neo; FRT]82B$
 $y\ w\ P[ry^+; hs-neo; FRT]82B\ P[mini-w^+; hs-\pi M]87E\ Sb^{63b}\ P[ry^+; y^+]96E$ \times Y Ly

Orange eyes, Stubble females.

white eyes, yellow,
Stubble⁺, Lyra males.

Select for Stubble, Lyra⁺, yellow⁺, orange eyes, virgin females:

$y\ w\ P[ry^+; hs-neo; FRT]82B, P[mini-w^+; hs-\pi M]87E\ Sb^{63b}\ P[ry^+; y^+]96E$
 $y\ w\ P[ry^+; hs-neo; FRT]82B$ \times $y\ w\ Y$ Ly
 $TM6B, Hu$
 Crossing over occurs here.

yellow, white,
Lyra, Humeral males.

Select for Humeral, white eyes, Stubble⁺, yellow⁺ virgin females and males to establish the line.

$y\ w\ P[ry^+; hs-neo; FRT]82B\ P[ry^+; y^+]96E$
 $y\ w\ P[ry^+; hs-neo; FRT]82B\ P[ry^+; y^+]96E$

The homozygous phenotype
breeds true.

Figure II.3 Construction of line 2

Line 2 was constructed as in Figure II.2 except that the reciprocal crossover chromosome was selected in the F₂. Flies phenotypically Hu, Ly⁺, Sb⁺, white eyes and yellow⁺ body color were selected over the TM6B balancer to establish the line. The P[ry⁺; hs-neo; FRT] homozygotes are viable and fertile and therefore non-balancer flies segregate in the stock.

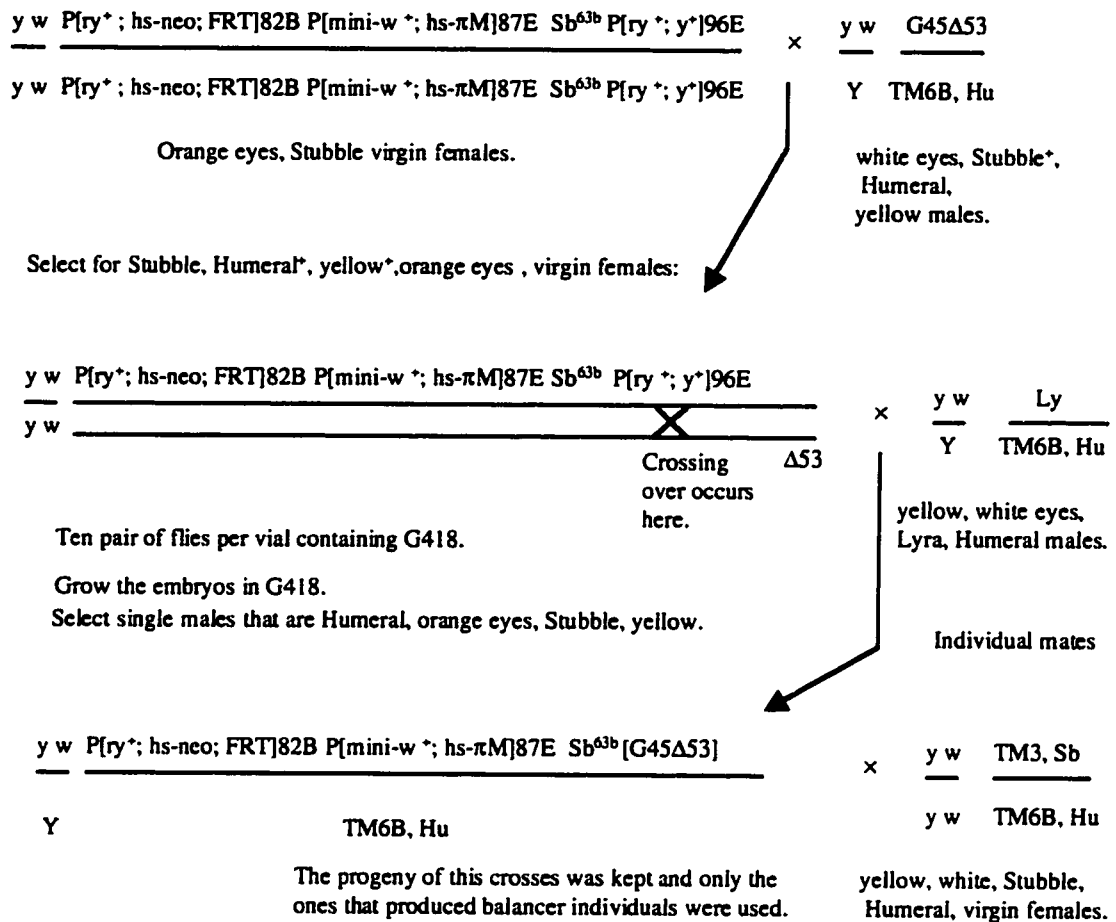


Figure IL4 Construction of line 3

To construct line 3, the original deficiency line G45Δ53 was crossed to females from a balancer stock $y\ w/y\ w$; $Ly/TM6B, Hu$ in order to construct a line carrying the deficiency chromosome in a yellow white background ($y\ w/y\ w$; $G45\Delta 53/TM6B, Hu$). This would allow later selection of the chromosome carrying the Sb^{63b} allele, the $P[ry^+; y^+]$ (yellow⁺ marker) and the $P[mini-w^+; hs-pM]$ (orange eyes) cassettes. Then homozygous females from the FRT line 2045 (Table II.1) were crossed to males obtained as above that carried the deficiency chromosome in a yellow white background. The offspring selected were phenotypically Stubble, Humeral⁺, orange eyes, and females. These females carried the deficiency chromosome and its homologue carried the 2045 insertions. In order to obtain the desired recombinants, the females were crossed to balancer males (10 females and 10 males per vial) phenotypically yellow, white, Lyra and Humeral in vials containing G418. Single males were selected. These males had orange eyes for the $P[mini-w^+; hs-pM]$ cassette, Stubble bristles for the Sb^{63b} allele, yellow body color indicating the loss of the $P[ry^+; y^+]$ cassette, and a Humeral phenotype. These males should carry the neomycin gene in the FRT cassette because they were resistant to G418. These males were mated individually to a balancer line that carried $TM6B, Hu/TM3, Sb$ in a yellow white background. The progeny of these crosses were kept and scored for more than two generations. Those lines that produced only balancer individuals, implying that the deletion G45Δ53 was recombined onto the FRT chromosome, were retained.

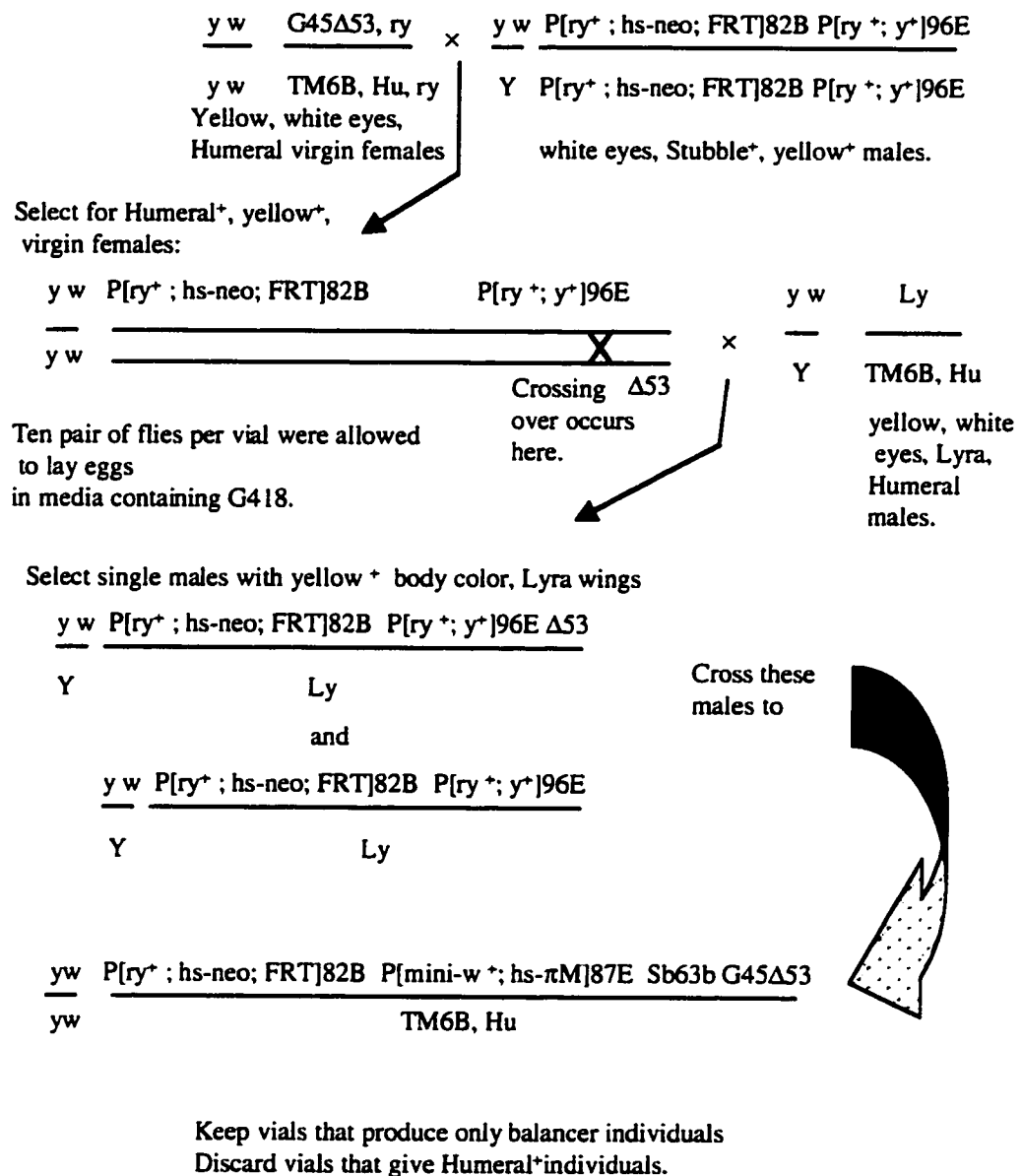


Figure II.5 Construction of line 4

Construction of line 4 had the purpose of recombining G45Δ53 distal to the P[ry⁺; y⁺] cassette. Females from the deficiency line carrying the deficiency chromosome G45Δ53 in a yellow white background, were crossed to males homozygous for the P[ry⁺; hs-neo; FRT] and P[ry⁺; y⁺] cassettes (see line 2 above) in a yellow white background. The progeny selected were yellow⁺, Humeral⁺ females. Ten females were placed in vials containing ten yellow, white, Lyra/ TM6B Humeral males, with medium supplemented with G418 as in the construction of line 3. After allowing them to lay eggs from two to three days the parents were removed and the offspring selected were single males phenotypically Lyra, yellow⁺ which were crossed to a recombinant line carrying Δ53. The recombinant chromosome was easily identified as it was the one carrying the yellow⁺ marker (P[ry⁺; y⁺] cassette). Therefore, y⁺ Hu flies were crossed to establish line 4.

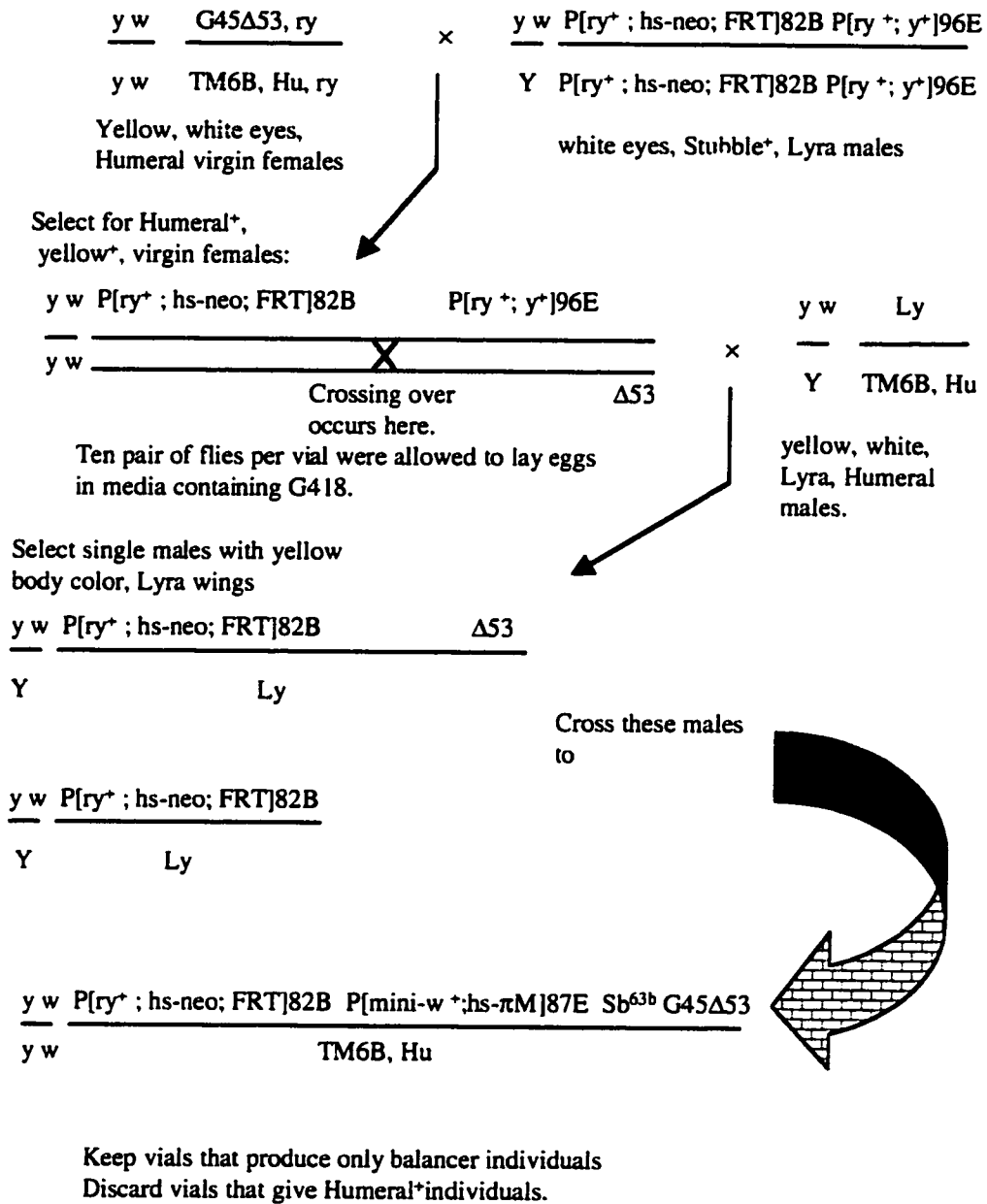


Figure II.6 Construction of line 5

Line 5 was constructed by crossing females of the deficiency line in a yellow background to males of line 2 constructed as shown in Figure II.3. The offspring selected were yellow⁺, Humeral⁺ females. These females were crossed to yellow white Ly Hu males. The offspring were selected in G418 as in Figure II.5, except that the males were phenotypically yellow Lyra and yellow Humeral. These males were crossed individually to yellow, white P[ry⁺; hs-neo FRT]82B P[mini-w⁺; hs-πM] 87E Sb^{63b} G45Δ53 /TM6B, Hu ry and vials were scored for the presence of balancer flies.

II.4 β -galactosidase staining

Staining for β -galactosidase was performed on imaginal discs and embryos. To stain imaginal discs, larvae were dissected in Phosphate-buffered saline (PBS) and fixed in glutaraldehyde-PBS (30 μ l of 25% glutaraldehyde/ml PBS) for 15 min at RT, then washed in PBS 3 X. Staining was performed by adding 20 μ l of a 10% solution of 5-Bromo, 4-chloro, 3-indolyl galactose (Xgal) in dimethyl formamide per ml of staining solution (25 mM NaPO₄, pH: 7.2, 140 mM NaCl, 3.1 mM K₃[Fe(CN)₆], 3 mM K₄[Fe(CN)₆]). After adding the staining solution, the samples were incubated at 37°C from 1 h to overnight until β -galactosidase activity was detectable. Embryo staining was performed as by Ghysen and Kerridge (1989), with minor modifications. Embryos were collected in egg-laying chambers on plates with standard medium. A solution of 0.7% NaCl and 0.03% Triton X-100 was added to the plate and a soft paint brush was used to remove the embryos. Then embryos were transferred to a basket made from a cut off Eppendorf tip closed with a nylon mesh at one end, dechlorinated in 2.6 % sodium hypochlorite (1:1 dilution of commercial bleach) by immersing the basket containing the embryos in a small beaker. When embryos acquired a bright surface and floated (3 min approximately) they were washed with tap water to remove the bleach and then transferred into a glass scintillation vial containing 3 ml of 4% formaldehyde in PBS. An equal volume of n-heptane was added immediately followed by bursts of vigorous mixing spread over 15 min. The heptane (upper phase) was removed and replaced with PBS. The embryos were then transferred to an Eppendorf tube and spun down in a microfuge at maximum speed, the PBS was removed and replaced with 1 ml of PBS+0.2% Triton X-100. When embryos sank the solution was replaced with Xgal staining solution (10 mM NaPO₄, pH: 7.2, 150 mM NaCl, 1 mM MgCl₂, 5 mM K₃[Fe(CN)₆], 5 mM K₄[Fe(CN)₆] 0.2% w/v Xgal). The embryos were incubated in the dark at 37°C and examined at intervals until staining developed. Stained embryos were mounted on microscope slides in 30% glycerol in PBS for observation under the compound microscope.

II.5 DNA work

Genomic DNA preparation from flies was performed as follows. 100 flies were isolated and transferred to an Eppendorf tube and 300 μ l of buffer I (10mM Tris pH 7.5; 60mM EDTA; 0.15 mM Spermidine, 0.15 mM spermine) was added to the sample. Flies were ground by using a pestle. 3 μ l of proteinase K (20 mg/ml) was added and incubated for 60 min at 37 °C. Then 300 μ l of buffer II (200 mM Tris pH:9.0, 30 mM EDTA and 2% SDS) was added, and the mix was incubated for 30 min at 55°C. One volume of phenol: chloroform: isoamyl alcohol 25:24:1 (P:C:I 25:24:1) was added to the mix, mixed and spun down for 5 min at 12000 rpm in an Eppendorf microfuge to separate the aqueous and organic phases. Then the aqueous phase (top) was transferred to a new tube and a second de-proteinization with P:C:I 25:24:1 was performed. Then an equal volume of chloroform was added and extracted as before. NaCl was added to a final concentration of 200mM (15.2

μl from a 5 M stock) and to precipitate the DNA one volume of isopropanol was added to the mix, which was spun down for 10 min at maximum speed in a microfuge. The pellet was washed with one ml of 70% ethanol and spun down as above. The ethanol was removed with a micropipette and the pellet dissolved in TE (300 μl) at RT. RNase was added to a final concentration of 100mg/ml (3μl from a 10mg/ml stock) and incubated at 37°C for 15 min. 200 μl of TE were added and the sample was extracted twice with P:C:I 25:24:1 as above. The DNA was precipitated by adding sodium acetate (pH 5.2) to 300 mM, and two volumes of 95% ethanol, then placed on ice for 10 min. The precipitated DNA was transferred to a new Eppendorf tube with a Pasteur pipette, washed with 70% ethanol and in TE.

Small scale plasmid preparation (minipreps), large scale phage preparation, preparation of plates, plating cells, storage medium for phages and phage titring, subcloning into Bluescript[®] II KS⁺ (Stratagene Cloning Systems), gel electrophoresis, and separation of dNTP's was performed according to Sambrook et al. (1989). Plasmid/cosmid medium scale preparation (midiprep) was performed according to Qiagen[™] plasmid handbook, 1995, using Qiagen resin columns. DNA was purified from gels using a glassmax[™] kit (BRL) according to the manufacturer's specifications. Transformation of bacterial cells was performed according to the Electroporation Manipulator[™] 6000 electroporation protocol, or by the chemical method (Inoue, 1990). Labeling DNA with [α -³²P]dCTP by random priming was performed using the Oligolabelling kit (Pharmacia Biotech) according to the manufacturer's instructions. If DNA was to be labeled with non-radioactive dNTPs, the DIG DNA Labeling and Detection Kit (Boehringer Mannheim) was used instead of the Oligolabelling kit.

II.6 Blot techniques

Southern analysis was performed on DNA samples which were run on 1% agarose-TAE gels. GeneScreenPlus membrane (Dupont) was used in Southern transfers by capillary blots. The conditions for transfer and hybridization are described in the manual supplied with the membrane. To screen a cDNA library, Hybond[™]-N nylon membranes (Amersham life science) were used to lift plaques from the plates and hybridized according to the protocol supplied with the membranes.

II.7 *In situ* hybridization to polytene salivary gland chromosome from larvae

For dissection of salivary glands, third instar larvae of the required genotype were grown at 18°C until late third instar. Third instar larvae were taken out of the vials, washed in PBS and then placed on top of a slide. Salivary glands were dissected in a solution of 45% acetic acid, then transferred to a siliconized coverslip with a drop of 45% acetic acid. Salivary glands were squashed on a slide and frozen in liquid nitrogen for 5 min. The coverslip was flipped off with a razor blade. The slide containing

the chromosome was fixed for 10 min in a solution of 3:1 acetic acid: ethanol, then transferred to 70% ethanol for 5 min, then to 95% ethanol for 5 min and dried overnight for examination under the microscope for the presence of clear bands. Slides were incubated for 30 min at 60°C in 2 X in SSC and rinsed briefly in the same solution at RT. To denature the chromosomes the slides were immersed in freshly made 70 mM NaOH for 2 min at RT, then rinsed 2 X for 5 min in 2 X SSC, then immersed 2 X in 70% ethanol and 5 min in 95% ethanol. Chromosomes were dried at RT and the chromosome region marked with waterproof ink.

The probe was labeled with digoxigenin-labeled dNTP's as described above and it was added to the hybridization solution (45% deionized formamide, 6.5% dextran sulfate, 575 mg/ml yeast tRNA, 1.4 mg/ml sonicated salmon sperm DNA) to a final concentration of 30 ng/ml. The hybridization solution was heated at 75°C for 10 min to denature all the nucleic acids and quenched on ice for 5 min. 10-20 µl was added per slide. Hybridization was performed in a humidified chamber at 37°C. After 18 h in the chamber, the coverslips were removed and the slides were washed twice in 2 X SSC for 10 min at 37°C, then twice in 2 X SSC at RT for 10 min, finally twice in PBS at RT for 10 min. To detect the signal, slides were first blocked by immersion in "blocking buffer" (buffer I plus 0.5% blocking reagent (Boehringer Mannheim); buffer I is Tris-HCl 100mM; NaCl, 150mM; pH: 7.5) for 20 min at 42°C, then placed in blocking buffer for 10 min at RT, and finally rinsed briefly in buffer I and flicked dry. The antibody anti-Dig that has the alkaline phosphatase enzyme (AB-AP conjugate, Boehringer Mannheim) was diluted 1/1000 in buffer I and 40µl of that dilution was added per slide. Incubation was carried out in a humidified chamber at 4°C. To wash the antibody-conjugate, the slides were rinsed once for 1 min in buffer I at RT to remove the coverslip, then three X for 10 min in buffer I at RT. To activate the alkaline phosphatase, slides were immersed in buffer 3 (Tris-HCl, 100 mM, NaCl, 100 mM, MgCl₂, 50 mM; pH: 9.5) for 2 min at RT. To develop the slides, 40 µl of color solution (4.5 µl NBT-solution, 3.5 µl of X-phosphate in 1 ml of buffer 3) was added per slide. Usually, the signal appeared between 1-2 h. To remove the color solution, slides were rinsed for 2 min at RT in TE. In order to observe the slides under the microscope, a solution of 15% glycerol in TE was added on top of the slides, then sealed with a coverslip and rubber cement.

II.8 Embryo and imaginal disc *in situ* hybridization

Hybridization to embryos was performed with non-radioactive probes. Embryos were collected and dechorionated as described in the lacZ staining protocol. To fix the embryos they were transferred to scintillation vials and a mixture of 50% heptane and 50% fixative (10% formaldehyde, 50 mM EGTA pH: 8.0, in PBS) was added and fixation performed at RT for 20-30 min. To devitellinize the embryos, fixative and heptane were removed and replaced with methanol. Embryos were shaken vigorously for several min. After they had sunk they were rinsed with methanol, then 3 X with 95% ethanol and stored at -20°C until used. They were rinsed in 100% methanol, 50% methanol 50% PBT plus 5% formaldehyde (PBT=PBS, 0.1% Tween 20).

Embryos were rinsed in PBT 3 X 2 min each then incubated for 3-5 min at 37°C in PBT plus 50mg/ml of freshly prepared proteinase K solution. To stop the digestion embryos were rinsed 2 X with 2mg/ml glycine in PBT, then rinsed twice in PBT, post fixed for 20 min in PBT plus 5% formaldehyde, and rinsed 5 X in PBT. To hybridize, the embryos were transferred to Eppendorf tubes and rinsed in a solution of 1:1 hybridization solution (50% deionized formamide; 5 X SSC, 100mg/ml denatured, sonicated, salmon sperm DNA; 100mg/ml tRNA from *E. coli*; 50mg/ml heparin; and 0.1% Tween 20); PBT and then rinsed in 100% hybridization solution. Prehybridization was performed for 2 h at 48°C.

Hybridization was done at 48°C overnight in a small volume (100 µl) with approximately 100ng/ml denatured probe. To wash off the excess probe, embryos were washed at 48°C for 20 min in hybridization solution, for 20 min in 50% hybridization solution, 50% PBT and 5 X for 20 min in PBT using a volume of 1 ml each time. The antibody-alkaline phosphatase conjugate was then added to the embryos and incubated overnight at 4°C. The antibody was preadsorbed against one volume of fixed embryos. The dilution added was 1:2000. The antibody was washed 4 X for 20 min in PBT, rinsed twice in a solution of 100mM NaCl, 50mM MgCl₂, 100mM Tris-HCl pH: 9.5, 1 mM Levamisol, and 0.1% Tween 20. Each wash was 1 ml. To develop the stain, 4.5 µl NBT-solution and 3.5 µl of X-Phosphate was added per ml of the last wash. The reaction was monitored until color developed. To stop the reaction, embryos were washed with PBT several times and then mounted for observation under the microscope.

In situ hybridization to imaginal discs was performed by everting larval heads in PBS (imaginal discs remained attached to the head) and transferring them to an Eppendorf tube containing 4% formaldehyde in PBS. Fixation was performed for 7 min at RT. The tissue was rinsed in 1:1 methanol: fixative (4% formaldehyde, 1% Triton X-100, 100mM PIPES pH: 7.0, 2mM MgSO₄, 1mM EGTA pH: 6.4), and washed twice in methanol for 5 min and then the embryo protocol above was followed without modification from the methanol rinse (methanol: PBT plus 5% formaldehyde) step. After staining, discs were dissected free of other tissue and examined.

III. RESULTS

III.A A search of cDNAs using the G45 genomic flanking region obtained by plasmid rescue

I screened for cDNAs using a genomic flanking region (FLR) as a probe. The purpose of this screen was to obtain a preliminary set of cDNAs as a starting point to find a transcript expressed under regeneration conditions. The G45 insertion line only reports expression in imaginal discs under regeneration conditions, but does report expression in the embryo. Therefore, an embryonic cDNA library was used for the search for cDNAs that might be later expressed in imaginal discs under regeneration conditions. The embryonic libraries we decided to use were made from 3 to 12 h and from 12 to 24 h embryo mRNA. This decision was based on the embryonic stage at which β -gal expression first appears, which is approximately stage 9. I screened approximately 70,000 plaques. I did four rounds of rescreening. The probe (FLR) was used to hybridize the two libraries mentioned above.

Fourteen putative positives were detected in the first screen. These were named G45-1 to G45-14. In the second rescreen only the plaques G45-1, 4, 6, 7, 8, 11, 12, and 14 showed signal. The other G45 putative positives were considered false positives and were not reprobed further. In the fourth screen all the positives detected in the second screen were still retained for further analysis. These positives differed in the intensity of the signal detected in the screen.

III.B Analysis of the cDNAs detected by the screen

III.B.1 Cross hybridization experiment

In order to analyze the size of the cDNAs, the phages were digested with EcoRI, which is the restriction enzyme used to construct the library. The sizes of the fragments were estimated from the gel and are given in Table III.1. Since some of the cDNAs produced fragments of the same size when digested with EcoRI, I tentatively concluded that some of them might be reisolates of the same primary clone.

To see whether they hybridized to one another and to FLR I did a cross hybridization experiment with these cDNAs. The probes for this experiment were prepared by recovering cDNA fragments from the gel after digesting the phage that contained the cDNA with EcoRI. This was done in order to make sure that most of the sequences came from the insert and to minimize contamination with the phage or other sequences. To analyze the cDNAs, the phage were digested with EcoRI, then blotted to a membrane by Southern transfer. Five replicates of the same blot were probed with

random primed-labeled cDNAs using radioactive ^{32}P -alpha dCTP. The five blots were probed with labeled cDNAs G45-7, G45-8, G45-11, G45-12 and G45-14 (Figure III.1 A, B, C, D, E respectively). cDNA G45-7 hybridizes to the 1.4 kbp band of G45-4 and G45-8, to G45-5 and G45-6 and to itself (Figure III.1A). cDNA G45-8 hybridizes to itself and to both bands of G45-4, consistent with the idea that they represent the same cDNA, and to G45-5, G45-6 and to the 1.2 kbp band of G45-7 (Figure III.1B). cDNA G45-11 hybridizes to G45-1 and G45-12 (Figure III.1C). cDNA G45-12 hybridizes to G45-1 and G45-11 (Figure III.1D). cDNA G45-14 hybridizes to G45-5 and G45-6 (Figure III.1C).

The five replicates were then stripped and probed with a second set of probes. In choosing the second probe for each stripped blot I avoided using a cDNA with a similar restriction pattern and size that might represent the same clone. For example, G45-5 and G45-6 showed a similar size (Table III.1). Consequently, if one blot was first probed with G45-5 cDNA, it was not reprobed with G45-6. This minimized the chances of picking up the same signals after stripping the blot. cDNA G45-1 showed hybridization to G45-11 and with G45-12 (Figure III.2 A). cDNA G45-4 hybridized to the same bands as did G45-8, supporting the hypothesis that these two cDNAs are identical (Figure III.2 B). cDNA G45-5 hybridized to G45-5, G45-6, and weakly to the large bands from G45-4, G45-8 and G45-7. It also showed a weak hybridization to G45-14 (Figure III.2 C). This blot was probed with G45-12 first. G45-14 must be genuine signal and not an old signal (notice arrow marking old signal from G45-12) since G45-12 does not hybridize to G45-14 (Figure III.1D).

The cDNA G45-6 probe hybridized to the same bands as G45-5. This is evidence that G45-5 and G45-6 may represent the same cDNAs. If so, the lack of signal at the position corresponding to the G45-12 band is a confirmation of the old signal in blot of Figure III.2 C. The flanking region (Figure III.2 E, F) was used as probe to confirm that the cDNAs had some degree of similarity to the genomic flanking DNA. Figure III.2 E shows the blot that had been probed with G45-8. The arrow-head and arrow mark the position of the 0.6 kbp bands produced by G45-4 and G45-8 EcoRI digestion. These bands are detected either because of the homology to the FLR probe or because of the remaining signal of the previous probe. A half-hour exposure of the same blot (Figure III.2 F) was done to see which bands are most intense. The strongest bands are G45-4 and G45-8 1.4 kbp, G45-5 and G45-6 and the largest band of G45-7. The weakest ones are G45-11, G45-12 and G45-14. The signal detected in the G45-1 band is extremely faint but visible above background. The intensity of this signal is consistent with the one seen in the initial screen of the cDNA library (Table III.1).

These results can be summarized as follows. First, the cDNAs fall into two groups that do not cross hybridize. One group comprises cDNAs G45-1, G45-11, and G45-12. The other group is composed of cDNAs G45-4, G45-5, G45-6, G45-7, G45-8, and G45-14. Second, based on their similarity in size, EcoRI site, and intensity of signal, G45-4 may be identical to G45-8, and G45-5 may be the same as G45-6. These two groups of cDNAs can be arranged in separate contigs that might represent different transcripts. Therefore, the flanking region may hybridize to two different transcripts.

Table III.1. cDNA's detected by the flanking region		
cDNA	Intensity of the signal.	Size of the fragment produced by EcoRI digestion of the cDNA (kbp)
G45 1	very weak	1.6
G45 4	strong	1.4 + 0.6
G45 5	strong	1.2
G45 6	strong	1.2
G45 7	strong	1.2 + 0.5
G45 8	strong	1.4 + 0.6
G45 11	weak	0.6
G45 12	weak	1.2
G45 14	weak	0.7

Cross Hybridization Experiment

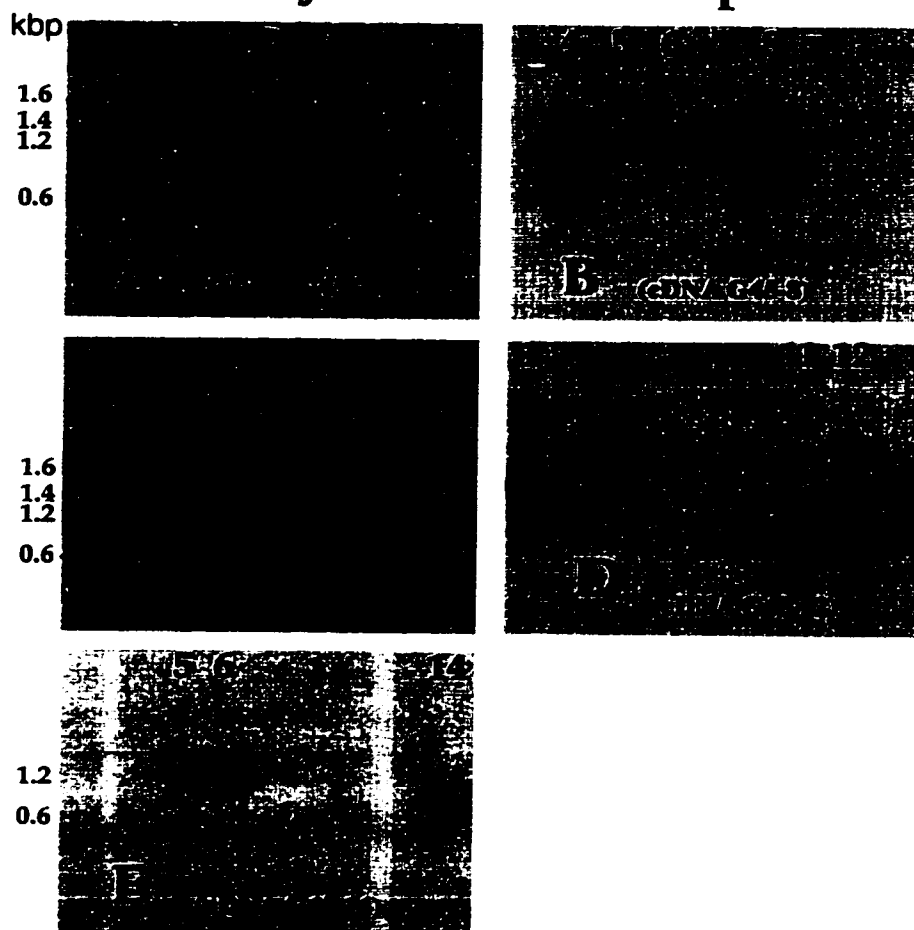


Figure III.1 Cross hybridization experiment I. Each blot contains DNA from the lambda cDNA clones isolated in the screen. In all the blots, lambda clones containing the insert of the cDNAs G45-1, 4, 5, 6, 7, 8, 11, 12, and 14 were digested with EcoRI to release the cDNAs separated by gel electrophoresis, stained with ethidium bromide to make sure that the visualized band of DNA corresponded to the expected size, then blotted to a membrane by Southern transfer and probed with radioactively labeled cDNAs (probes used are in brackets in the corresponding blot). After washing the probe at high stringency (Materials and Methods) filters were exposed for 1 h in a intensifying screen. Kilobase pairs are shown on the left side of A, C, and E and are aligned for B and D. Numbers on top of each blot represent cDNAs that had hybridization signals (see also text). DNA standards of known molecular size were loaded to the gel and transferred to the membrane but none of the bands was detected by the probes.

Cross Hybridization Experiment

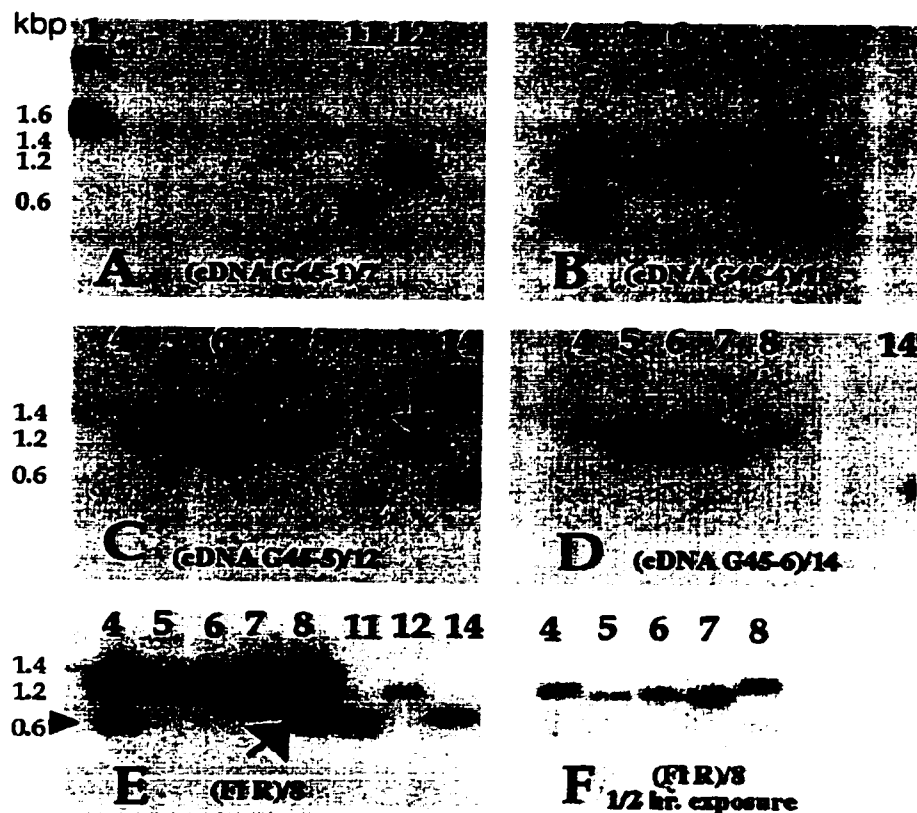


Figure III.2. Cross hybridization experiment II. These are the same blots used in Figure III.1 with a different set of probes from the cDNA screen. Blots were stripped and reprobed as in Figure III.1. Probes are indicated in brackets, previous probes used on the blots are after the "/" character. Arrows in C indicates old signal from cDNA G45-12. All the blots were exposed for 1 h except E, 24 hrs and F, 1/2 h. Arrows in E indicate probable signal probably from the previous blot, though a weak hybridization between the flanking region (FL R) and the two 0.6 kbp fragments cannot be ruled out.

III.B.2 Comparison between Embryonic cDNA and G45-lacZ expression

The next question I asked was whether either of these cDNA clones represented endogenous genes that were expressed in the appropriate embryonic pattern. To answer these questions I used G45-11 as a representative of one of the groups and G45-7 as one of the other group as probes in *in situ* hybridization experiments using wild type embryos. G45 embryos were first stained for β -gal expression as a control for the *in situ* experiments. G45 reported expression in bilaterally arranged single cells near the midline of each segment of the embryonic nervous system and the brain lobes (Figure III.3).

Based on the morphology of stained embryos, G45 is first expressed in this pattern at about stage 8 (3 hrs 45 min to 4 hrs 30 min) when germ band extension takes place. At this stage β -gal expression was seen on the dorsal and ventral sides in cells that are located along the midline (Figure III.3A). Expression is also detected in later stages around stage 13 (Figure III.3B). This stage is characterized by a complete retraction of the germ band, and the β -gal -expressing cells are seen only in the ventral part of the embryo. Only two cells are stained per segment in the midline in 13 segments, this corresponds to the three thoracic and ten abdominal segments. The latest stage β -gal is seen was stage 16 (Figure III.3D) identified by the epidermis showing signs of segmentation as shown by the folding of the edges. At this stage, expression was stronger in the brain lobes and in bilateral foci in each segment of the subesophageal ganglion.

To see whether either of the cDNAs would show a similar pattern of expression I did *in situ* hybridization on a 24-h embryo collection using G45-7 and G45-11 as probes. These probes were labeled with non-radioactive Dig-dUTP nucleotides. G45-7 hybridized in a pattern similar to the β -gal reporter gene expression in G45, but the pattern was incomplete. Only the midline bilateral cells of the CNS were stained. This probe did not detect any signal in the brain lobes (Figure III.4). The cDNA G45-11 probe showed the complementary pattern to G45-7 since only hybridization to the brain lobes was detected (Figure III.4). The embryos were staged according to morphological features as above and expression of the transcripts represented by the cDNAs. The embryos shown in Figure III.4. A, B. showed a condensation of the nervous system that is typical of a late stage. The embryo shown in Figure III.4 A is a stage 15 embryo because the nervous system is condensed, dorsal closure is complete but the gut is not seen as a convoluted tube.

III. B. 3 Comparison between imaginal disc cDNA hybridization pattern and G45-lacZ expression

The *in situ* hybridization of flanking sequence probes to imaginal discs had raised the possibility that the flanking region (FLR) might include exon sequences corresponding to two transcripts that would be transcribed in opposite directions. Also, the cross hybridization experiment shows that two groups of cDNAs are detected by FLR. This suggested a possible correspondence between the two putative transcripts and the two groups of cDNAs from the cross hybridization experiment.

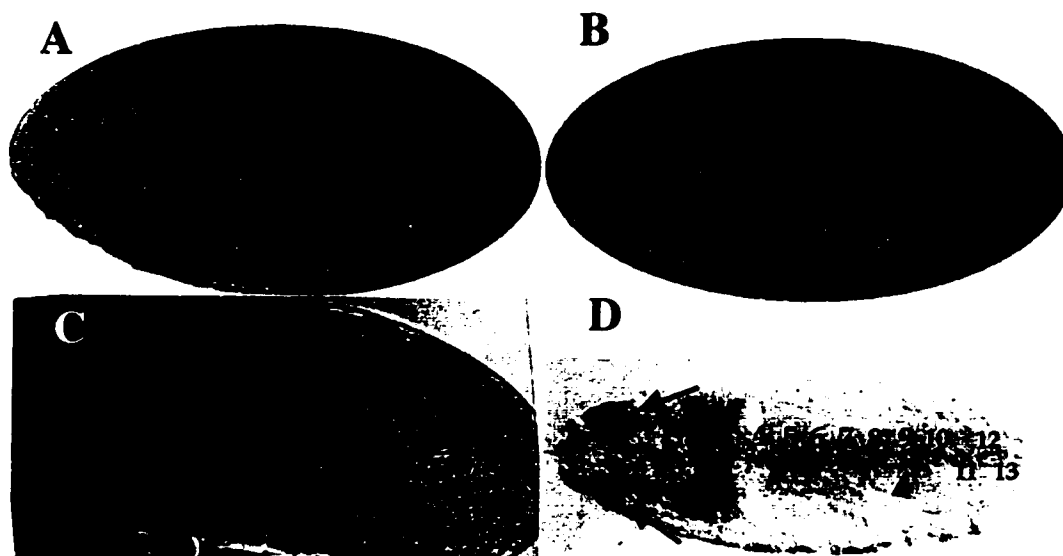


Figure III.3. G45 embryo β -gal expression. A, B, and D, ventral views. C is a ventrolateral view. Anterior is to the left. A. Stage 8 embryo. The arrows mark lacZ expression in the lateral cells. B. Stage 13 embryo, showing expression in pairs of cells in 13 segments. C. β -gal is restricted to the midline. Arrows in C mark the anterior and posterior limits of the segmental expression in the midline of the CNS. D. Stage 16 (approximately). The metameric divisions are visible on the lateral surface of the embryo. Arrows indicate expression in the brain lobes. Pairs of cells expressing β -gal in the midline are numbered 1-13, which coincides with the number of segments. The expression is mainly restricted to the midline as in the embryos shown in B and C. Notice the single cell in segment 9 showing β -gal expression (arrowhead). This variable pattern of staining was also observed in wild type embryos probed with cDNA G45-7.

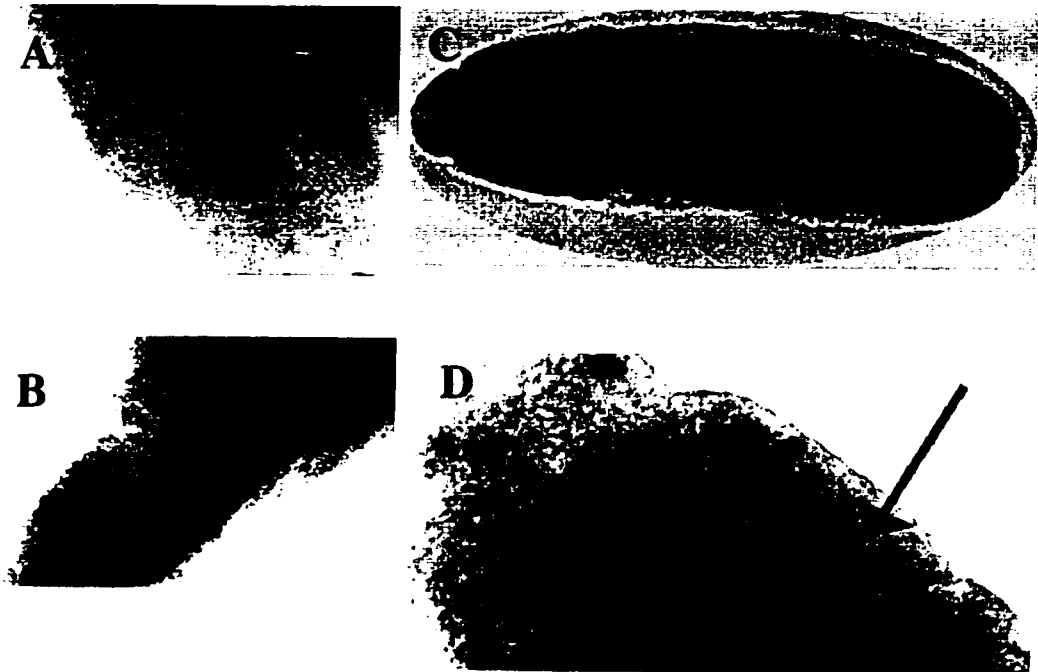


Figure III.4. Wild type embryos stained by *in situ* hybridization with non-radioactively labeled cDNA G45-7 (left). A. Wild type embryo at about stage 15 stained by *in situ* hybridization with non-radioactively labeled cDNA G45-7. B. Same staining as in A except the stage is 16, when the nervous system is more condensed. C. Dorsal view, anterior is to the left. Stage 14 embryo stained by *in situ* hybridization with non-radioactively labeled cDNA G45-11. D. Same as C. Hybridization was seen in late embryos in the brain lobes (arrows). Unlike cDNA G45-7 no hybridization was observed in the midline cells of the nervous system suggesting that G45-11 and G45-7 represent different transcripts.

To see how these two groups of cDNAs hybridized to third instar imaginal discs under regeneration conditions, I did *in situ* hybridization on imaginal discs from 29°C treated su(f)¹² third instar larvae using the same cDNAs as before. Flies of the y v f su(f) genotype were allowed to lay eggs at 22°C and the progeny were incubated at the same temperature until the larvae reached third instar. Then they were cultured at 29°C for 48 h followed by a 24 h. recovery at 22°C (Russell, 1974). Then the larvae were processed for *in situ* hybridization. The probes used were the same as in the embryo *in situ* experiment. G45-7 detected a signal posterior to the morphogenetic furrow in the third instar eye-antenna imaginal disc, but no signal was evident in any of the other discs in the same experiment (Figure III.5). G45-11 detected a signal in all imaginal discs Figure III.5. No specific pattern was seen, indicating a general expression of the homologous gene. Controls showed a weak staining in a general pattern. These results are similar to those reported by W. Brook (1994) using the G45 flanking sequences T₇ and T₃ single strand probes respectively (Table III.2).

The similarity between the T₇ single strand probe and the G45-7 cDNA signals suggests that the flanking region contains exon sequences from a gene transcribed in the midline of the CNS in the embryo and in differentiating ommatidia which may be the template for G45-7 cDNA. This gene is not differentially transcribed in regenerating discs. The similarity of the T₃ single strand probe and G45-11 signals is evidence of exon sequence shared between the genomic DNA flanking the insertion of the P-element and the gene for the G45-11 cDNA. This gene may be the one induced in a general pattern in imaginal discs under regeneration conditions. Further evidence for such a gene is its embryonic expression in the head region (brain lobes) in embryos. The G45 enhancer-trap appears to report the embryonic expression of both these genes.

To confirm that the two cDNA contigs included at least some exonic sequence in the flanking region I probed a Southern blot that contained phage DNA plus genomic DNA insert. These phage were originally isolated by screening a genomic library in lambda EMBL4 using the flanking genomic region of 2.3 kbp as probe (Brook, 1994). DNA was isolated from lysates of these phages, digested with several restriction enzymes and blotted by Southern transfer and probed with the rescued FLR that maps to 100E (Brook, 1994). I grew two of them, named λ7 and λ9 by W. Brook, restricted with HindIII and EcoRI, then blotted by Southern transfer and probed with cDNA G45-7 and G45-11. The results (Figure III.6) suggested that cDNA G45-7 maps at or near the location 100E because the restriction pattern detected with the flanking region as a probe (Brook, 1994) was the same as the one detected using G45-7 as a probe. However, no hybridization was detected using G45-11 as a probe. The flanking region has been shown to map to a unique site at 100E by *in situ* hybridization to polytene chromosomes (Brook, 1994). Therefore, it seemed very likely that the genomic and G45-7 clones identified with strong hybridization to it all come from the same cytological location. However, subsequent sequencing data showed these conclusions to be incorrect, probably due to a cloning artifact.

Table III.2 Comparison between T3, T7, single strand probes, G45-7 and G45-11 cDNAs signals in heat-treated su(f) third instar larvae imaginal discs.

T3 single strand probe	T7 single strand probe	G45-7 cDNA probe	G45-11 cDNA probe
Staining in all discs (general expression)	Staining in eye-antenna imaginal discs, posterior to the morphogenetic furrow	Staining in eye-antenna imaginal discs, posterior to the morphogenetic furrow.	Staining in all discs (general expression)

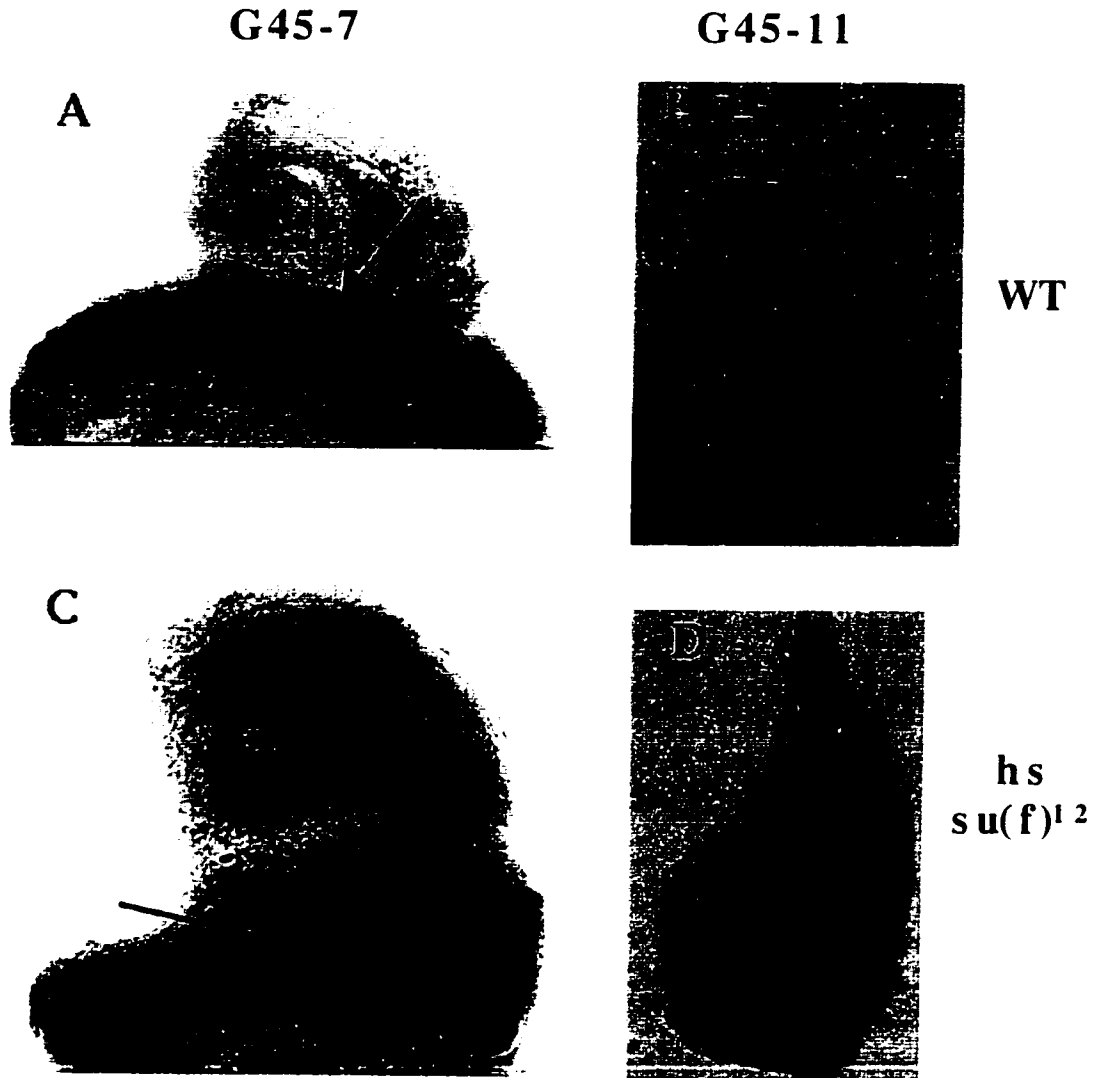


Figure III.5. cDNA G45-7 and G45-11 hybridization pattern in wild type and heat-treated $su(f)^{12}$ imaginal discs. A and B are control discs. C and D are $su(f)^{12}$ heat-treated discs to induce death. A. Canton-S control discs hybridized with G45-7 probe. Hybridization was only seen in the eye antenna imaginal disc behind the morphogenetic furrow (arrow). B. Canton-S control leg disc hybridized with G45-11 probe. C. Heat-treated $su(f)^{12}$ eye-antenna disc hybridized with G45-7. The same pattern as in A is detected only in eye antenna imaginal disc after cell death. A similar pattern was also observed when T_7 single strand probes were synthesized with the FLR as a template (Brook, 1994). D. Heat-treated $su(f)^{12}$ leg imaginal disc hybridized with G45-11. General staining was observed in all discs.

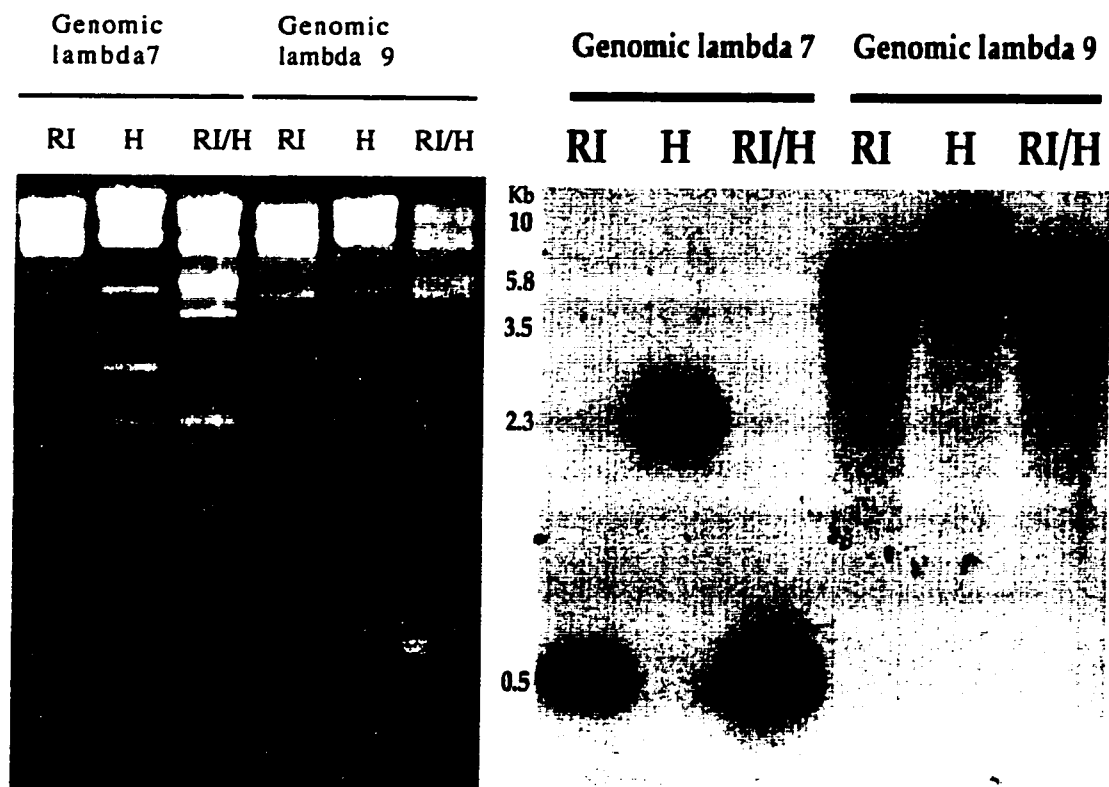


Figure III.6. Genomic lambda clones from a EMBL4 library isolated in a screen using the rescued genomic flanking region as a probe. Lambda phage containing genomic inserts were digested as indicated (RI: EcoRI, H: Hind III), separated by 1% agarose gel electrophoresis, and stained with ethidium bromide (shown on the left picture) blotted to a filter membrane and probed with radioactively labeled cDNA G45-7 (shown on the right picture). The same pattern of hybridization was detected when the flanking region was used as a probe. This blot was stripped and reprobed using the cDNA G45-11, and no hybridization was detected.

III.B.4 A caveat

Several pieces of evidence are against the conclusion that two genes are represented by the genomic flanking region. Firstly, G45-11 did not hybridize to the blot shown in Figure III.6, and attempts to map cDNAs G45-7 and G45-11 to polytene chromosome of the salivary of third larval instar did not show any signal at 100E. Secondly, the genomic flanking region was partially sequenced from both ends. The terminal 50 bp at the T₇ promoter end was identical to part of a Sequence Tagged Site (STS) of 229 bp in length. This STS is part of a cosmid mapped by the European Drosophila Genome Project (EDGP) to the X chromosome (Madueño et al., 1995; cosmid clone 65F1, EMBL nucleic acid sequence database, accession number Z32239). Thirdly, G45-7 was sequenced and compared to the genomic flanking region and the STS from the clone DM65F1T. Sequence similarity was found among the three (Figure III.7). Finally, a Southern blot containing genomic DNA from flies of the genotypes PZG45/PZG45 and PZG45/ Δ 53 digested with EcoRI was probed with the G45-7 1.2 kbp fragment but failed to hybridize differentially (see below). This indicates that G45-7 is probably not within the region deleted by Δ 53. An alternative explanation would be that the sensitivity of the experiment was not enough to discriminate between one or two copies of the G45-7, or the part of the cDNA used as probe is not deleted in Δ 53.

To summarize, several lines of evidence indicated that the FLR might contain chimeric sequences. Firstly, the failure to map cDNAs G45-7 and G45-11 to the site of insertion at 100E by *in situ* to polytene chromosomes. Secondly, a sequence tagged site (STS) of 229 bp, which is part of the cosmid 65F1 that maps to the X chromosome (Madueño, 1995; cosmid clone 65F1, EMBL nucleic acid sequence database, accession number Z32239), was also found in the cDNA G45-7 and in the FLR (Figure III.7). This suggested that at least part of the FLR contains sequence not from 100E.

To confirm that the FLR is chimeric I decided to do a Southern blot experiment using the cosmid 65F1 as well as three overlapping cosmids that were previously mapped to 100E (cosmid clones are shown in Figure III.8), (Sیدن-Kiamos et al., 1990). The cosmids were digested with HindIII, separated on an agarose gel and transferred to a membrane by Southern transfer. As positive controls, cDNA G45-7 and the FLR were also included. The membrane was probed with radioactively labeled FLR DNA fragment to see whether it would hybridize to the cosmids from 100E or to both cosmids from 100E and chromosome X. Exposure for 20 min showed a very intense signal suggesting that the three cosmids from 100E contained most of the sequence from FLR. However, a faint band is clearly seen in lane 4 that correspond to the STS DM65F1T. This adds evidence in favor of a chimeric hypothesis and suggests that the FLR hybridizes to a secondary site (on chromosome X) not shown by the *in situ* hybridization to polytene chromosomes in previous work (Brook, 1994). Longer exposure permitted the visualization of a darker band from the digestion of cosmid 65F1 at the position of the faint band when exposed for 20 min (not shown) which confirms the existence of a genuine hybridization signal that with all likelihood correspond the STS DM65F1T, which is part of the cosmid clone 65F1.

To further analyze the relationship between the cDNAs and the cosmids I did a second hybridization experiment with the blots previously used in the cross hybridization experiment. Here I labeled the entire three cosmids from 100E and from the X chromosome (Figure III.9). Only hybridization with cosmid 65F1 was obtained after a 72-h exposure. This hybridization signal was seen with the 1.2 kbp fragment of cDNA G45-7 and with G45-5 and G45-6. None of the other cDNAs gave a signal with any of the probes. This result added more evidence that the FLR is chimeric since the cDNAs obtained by screening with these probe do not map to 100E. To confirm that G45-7 and G45-11 did not have overlap to cosmids from 100E that had hybridized strongly to the FLR (129G12 and 12C5 in Figure III.9) I did a third hybridization experiment.

Cosmids 129G12 and 12C5 were digested with HindIII or EcoRI, separated on agarose gels and transferred to a membrane by Southern transfer. A digest of the FLR and EcoRI digested λ 7 and λ 9 clones (Figure III.6) were included as positive controls. G45-7 detected no hybridization to the cosmids but it did to FLR and λ 7 and λ 9 clones (Figure III.10). Finally, DNA from λ clones 7, 9, from cosmid clones 12C5 and 129G12 was digested and transferred to a membrane. As a positive control I used the FLR DNA. G45-11 was labeled as before and hybridized to the blot. The probe did not hybridize either to the cosmids or to the λ 7 and λ 9 clones but it did to FLR (Figure III.11). This result added evidence that G45-11 also may not map to 100E.

These experiments suggested that the FLR had a chimeric structure and so it might have picked up cDNA clones from secondary sites in the genome in the library screen. The compelling evidence that the FLR hybridized to a HindIII fragment of about 4.1 kbp from the cosmid 12C5 and to G45-7 (Figure III.8) while G45-7 did not hybridize to any band in the 12C5 HindIII digest (Figure III.10) indicates that G45-7 may not have any relationship to the part of the FLR that maps to 100E. Indeed, the fact that the X-chromosome STS sequence is contained in G45-7 is evidence that this cDNA may come from the X chromosome, along with the portion of FLR that cross-hybridizes with the STS.

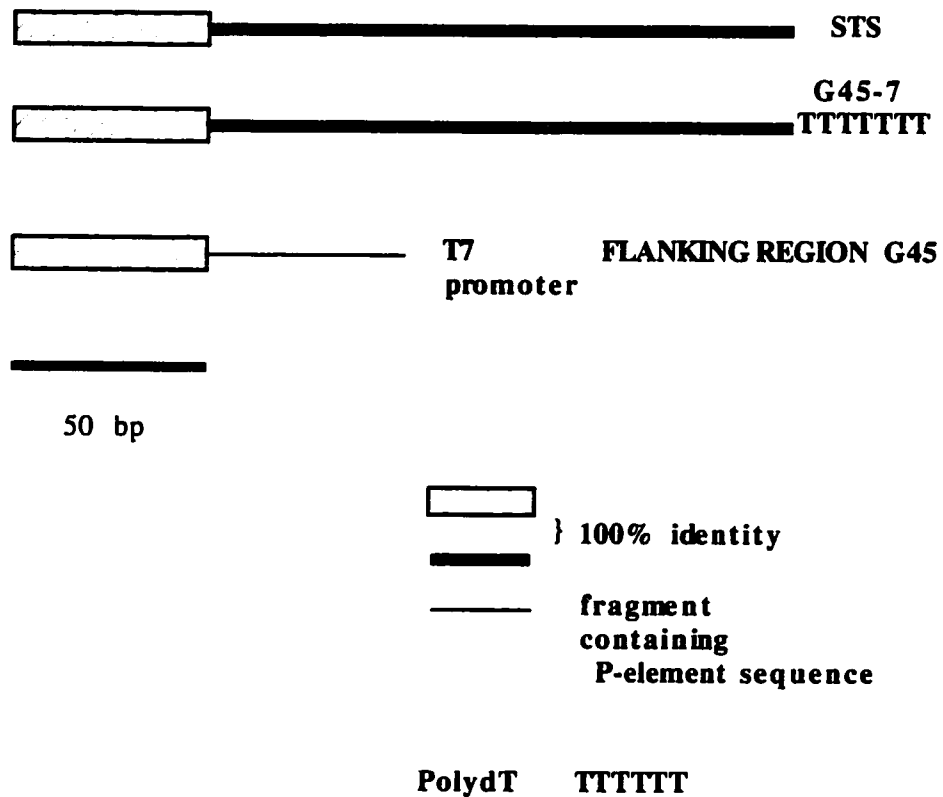


Figure III.7. Schematic representation of sequence relationship between the STS from the cosmid 65F1, the FLR and the cDNA G45-7. A partial sequence obtained from polydT end of cDNA G45-7 (200 bp) was found to have 100% identity to a sequenced STS of 229 bp (DM65F1T) reported by the EDPG (Madueño et al., 1995), included in a cosmid mapped to the chromosome X. Partial sequence from the T₇ promoter of the FLR which had been subcloned in pBS SK⁻ showed a 50 bp sequence that is common to the STS, and to G45-7.

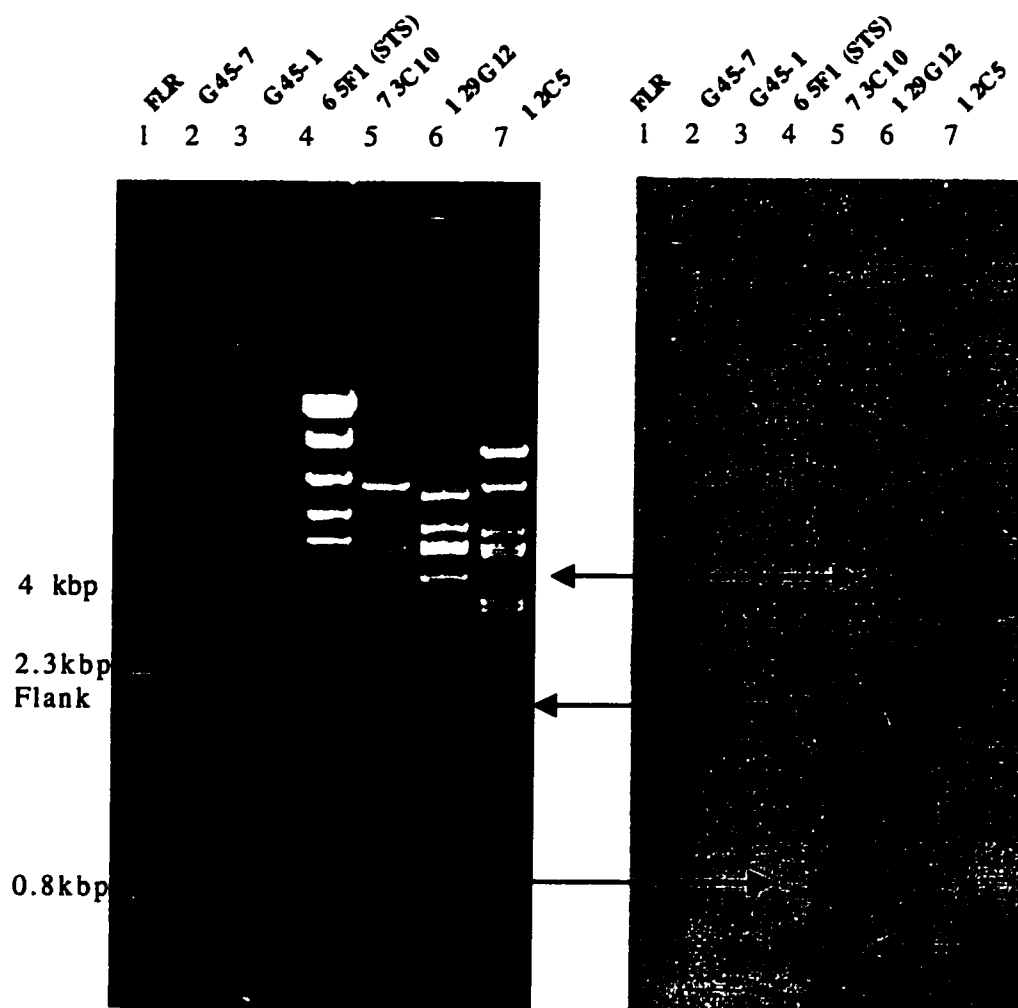


Figure III.8 The 2.3 kbp genomic flanking region (FLR) is chimeric. Lane numbers are on top of the figures. Cosmids were digested with HindIII, separated on 1% agarose gel by electrophoresis, stained with ethidium bromide (A), transferred to a filter membrane by Southern transfer, and probed with radioactively labeled FLR; washed as described in Materials and Methods and exposed for 20 min (B). Lane 1: FLR (positive control). Lane 2: cDNA G45-7 (1.2 kbp fragment). Lane 3: cDNA G45-1. Lane 4: 1 μ g of cosmid 65F1 (containing STS DM65F1T). Lane 5: 1 μ g of cosmid 73E10 (100E). Lane 6: 1 μ g of cosmid 129G12 (100E). Lane 7: 1 μ g of cosmid 12C5 (100E). B. Cosmids 73E10, 129G12, and 12C5 contain a single band of 0.8 kbp, 1.8 kbp, and 4.1 kbp respectively, showing that the FLR is included in these cosmids, and confirming the hypothesis that FLR maps to 100E. Cosmid 65F1 (chromosome X) showed a faint band of approximately 0.5 kbp (single head arrow). This signal was comparable to the signal of G45-7 in this blot when exposed for 2 h.

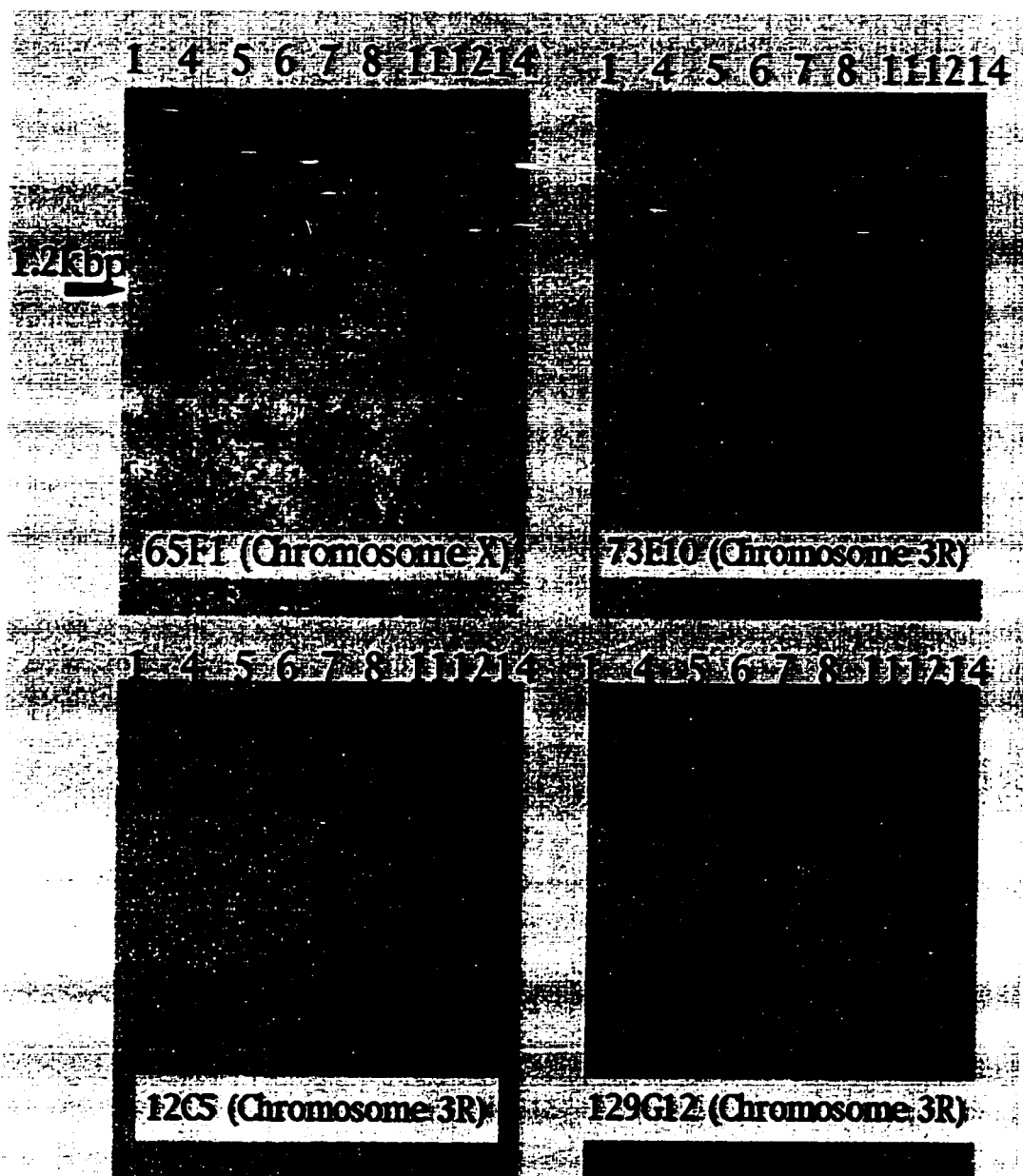


Figure III.9 cDNAs G45-5, 6, and 7 hybridize to a cosmid that maps to the X chromosome. Blots shown in this figure were also used in the cross hybridization experiment. All the blots are repeats containing cDNAs 1-14 from the screen, as indicated by the numbers on top of each blot. Templates for the probes were the cosmids obtained from the EDGP consortium, which are shown at the bottom of each blot. Chromosome location for each of the cosmids is indicated in brackets. Only cosmid 65F1 hybridized to cDNAs G45-5, 6, and 7 (1.2 kbp band). Blots were exposed for 72 h. Clone 65F1 includes the STS also found in cDNA G45-7.

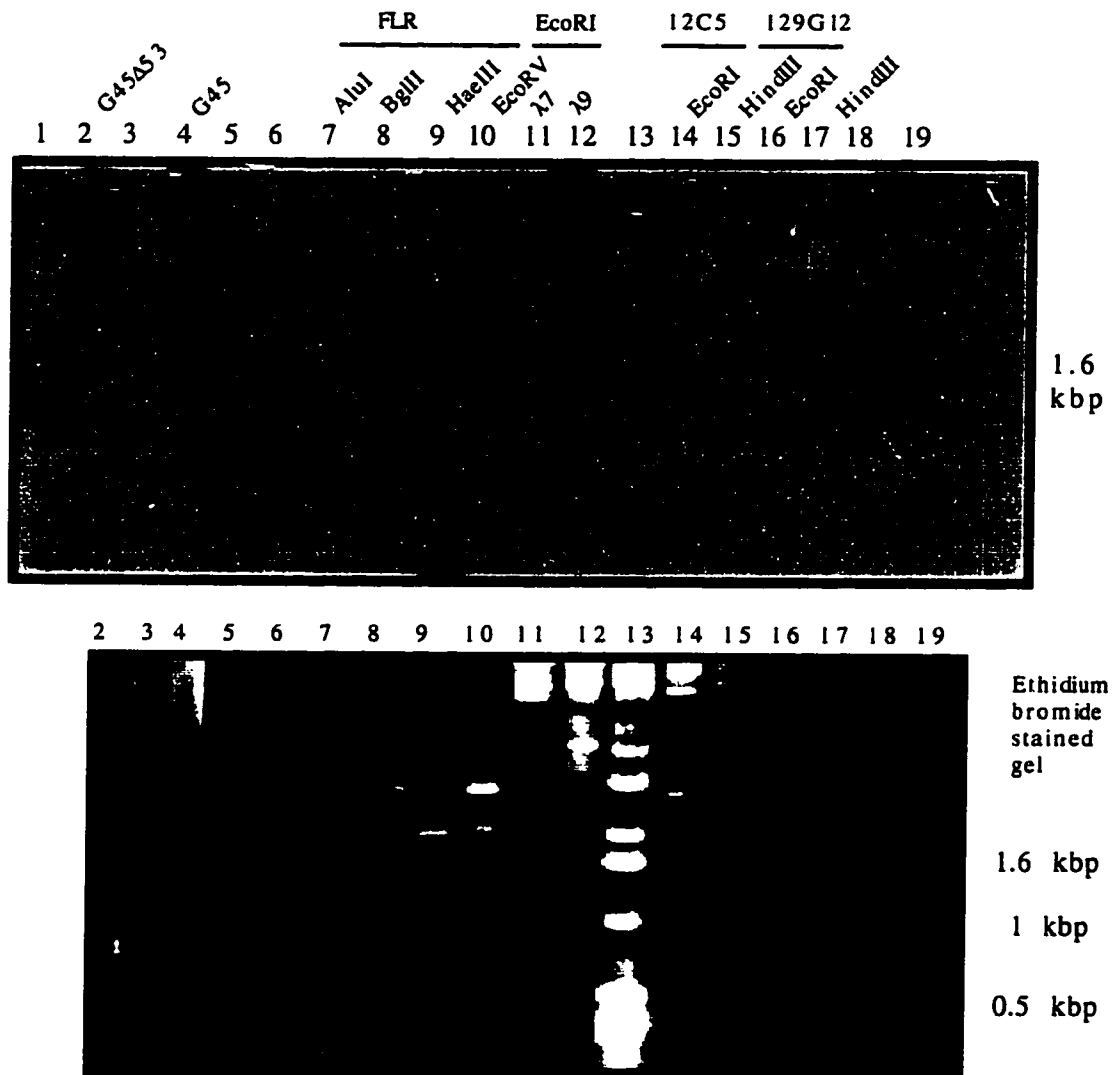


Figure III.10 cDNA G45-7 does not map to 100E. Digested DNA was run on 1% agarose gel electrophoresis, then stained with ethidium bromide (bottom picture). Digested DNA was transferred to a filter membrane by Southern transfer, which was hybridized to a labeled G45-7 probe, washed according to Materials and Methods, and exposed for 2 1/2 h. Lane numbers are shown on top of the figures. Lanes 3, 5, 6, and 18 were not loaded. Lanes 1, 13, and 19: 1 kbp ladder (BRL). Lane 2: 15 μ g of genomic DNA from flies genotypically G45/ Δ 53 digested with EcoRI. Lane 4: 15 μ g of genomic DNA from flies genotypically G45/G45 digested with EcoRI. Lanes 7, 8, 9, 10: (positive control) 1 μ g of pBluecript SK⁻, which contains the FLR insert in the HindIII single cloning site, was digested with HindIII and AluI; HindIII and BglII; HindIII and HaeIII; and HindIII and EcoRV respectively. Lane 11 and 12: 1 μ g of lambda EMBL4 clone 7 and 9 respectively, digested with EcoRI. Lane 14: 1 μ g of cosmid 12C5 and (100E) digested with EcoRI. Lane 15: same as lane 14 but digested with HindIII. Lane 16: 1 μ g of cosmid 129G12 digested with EcoRI. Lane 17: same as lane 16 but digested with HindIII. The probe did not detect any band in the cosmid digestions, but it did detect a band from the FLR digest, and the lambda clones.

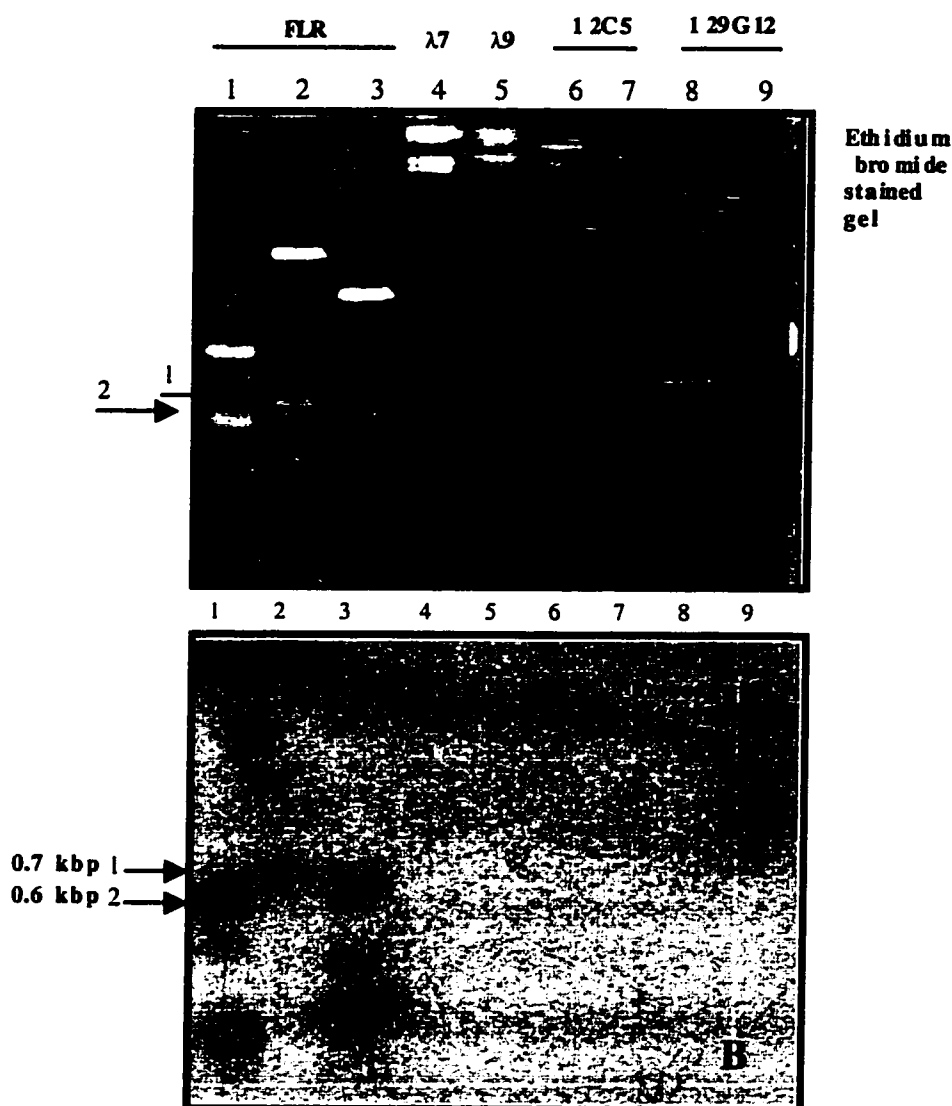


Figure III.11 cDNA G45-11 does not map to 100E. Digested DNA was separated on 1% agarose gel electrophoresis, stained with ethidium bromide (A). Digested DNA was transferred to a filter membrane by Southern transfer, which was hybridized to labeled G45-11, washed according to Materials and Methods, and exposed for 21 h (B). Lane numbers for both figures are shown on top of the figure A. Lanes 1, 2, and 3: (positive control) 1 μ g of pBluecript SK which contains the FLR insert in the HindIII single cloning site, double digests with HindIII and AluI, HindIII and BglII, and HindIII and HaeIII respectively. Lane 4 and 5: 1 μ g of lambda EMBL4 clone 7 and 9 respectively, digested with EcoRI. Lane 6: 1 μ g of cosmid 12C5 (100E) digested with EcoRI. Lane 7: same as lane 6 but digested with HindIII. Lane 8: 1 μ g of Cosmid 129G12 digested with EcoRI. Lane 9: same as lane 8 but digested with HindIII. The probe did not detect any band in the cosmid digestion, but it did detect two bands (arrow number 1 and 2 mark the position of the bands of approximately 0.6 and 0.7 kbp) from the FLR digest, lambda clones were not detected, suggesting that G45-11 is not related to the contig that contains G45-7.

III. C Clonal analysis with a G-45 deletion line generated by imprecise excision of the P-element

To test the hypothesis that a gene involved in patterning is located at the insertion site 100E, which is the site where the P-element maps in G45, I generated homozygous clones of mutant cells using one of the imprecise excision derivatives of G45, $\Delta 53$. I used this line because the original G45 insertion line has a wild type phenotype and so homozygous clones are not expected to cause any phenotypic effects. Because $\Delta 53$ is an embryonic lethal line (homozygous mutants die as embryos) it was necessary to induce homozygous mutant clones in the larval stage.

Analysis of changes in gene expression in imaginal discs was not done since I did not know what gene could be affected. Instead, if a mutant clone affects cell fates in imaginal discs, re-specification of cell fates can be seen as changes in the pattern of adult structures derived from imaginal discs. These changes are expected to correlate with the presence of marked clones. Since the conditions of the original screen were selected so that genes affecting patterning could be identified I expected phenotypic changes in the pattern of the adult structures such as wing, legs, eye ommatidia and thorax.

If a gene in $\Delta 53$ is involved in the specification of compartmental cell fates (e.g. a selector gene), changes such as posterior-to-anterior or dorsal-to-ventral in a cell-autonomous way are expected. If, instead, the role of the gene in $\Delta 53$ is repression or activation of patterning genes acting downstream of compartment specification genes (e.g. *wg*, *Notch (N)*), then changes such as ectopic formation or absence of normal cuticular structures are expected. In the latter case, either a non-autonomous or autonomous effect is possible.

I constructed 5 recombinant lines for this study which could be used to make genetically marked clones homozygous for the deletion (Table II.2). These were derivatives of the lines carrying an hsFLP cassette on the X chromosome, an FRT cassette and a series of markers on the right arm of the third chromosome (Xu and Rubin, 1993) and the deficiency line G45 $\Delta 53$ generated in this lab. A complete description of the construction of these lines is presented in Materials and Methods.

III.C.1 Results of the first clonal analysis experiment

This experiment was set up so to obtain $\Delta 53$ clones marked with yellow *Sb* and white, along with twin clones marked with *Sb*⁺. The method was to construct flies that had the hsFLP construct in the first chromosome, and were homozygotes for P[ry⁺; hs-neo FRT] cassette at the cytological position 82B, and heterozygotes for P[mini-w⁺; hs- π M]87E *Sb*^{63b} G45 $\Delta 53$, and P[ry⁺; y⁺] cassette. This genotype permits the expression of the Flip recombinase enzyme to induce mitotic clones in the first instar larvae.

A control cross was made without the $\Delta 53$ but with the same gratuitous markers, which are described in Figure III.12A and Figure III.12B. Larvae were heat-shocked at first instar to induce the expression of the hsFLP, and thus produce mitotic clones. The resulting adult females and males with orange eyes, Sb and yellow⁺ (target class of progeny) were scored for the presence of marked clones to make sure that the mitotic clones were effectively produced (red ommatidia, Sb/Sb yellow bristles; white ommatidia, (Sb⁺ yellow⁺). In the experimental cross (Figure III.13) I screened for abnormalities on cuticular structures derived from imaginal discs (i.e. legs, wings, notum, head capsule, ommatidia, palp and ocelli) in more than 50 flies of the target class and from the internal controls. No abnormalities were found in the controls except for the presence of wing blisters in the w⁺ Sb^{63b} G45 Δ 53 /TM3, Sb progeny. These blisters were seen at a frequency of only 3% (3/98 flies). Other phenotypic effects were found in flies of the target class Sb^{63b} G45 Δ 53/ y⁺ in the head, thorax and wings. No abnormalities were observed in legs or abdomen.

Abnormalities in the head were observed in the eyes, ocellar region and palpus organ. Δ 53 eye clones marked with two doses of w⁺ (red ommatidia) were seen in 16/60 eyes scored (27%). In most cases, red clones were accompanied by a white twin clone. In 11/16 cases (69%), the red clones showed a disorganized arrangement of ommatidia as compared to the white twin clones, which did not show any evidence of such a phenotype. The red G45 Δ 53 clones were generally smaller than neighboring wild type twin clones (white ommatidia). Examples of these clones are shown in Figure III.14. Not all of the mutant clones (red clones) showed disorganized ommatidia (i.e. 5/16 eyes were apparently normal).

Because disorganized ommatidia are sometimes seen at a low frequency in wild type lines I examined the frequency of this phenotype elsewhere in the 60 eyes of the target class. Disorganized ommatidia were found in 13/60 eyes. However, in 11/13 eyes (80%) the disorganized ommatidia were found in association with marked red ommatidia, while only 20% (2/13 eyes) showed disorganized ommatidia not associated with the red pigment. If the 60 eyes are considered, then 3% of the eyes (2/60 eyes) have unmarked disorganized ommatidia.

To see if this phenotypic effect was also found in other genotypes or if it was part of the phenotype associated with the clones that carried the deficiency chromosome, I recorded the frequency of disorganized ommatidia in flies of the genotypes listed in Table III.3. These are y w; P[ry⁺; hs-neo; FRT]82B G45 Δ 53 /TM6B, Hu; G45PZ/ G45PZ; Oregon R and the control lines (Figure III.12A, Figure III.12B) y w; P[ry⁺; hs-neo; FRT]82B, P[mini-w⁺; hs- π M]87E, Sb^{63b}/ P[ry⁺; hs-neo; FRT]82B P[ry⁺; y⁺] after heat-shock for 1 h at 38°C first instar. Table III.3, shows the frequency of eyes with disorganized ommatidia in these various genotypes.

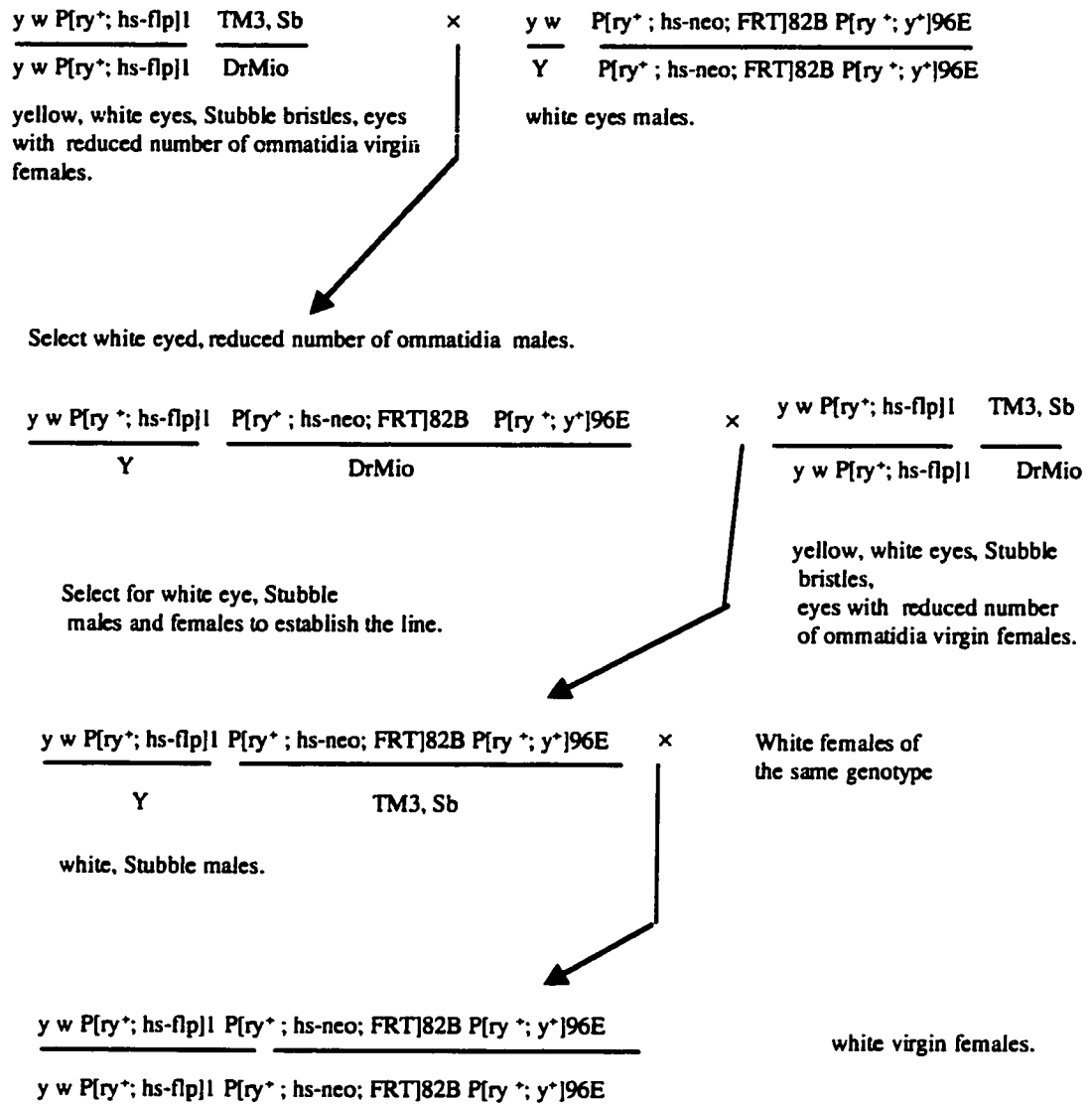


Figure III.12A. Crossing scheme used to generate control clones for the first and second clonal analysis experiments

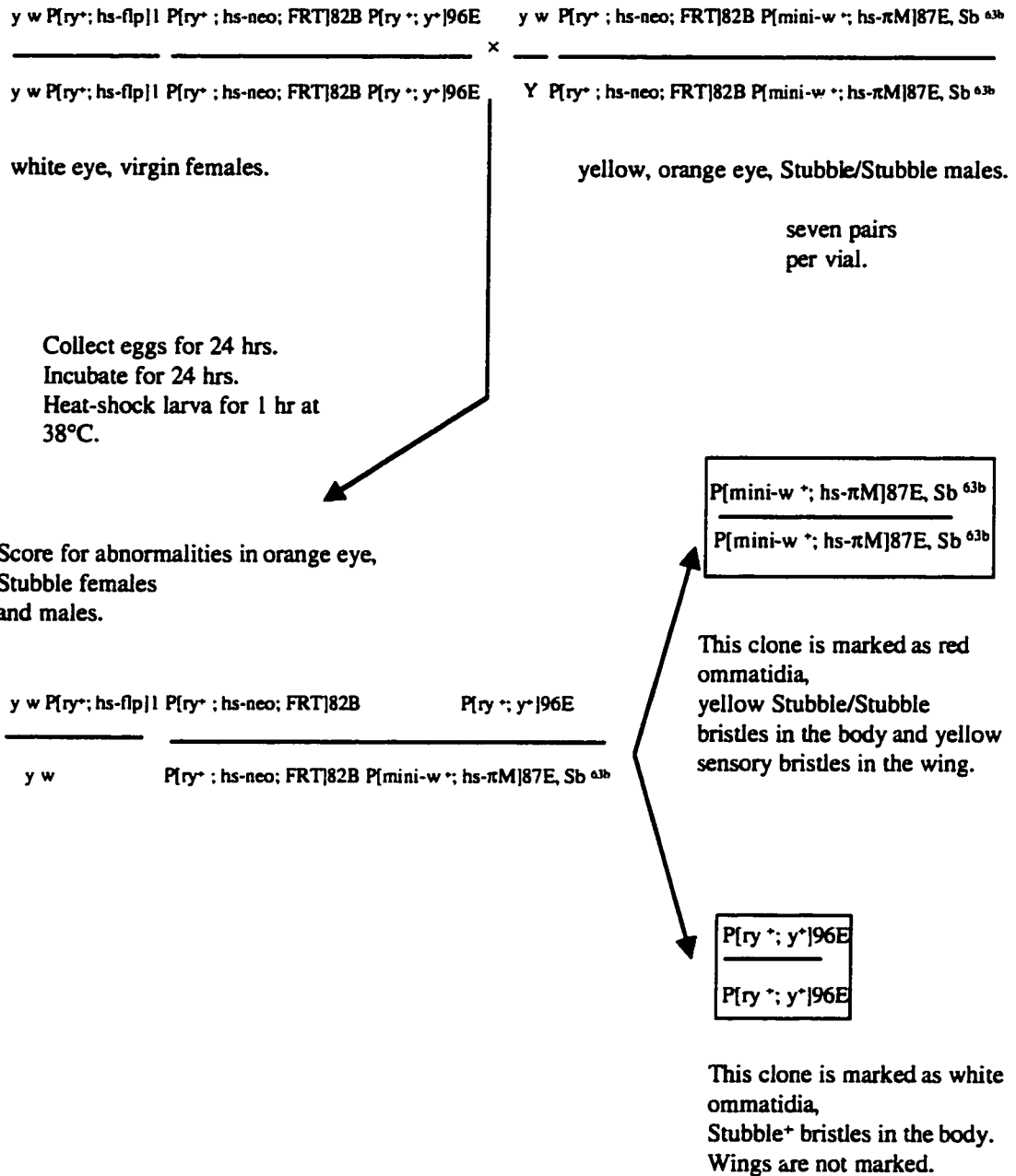


Figure III.12B. Crossing scheme used to generate control clones for the first and second clonal analysis experiments

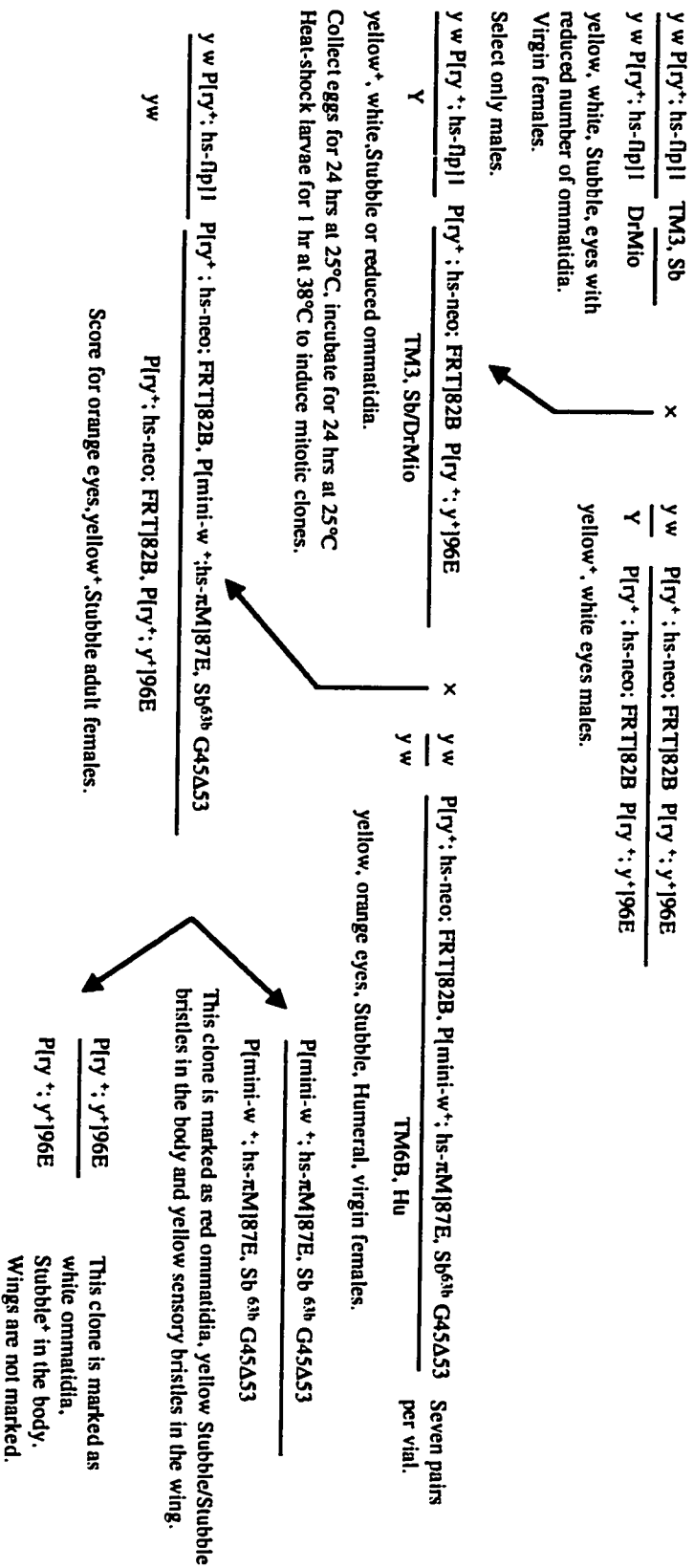


Figure III.13 Crossing scheme used to generate clones in the first clonal analysis experiment. The males were crossed to females from line 4 (Table II.2). The flies were allowed to lay eggs for 24 h at 25°C, parents were removed and embryos incubated for 24 h and larvae were heat-shocked for 1 h at 38°C to activate the expression of the Flp recombinase enzyme in the first larval instar. Mitotic clones would be induced only in the yellow⁺, Sb, orange eyed females, which carried both FRT chromosomes and one copy of the P[ry⁺; hs-FLP1] construct. The other classes of flies in this cross provide an internal control for any effects that might be caused by the heat-shock treatment.

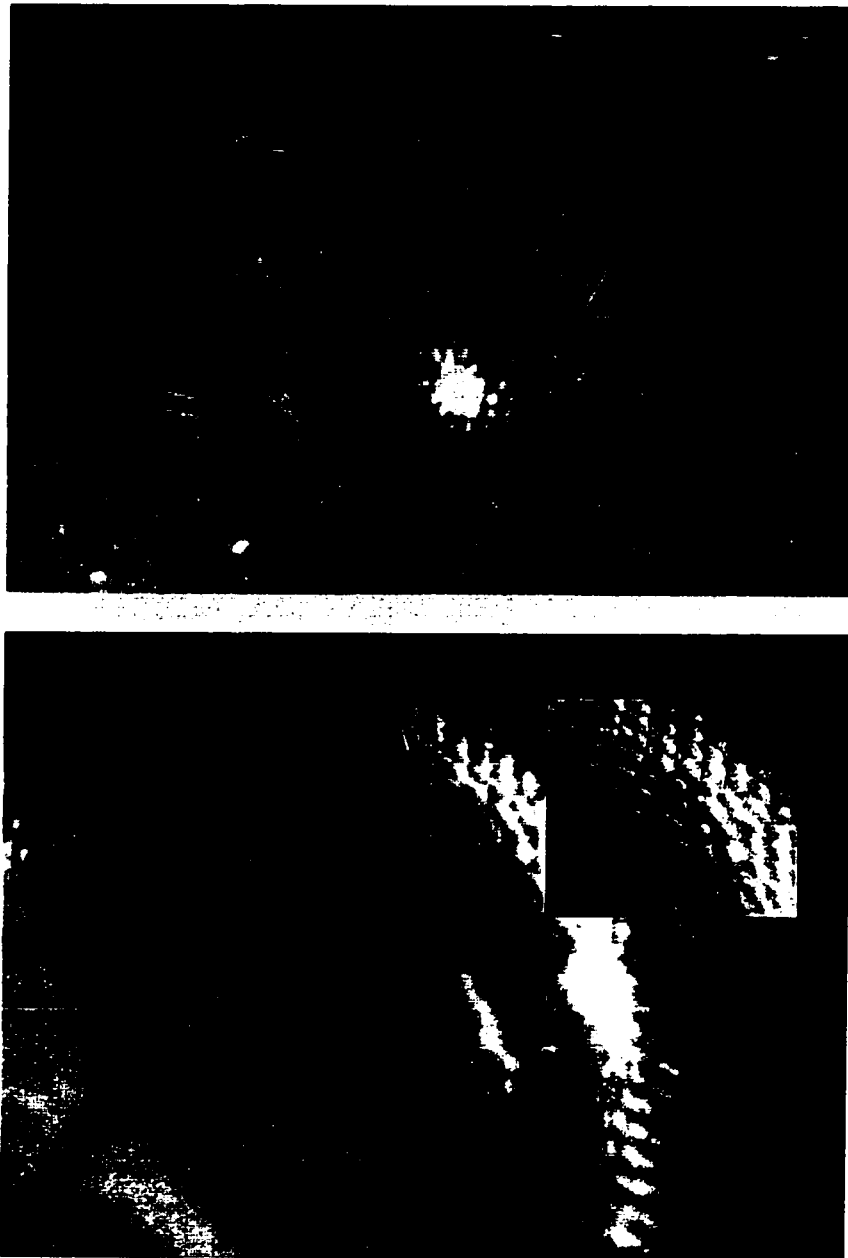


Figure III.14. Eye abnormality of an orange-eyed fly of the first clonal analysis experiment (Figure III.13) genotypically $y\ w\ P[ry^+ \text{hs-FLP}]/y\ w; P[ry^+ \text{hs-neo FRT}]82B\ P[\text{mini-}w^+ \text{hsPiM}]87E\ Sb^{63b}\ G45\Delta53/P[ry^+ \text{hs-neo FRT}]82B\ P[ry^+;y^+]96E$. Top picture. Left arrow indicates the position of the red ommatidia (mutant clone). Top and right arrows indicate the position of two twin clones. Note the white twin clone is much larger than the red $\Delta53$ clone. Bottom picture. Arrow points to the position of a clone marked with red ommatidia that shows the disorganized phenotype.

Table III.3. Frequency of disorganized ommatidia in different genotypes		
Genotype	Frequency of unmarked disorganized ommatidia	Heat-shocked at 38°C for 1 h in first or second instar.
y w ; P[ry ⁺ ; hs-neo; FRT]82B G45Δ53/TM6B Hu	5%, (16/314 eyes)	No
G45PZ/ G45PZ	12% (27/210 eyes)	No
Oregon R	9.6% (5/52 eyes)	No
y w/hsFLP; P[ry ⁺ ; hs-neo; FRT]82B, P[mini-w ⁺ ; hs-πM]87E, Sb ^{63b} / P[ry ⁺ ; hs-neo; FRT]82B P[ry ⁺ ; y ⁺]	2.2% (2/90 eyes)	Yes
y w/hsFLP; P[ry ⁺ ; hs-neo; FRT]82B, P[mini-w ⁺ ; hs-πM]87E, Sb ^{63b} G45Δ53/ P[ry ⁺ ; hs-neo; FRT]82B P[ry ⁺ ; y ⁺]	3% (2/60 eyes)	Yes

These results showed that disorganized ommatidia do occur at a low frequency in wild type flies and flies that do not carry $\Delta 53$ homozygous clones. However, the high frequency (80%, 11 marked/13 disorganized) of disorganized ommatidia in marked clones in the target class compared to the low frequency of not marked disorganized ommatidia in the same flies (20%, 2 unmarked/13 disorganized) suggests that $\Delta 53$ homozygous clones cause disorganized ommatidia at a much higher frequency. This is also supported by the fact that twin clones are always smaller than the mutant clones. Thus, the presence of disorganized ommatidia in marked clones in the target class cannot be explained by chance and is an effect of the $\Delta 53$ mutation.

Ocellar abnormalities observed in the heat-treated target class involved a reduced size, or absence of one of the lateral ocelli (Figure III.15). The frequency for this effect was 2 out of 30 flies. In both these cases, some of the neighboring microchaetae were also missing, and there were marked mutant (y Sb) and wild type twin (y^+ Sb⁺) bristles nearby (Figure III.15). However, the frequency of heads with one or more marked bristles in all heads, including normal ones, was 33% (10/30 flies). This high frequency of clones produced in the head is in agreement with the number of flies that show clones in other structures. The ocellus phenotype was only found in the target class (2/30 flies). This phenotype was not seen in any of the 90 flies of the control class scored. This suggests that a missing or reduced ocellus may be due to the $\Delta 53$ clones in the head. A similar phenotype was observed in the target class of flies of the second clonal analysis experiment and none of the controls showed any similar effect. This phenotypic effect is strikingly similar to the one produced by clones that misexpress *wg* (Royet and Finkelstein, 1996).

Phenotypic effects seen in the maxillary palpus involved a reduced palp size or absence of one of the palp organs (Figure III.16). The frequency of these effects was also 2/30 flies. The lack of specific cuticle markers and the low density of micro and macrochaetae in the palpus made it difficult to establish a strong correlation between this phenotype and the presence of marked bristles. However, the presence in both cases of marked Sb/Sb and Sb⁺ bristles close to the palp organ, and the fact that no similar defects were seen in more than 100 control flies suggests that $\Delta 53$ clones may be responsible for these effects.

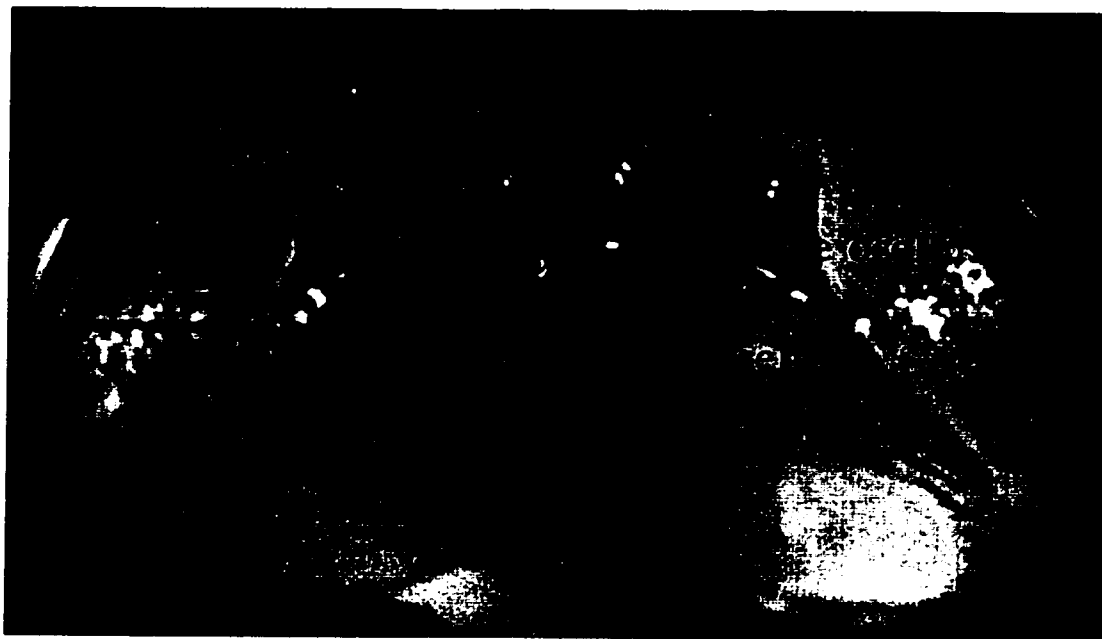


Figure III.15. Ocellus abnormality.

Dorsal view (anterior is up) of a head of an orange-eyed, yellow⁺, Sb fly of the first clonal analysis experiment (Figure III.13) genotypically $y^w P[ry^+; hs-flp]/y^w; P[ry^+; hs-neo; FRT]82B P[mini-w^+; hsPiM]87E Sb^{63b}G45\Delta53/P[ry^+; hs-neo; FRT]82B P[ry^+; y^+]96E$, in which mitotic clones were induced. The left part of the figure shows part of the left eye. A reduced left ocellus is shown at the center of the head. The right ocellus, which has a wild type phenotype, is shown to the right of the defective one for comparison. The presumed position of the mutant clone (genotypically $\Delta53/\Delta53 Sb/Sb$) is marked by the arrow and the position of the twin (genotypically $Sb^+ \Delta53^+/\Delta53^+$) is marked by the arrowhead.

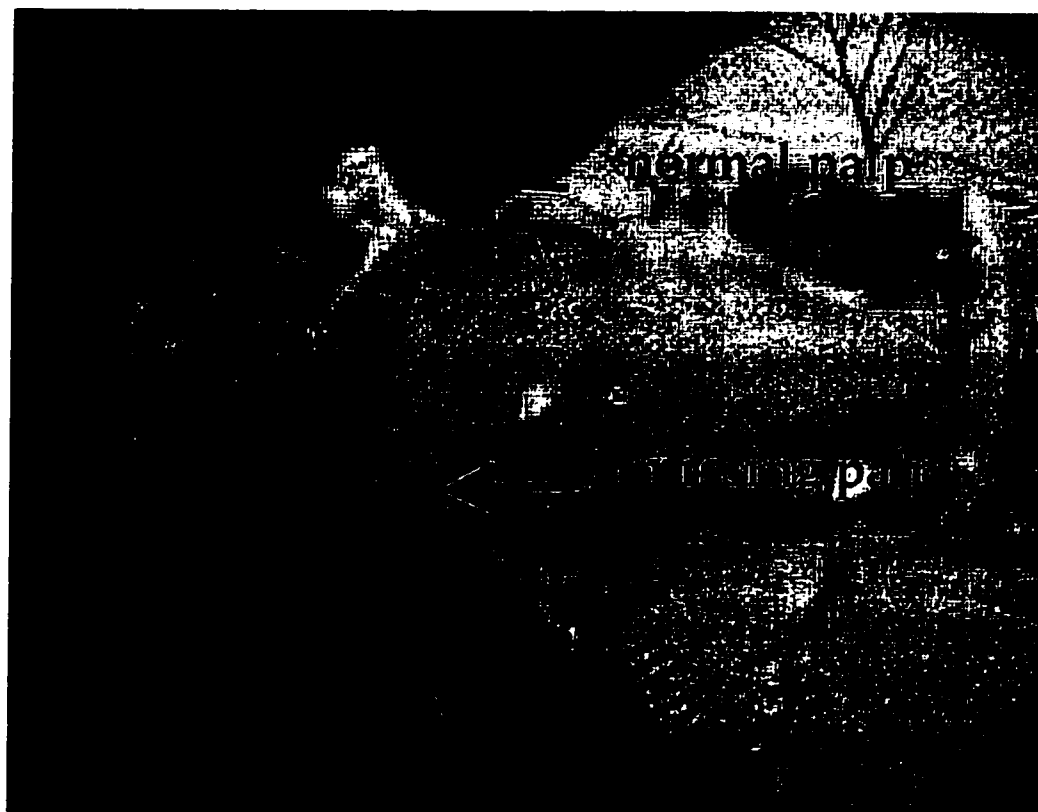


Figure III.16. Head of an orange-eyed fly of the first clonal analysis experiment (Figure III.13) genotypically $y\ w\ P[ry^+; hs-flp]/y\ w; P[ry^+; hs-neo; FRT]82B, P[mini-w^+, hsPiM]87E, Sb^{63b}G45\Delta 53/P[ry^+; hs-neo; FRT]82B, P[ry^+; y^+]96E$, in which mitotic clones were induced. Top arrow marks the position of a normal palp, and bottom arrow the position of a defective palp organ.

Thoracic abnormalities included pattern deficiencies and missing macrochaetae. These effects were seen only occasionally in the scutellum and were not studied further. More often, extra macrochaetae were observed in the scutellum and notum (Figure III.17, Figure III.18). The macrochaetae normally occupy fixed positions on the notum. Twelve particular thoracic bristles were individually scored in thirty thoraces of the target class to see if this phenotype was associated with marked clones. The total number of macrochaeta scored in each thorax was 12, and 6 out of 360 bristles were duplicated. In four of these cases one of the duplicated bristles was marked, either with $y\ Sb/Sb$ ($\Delta 53$ mutant clone), or with Sb^+ (wild type twin clone) (Table III.4). A statistical analysis of the data presented in Table III.4 shows that duplicated bristles are marked more often than expected by chance. A 2 by 2 χ^2 test (Steele and Torrie, 1960) indicates that the probability of this association occurring by chance is very low. The result of the statistical analysis supports the hypothesis that duplicated bristles are most likely due to the deletion at 100E in homozygosis. However, when duplicated, only one of the two bristles was ever marked, showing that the duplicated bristle pair is not one clone. Thus, a mutant clone may provoke the appearance of an ectopic bristle in tissue adjacent to a normal one. It is also interesting that in some cases the only marked bristle is the Sb^+ ($\Delta 53^+$) twin clone. This suggests that bristle duplication might be a non-autonomous effect of neighboring $\Delta 53$ mutant tissue that does not always form a bristle (see Discussion).

III.C.1.1 Wing abnormalities

The wing margin has three types of morphologically distinct bristle rows. The triple row is located at the anterior margin of the wing. It consists of a medial row of thick socketed sensory bristles, a more dorsal row of thinner bristles spaced by an average of four medial triple row bristles, and a ventral row of bristles, similar to the dorsal triple row, except that it runs ventral to the compartment border and is closely spaced. The double row runs along the distal margin and is characterized by socketed thin bristles. This row is composed of a ventral and a dorsal one including longer curved bristles that have sensory function (Whitlock, 1993). Finally, the posterior row has a dorsal and a ventral row of very thin bristles without sensory function.

Several types of phenotypic effects were observed in the wings. Blisters involving both layers of the wing were seen but their frequencies were not recorded as they were also observed in the balancer stocks and in the FRT line 2045 (Table II.1). This line carries a viable allele of Stubble, Sb^{63b} that has been reported to produce deformed legs and smaller wings than wild type flies when homozygous. However, some wing phenotypic effects (e.g. blisters) associated with Sb^{63b} in homozygosis may not have been reported. This would explain the observed blisters in the target and control classes.

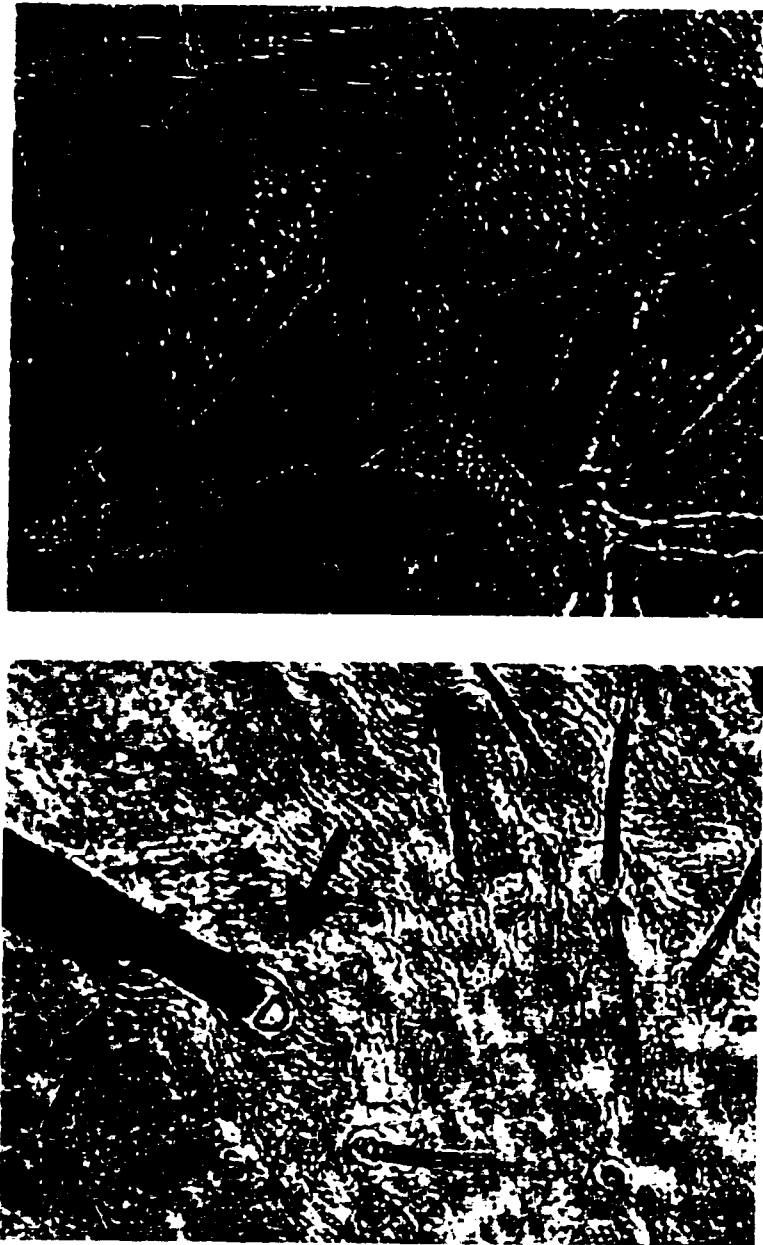


Figure III.17. Thorax abnormalities in the first clonal analysis experiment. Thorax of orange-eyed yellow⁺ Stubble flies (target class of the first clonal analysis experiment) (Figure III.13) genotypically $y\ w\ P[ry^{+};\ hs-FLP]/y\ w;$ $P[ry^{+};\ hs-neo;FRT]82B,$ $P[mini-w^{+};hsPiM]87E,$ $Sb^{63b}G45\Delta53/P[ry^{+};hs-neo;FRT]82B,P[ry^{+};y^{+}]96E,$ in which mitotic clones were induced.

A. Dorsal view, anterior up, of a thorax showing a marked ectopic macrochaetae, (medium size arrow) genotypically homozygous for $\Delta53$ and its twin (big and small arrows). B. A background ($Sb,$ yellow⁺) bristle duplication (big arrows) presumably caused by a non-autonomous effect of the neighboring clone genotypically $\Delta53$ homozygous (small arrow), which can be observed to the right (yellow microchaetae).

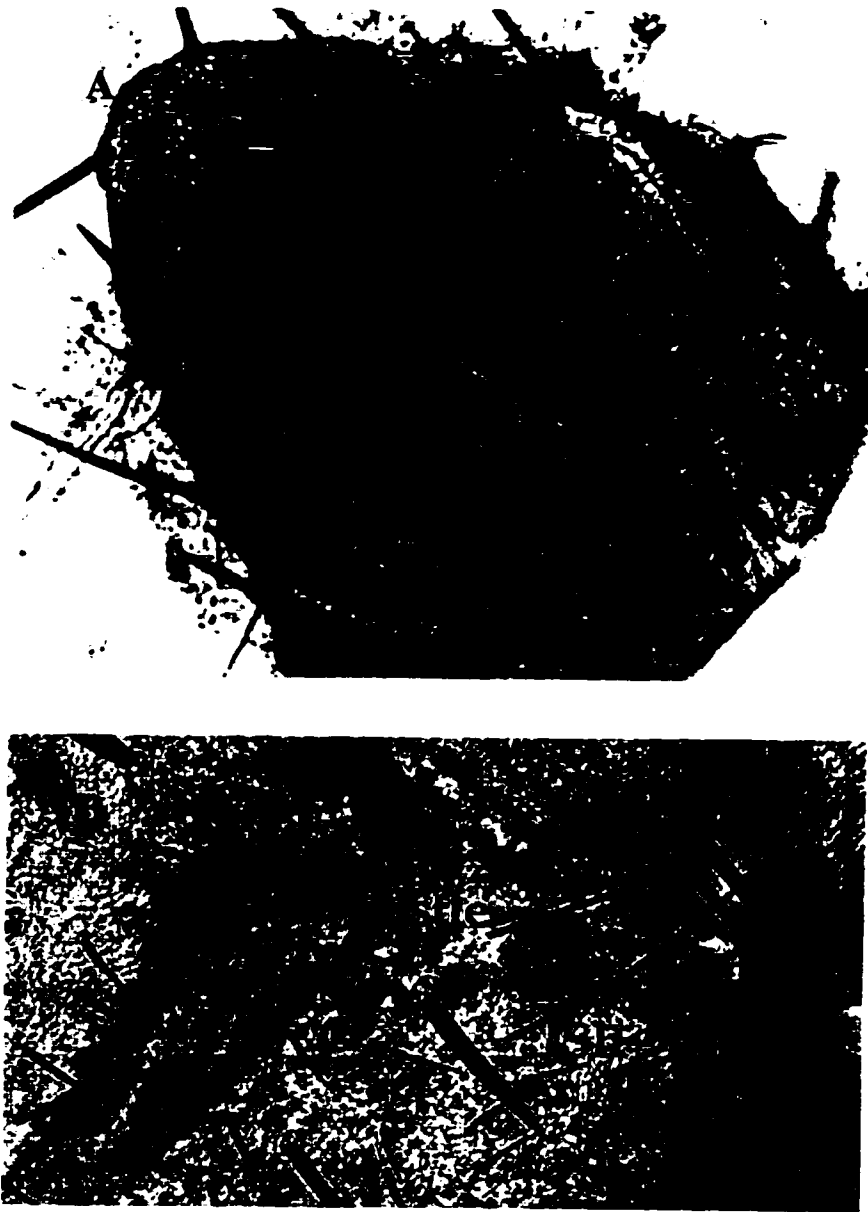


Figure III.18. Dorsal view of thoraces of orange-eyed flies of the first clonal analysis experiment (Figure III.13), genotypically $y\ w\ P[ry^+; hs-flp]/y\ w; P[ry^+; hs-neo; FRT]82B, P[mini-w^+; hsPiM]87E, Sb^{63b}G45\Delta53/P[ry^+; hs-neo; FRT]82B, P[ry^+; y^+]96E$, in which mitotic clones were induced. A. Example of a Sb^+ twin clone in which the bristle pattern is the wild type (arrows). B. An extra yellow Sb/Sb marked scutellar bristle, genotypically $\Delta53/\Delta53$ (long arrow) next to a Sb^+ twin clone (short arrow) that may have originated from the same mitotic recombination event.

Table III.4. Distribution of marked and duplicated thoracic bristles of flies from the first clonal analysis experiment

	Unmarked (y ⁺ Sb)	Marked (y Sb/Sb or y ⁺ Sb ⁺)	Total cases
Single macrochaeta	330	24	354
Duplicated macrochaeta	2	4	6
Total	332	28	360

A contingency X² test on these data is calculated as follows: $[(2 \times 24) - (330 \times 4)]^2 \times 360 / (332 \times 28 \times 354 \times 6) = 29.5$ P<0.005.

Ectopic patches of marginal bristles were observed only in the target class of flies of the first clonal analysis experiment. A summary of the position and frequency of the ectopic patches is given in Figure III.19 and Table III.5. They were found dorsally along the first vein, in the marginal cell, on the distal part of the second vein, in the submarginal cell, on the fourth vein and in the second posterior cell. Ventrally they were found along the first vein, marginal and submarginal cells and on the fourth vein (Figure III.20, Figure III.21, Figure III.22). These ectopic structures were located no further from the margin than about 15% of the total length of the longest elliptic diameter of the wing.

Compartment identity was retained. Patches of bristles in the dorsal anterior compartment had bristles like the ones found in the normal anterior dorsal margin (compare Figure III.20.A and Figure III.20.C {dorsal-anterior} with Figure III.20.E and Figure III.20.F {ventral-anterior}). In addition, the proximity of the ectopic structure to the margin seemed to determine the bristle type of the patch. For example, if a dorsal patch of ectopic tissue was closer to the triple row than to any other part of the wing margin, it produced only dorsal and medial triple row bristles (Figure III.20). If it was closer to the double row, it produced only dorsal double row bristles (Figure III.22).

In the anterior-dorsal part of the wing, patches found in the marginal cell or in the second vein had a mirror image-like pattern. Dorsal triple row bristles flanked the core of the patch, composed of medial triple row bristles. (Figure III.20 C). The ectopic patches of marginal bristles were either located on the plane of the wing surface (Figure III.20, Figure III.22) or they were associated with outgrowths projecting from the wing surface (Figure III.22C). These outgrowths were found dorsally in the submarginal cell and on the fourth vein no further from the margin than 10% of the total length of the longest elliptic diameter of the wing. Ventrally, they were found on the third vein, in the first posterior cell and on the fourth vein no further from the margin than 30% of the total length of the longest elliptic diameter of the wing. The distribution and frequency of outgrowths is given in Figure III.19.

It is important to note that most of the outgrowths (5 out of 6) were located very close to the anterior-posterior compartment boundary. This position is where a misexpression of *wg* causes formation of ectopic structures (see Discussion). The morphology of the ectopic outgrowth did not resemble a normal wing (Figure III.22C). Rather, it was an unpatterned mass of wing blade tissue that grew excessively on one surface. These ectopic structures always had bristles in the distal part. In all the cases, patches of ectopic tissue (ectopic bristles) showed compartment-specific wing bristle morphology.

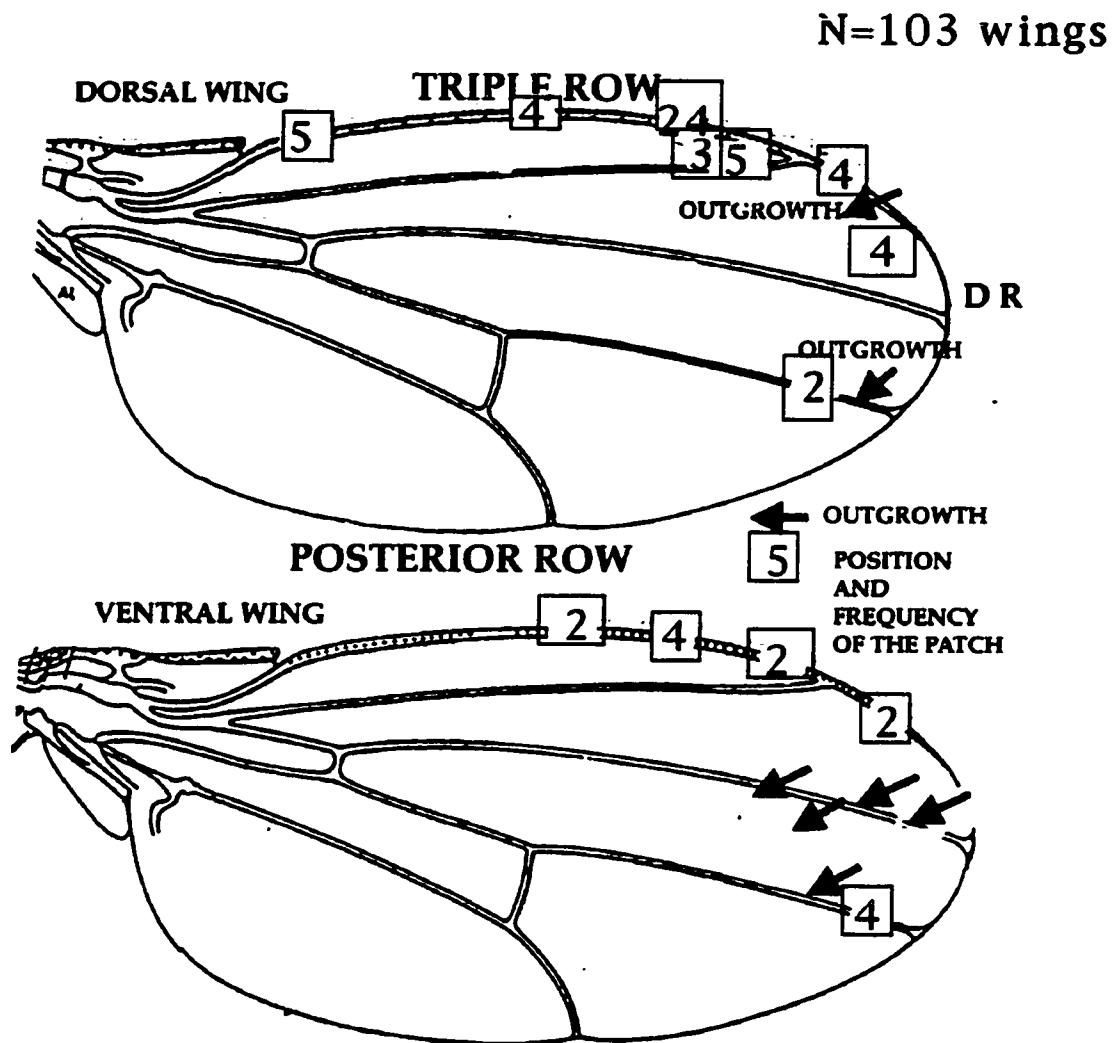


Figure III.19. Frequency and position of ectopic patches of marginal bristles found in the first clonal analysis experiment. Numbered rectangles represent the position and frequency of ectopic marginal patches among 103 wings scored from the first clonal analysis experiment (some examples are shown in Figure III.20). For example, a circle numbered 24 represents 24 wings in which an ectopic patch was observed on the distal part of the first vein of the dorsal compartment (e.g. Figure III.20 B). Arrows represent the position of each outgrowth (e.g. Figure III.22 B). Most of the outgrowths were observed in the ventral compartment. DR: double row.

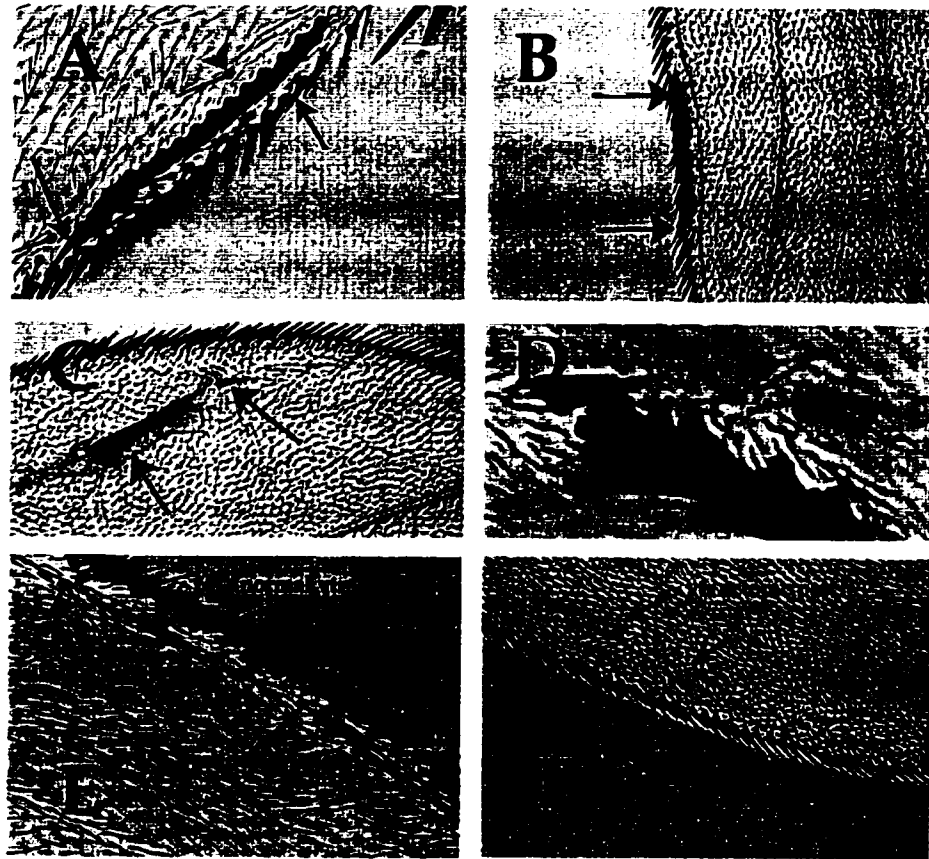


Figure III.20. Ectopic triple row bristles in the wing blade in the first clonal analysis experiment.

Wings of orange-eyed flies of the first clonal analysis experiment (Figure III.13) genotypically $y\ w\ P[ry^+; hs-flp]/y\ w; P[ry^+; hs-neo; FRT]82B, P[mini-w^+; hsPiM]87E, Sb^{63b}G45\Delta 53/P[ry^+; hs-neo; FRT]82B, P[ry^+; y^+]96E$ in which mitotic clones were induced. The point of this figure is to show the specificity of the ectopic marginal bristles according to position. A. An ectopic patch of bristles located in the anterior-dorsal compartment on the first vein. Arrows mark the position of the normal and ectopic yellow medial triple row bristles. Arrowhead indicates an ectopic dorsal triple row bristle. B. Anterior-dorsal ectopic patch of bristles located on the first vein. Top and bottom arrow mark the ends of the patch, composed of a medial and dorsal triple row bristles. C. Anterior-dorsal ectopic patch located on the second vein. The patch is organized as a mirror image-like duplication of the medial and dorsal rows (dorsal row bristles from both anterior and posterior to ectopic medial row bristles). Left arrow marks the position of a few yellow bristles; right arrow indicates smaller bristles, probably dorsal triple row. D. Higher magnification of an anterior-dorsal ectopic patch located on the marginal cell of the dorsal compartment. Several yellow (mutant) bristles are shown to the left. E. F. Ectopic patches of bristles located in anterior-ventral compartment. E. On the first vein. F. In the marginal cell. The patches of bristles in E and F are composed of only ventral triple row bristles, showing that the compartment identity is maintained.

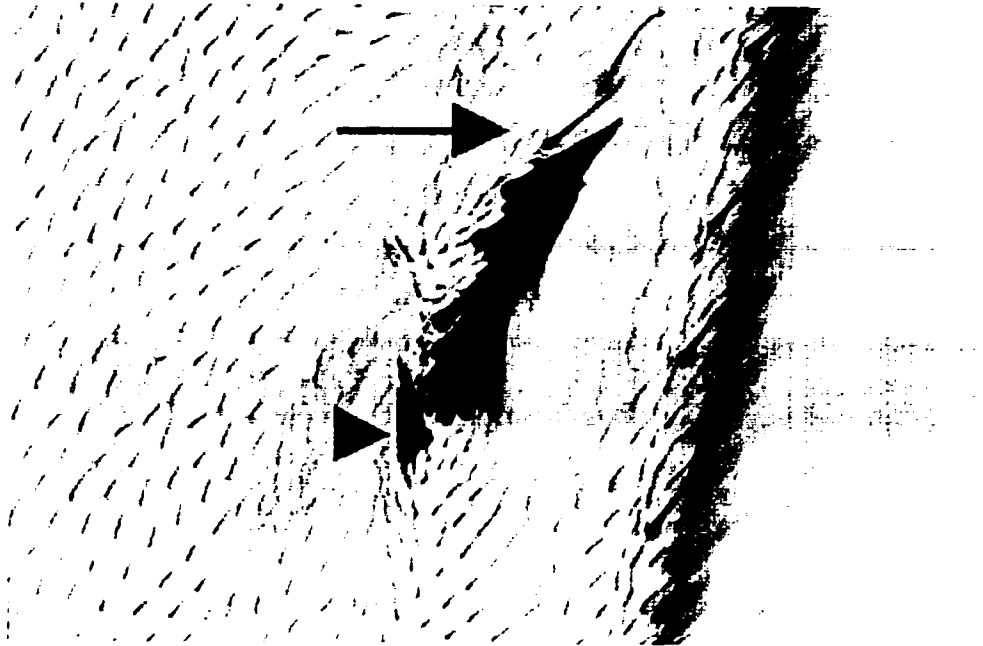


Figure III.21. Ectopic medial and dorsal triple row wing abnormalities in the first clonal analysis experiment.

Dorsal surface of a wing of an orange-eyed yellow⁺ Stubble fly (target class of the first clonal analysis experiment) (Figure III.13) genotypically $y\ w\ P[ry^{+};\ hs-flp] / y\ w; P[ry^{+};\ hs-neo;FRT]82B\ P[mini-w^{+};hsPiM]87E\ Sb^{63b}G45\Delta53 / P[ry^{+};hs-neo;FRT]82B\ P[ry^{+};y^{+}]96E$, in which mitotic clones were induced. Arrow marks the position of an ectopic dorsal triple row bristle, which is part of the ectopic patch. Thicker medial triple row bristles are usually not found in that position. Arrowhead marks the position of a dorsal yellow medial triple row bristle, also part of the ectopic patch, which is located in the marginal cell (see Figure III.19).

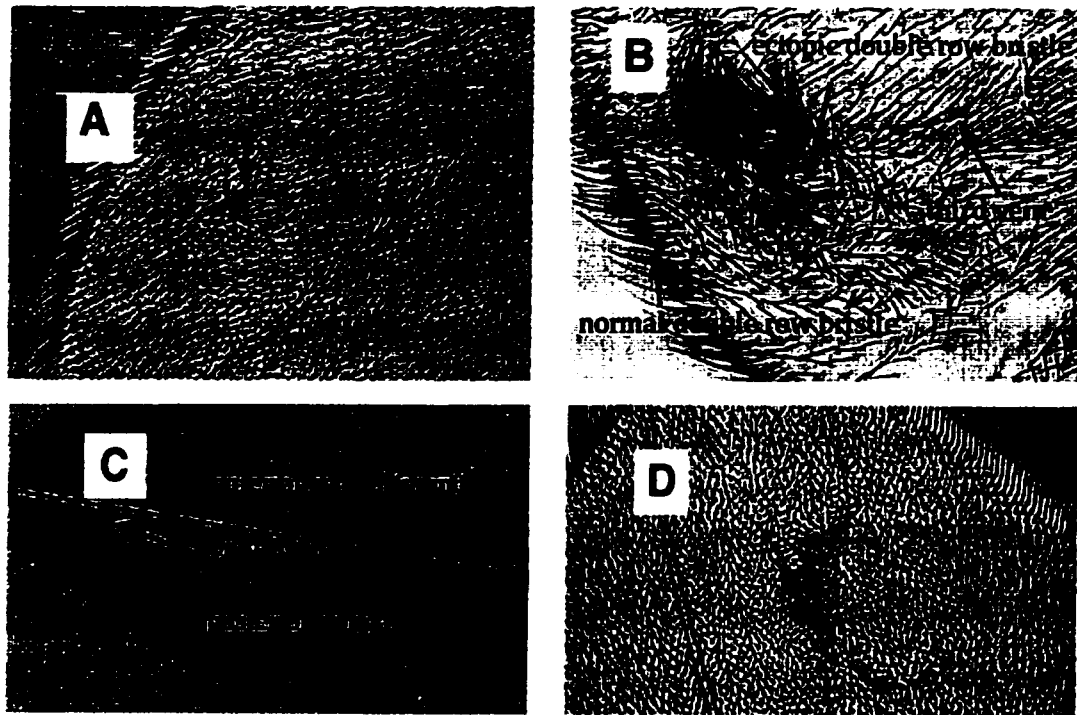


Figure III.22. Ectopic double row bristles and outgrowths in the wing blade in the first clonal analysis experiment.

A and B. Abnormalities observed in orange-eyed flies of the first clonal analysis experiment (Figure III.13) genotypically $y\ w\ P[ry^+; hs-flp]/y\ w; P[ry^+; hs-neo; FRT]82B\ P[mini-w^+; hsPiM]87E\ Sb^{63b}G45\Delta53 / P[ry^+; hs-neo; FRT]82B\ P[ry^+; y^+]96E$, in which mitotic clones were induced. A. A small ectopic patch composed of double row bristles in the dorsal surface. B. An ectopic patch composed of double row bristles on the ventral side of the wing. The ectopic patch has the same type of bristles as the neighboring normal margin, implying that the compartmental identity is retained.

C and D. Outgrowths in wings of the first clonal analysis experiment. Wing of orange-eyed yellow⁺ Stubble flies (target class of the first clonal analysis experiment) (Figure III.13) genotypically $y\ w\ P[ry^+; hs-flp]/y\ w; P[ry^+; hs-neo; FRT]82B\ P[mini-w^+; hsPiM]87E\ Sb^{63b}G45\Delta53 / P[ry^+; hs-neo; FRT]82B\ P[ry^+; y^+]96E$, in which mitotic clones were induced. C. Ventral outgrowth similar in position and morphology to the one reported for the ectopic expression of *wg* in clones (Axelrod, 1996). The outgrowth affects only the ventral compartment, and bristles maintain the compartment identity. The position of the outgrowth coincides with the anterior/posterior boundary (straight line). D. Ectopic patch on the third vein. Ectopic bristles have similar morphology to the posterior row since no sockets are observed at the base of the bristle.

Genotypically, the ectopic patches usually included some marked yellow bristles ($\Delta 53$ homozygous) and some unmarked yellow⁺ bristles (Figure III.20 C, D, E). Thus, the ectopic margin structures might be caused by a $\Delta 53$ clone, but if so must include cells transformed as a result of a non-autonomous effect of $\Delta 53$ homozygous clones on adjacent wild type cells. In addition, however, a few ectopic patches consisted only of unmarked yellow⁺ bristles. These results raised the possibility that the ectopic patches had marked yellow bristles only by chance and therefore that this phenotype was not caused by the $\Delta 53$ clones.

To test these possibilities I asked whether the ectopic patches were marked with yellow bristles at a higher frequency than the normal margin. Medial and dorsal triple row bristles were used for this analysis because the yellow genotype is most reliably scored there. I scored 103 wings taken at random from the target class of flies. The results are shown in Table III.5, Table III.6, and Table III.7.

I compared the frequency of yellow medial triple row bristles (ymtrb) in the dorsal ectopic patch to the frequency in the normal position (Table III.6 column 5, Table III.7). The statistical data for clones in the normal margin are presented in Table III.8. The frequency of dorsal triple row patches that showed at least one marked yellow bristle was 0.47 (21 out of 45 patches), (Table III.6; Figure III.20). Even though almost half of the ectopic patches are unmarked, the frequency of ymtr bristles in the dorsal ectopic patches was still significantly higher than the overall frequency of ymtr bristles in the normal margin (12.6% compared to 3.7%; $p < 0.05$), as shown by statistical analysis performed using a t-test assuming unequal variances (Microsoft Excel; Steele and Torrie, 1960). This result is strong evidence in favor of a clonal origin for this phenotype. However, the presence of many normal (y⁺) ectopic bristles must imply a non-autonomous effect of the $\Delta 53$ clones on neighboring wild type cells.

Further analysis of the data strengthened the conclusion of a clonal origin for this phenotype. To rule out the possibility that wings with ectopic patches have more clones I compared the frequency of yellow bristles in the normal margin in wings with dorsal ectopic anterior patches to the frequency in wings without ectopic patches (Table III.7 Group A + Group C and Group B + Group D). The average frequency of marked bristles in wings without ectopic patches was 5.5%; while the average of the same variable in wings with ectopic patches was only 1.6% (Table III.7). A statistical analysis using the same test as above is shown in Table III.8. The difference in frequency is significant at the 0.05 level. The result indicates that the higher frequency of yellow bristles seen in the ectopic patches compared to yellow bristles in the normal margin cannot be explained away by an increased general frequency of marked clones in these wings. It is also important to point out that all the yellow ($\Delta 53$ mutant) clones scored in normal margin showed a morphologically normal phenotype (Figure III.23). This means that the functions of any genes deleted in $\Delta 53$ are not required to make a normal wing margin, but rather to prevent the adoption of this fate in the wing blade.

Table III.5. Number of ectopic patches in 103 wings of the first clonal analysis experiment							
Triple row bristles		Double row bristles		Posterior row bristles		Outgrowths in ventral compartment	
Dorsal and Medial	Ventral	Dorsal	Ventral	Dorsal	Ventral	First post.	fourth vein
45	8	4+lout growth	3	2+lout growth	4	3	2

Table III.6 Phenotypes of the medial triple row bristles in the ectopic dorsal anterior patches in wings of the first clonal analysis experiment.

Ectopic patch.	Number of yellow bristles in patch	Number of y+ bristles in patch	Total bristles	Yellow bristles as a % of the total
1	1	9	10	10
2	0	3	3	0
3	0	14	14	0
4	0	20	20	0
5	3	7	10	30
6	0	3	3	0
7	0	7	7	0
8	0	1	1	0
9	4	35	39	10
10	5	22	27	18
11	0	10	10	0
12	0	16	16	0
13	2	8	10	20
14	0	1	1	0
15	0	4	4	0
16	1	1	2	50
17	0	7	7	0
18	0	1	1	0
19	0	3	3	0
20	1	4	5	20
21	1	4	5	20
22	0	8	8	0
23	0	6	6	0
24	3	3	6	50
25	0	3	3	0
26	3	7	10	30
27	3	27	30	10
28	9	30	39	23
29	1	9	10	10
30	0	1	1	0
31	0	12	12	0
32	0	10	10	0
33	6	1	7	85
34	0	8	8	0
35	0	14	14	0
36	0	3	3	0
37	0	3	3	0
38	2	13	15	13
39	10	12	22	45
40	1	8	9	11
41	2	6	8	25
42	2	8	10	20
43	6	30	36	17
44	15	16	31	48
45	0	22	22	0
Average	2	9	11	12

Table III.7 Percentage $\{100*(y/[y+y'])\}$ of bristles in normal margin in the first clonal analysis experiment (N=103 wings)							
Group A: wings with yellow bristles in normal margin and dorsal patches		Group B: wings with yellow bristles in normal margin. No dorsal patches		Group C: wings with dorsal patches but no yellow but no yellow bristles in normal margin		Group D: wings without margin clones or ectopic dorsal patches	
Number of wings	% of yellow bristles in normal margin	Number of wings	% of yellow bristles in normal margin	Number of wings	% of yellow bristles in normal margin	Number of wings	% of yellow bristles in normal margin
2	2	2	3	35	0	22	0
1	3	3	4	<p>Total for Group A: 13 wings with an average of 5.9% of yellow bristles</p> <p>Total for Group B: 33 wings with an average of 9.2% of yellow bristles</p> <p>Total Group (A+C): 48 wings with an average of 1.6% of yellow bristles</p> <p>Total Group (B+D): 55 wings with an average of 5.5% yellow bristles</p>			
2	4	3	6				
3	6	4	7				
2	7	4	8				
1	9	4	9				
1	10	1	10				
1	11	6	11				
		1	13				
		1	14				
		2	16				
		2	18				

Table III.8

t-Test: Two-Sample Assuming Unequal Variances			
	% of Yellow bristles in normal margin (see Table III.7)	% of Yellow bristles in ectopic patches (see Table III.6, column 5)	
Mean	$X_1=3.7$	$X_2=12.5$	
Variance	24	348	
Observations	103	45	
Hypothesized Mean Difference	$X_1-X_2=0$		
df	47		
t Stat	-3.1		
P(T<=t) one-tail	0.0014		
t Critical one-tail	1.7		
P(T<=t) two-tail	0.003		
t Critical two-tail	2.0		
t-Test: Two-Sample Assuming Unequal Variances			
	Groups A+C (see Table III.7)	Groups B+D (see Table III.7)	
Mean	$X_1=1.6$	$X_2=5.5$	
Variance	9.2	30	
Observations	48	55	
Hypothesized Mean Difference	$X_1-X_2=0$		
df	86		
t Stat	-4.5		
P(T<=t) one-tail	9.2E-06		
t Critical one-tail	1.6		
P(T<=t) two-tail	1.8E-05		
t Critical two-tail	1.9		

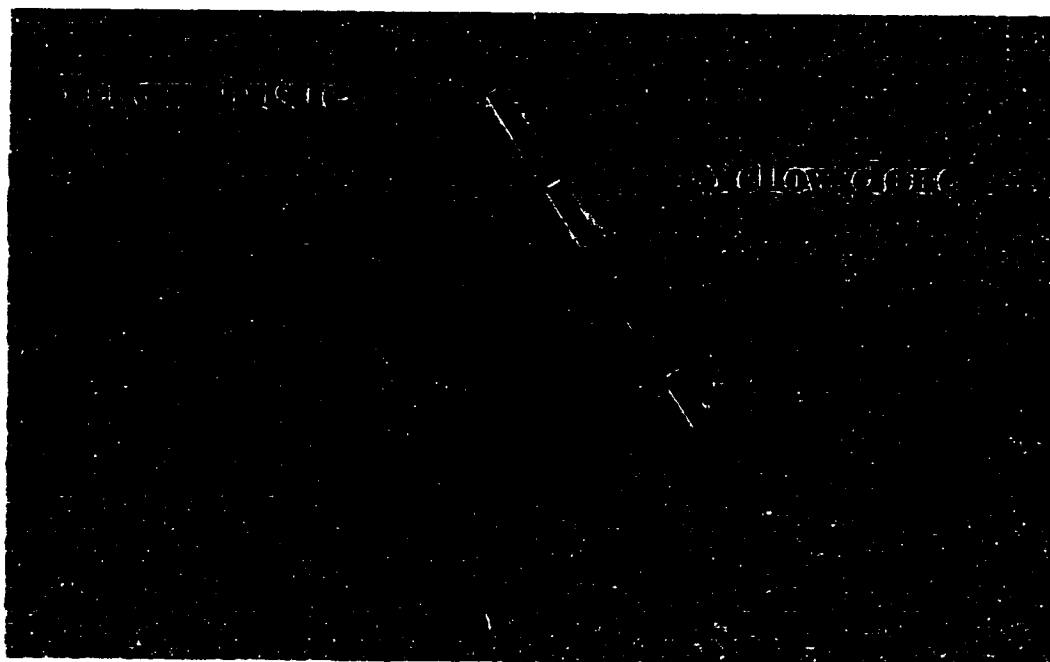


Figure III.23. Clones in the normal margin do not affect bristle phenotype. Wing of an orange-eyed yellow⁺ Stubble fly (target class of the first clonal analysis experiment) (Figure III.13) genotypically $y^w P[ry^+; hs-flp]/y^w; P[ry^+; hs-neo; FRT]82B, P[mini-w^+; hsPiM]87E, Sb^{63b} G45\Delta53/P[ry^+; hs-neo; FRT]82B, P[ry^+; y^+]96E$, in which mitotic clones were induced. Normal margin from a wing from the first clonal analysis experiment. The yellow clone does not affect the morphology where it intersects the normal margin. Dash line divides unmarked (yellow⁺ bristles) and marked (yellow clone) bristles.

III.C.2 Second clonal analysis experiment

Based on the first clonal analysis experiment I tentatively concluded that the abnormal phenotypes were probably due to the deficiency $G45\Delta53$ in homozygosis. In order to make sure that clones using FRT chromosomes did not cause any effects I also did another control for the first and second clonal experiment by removing $G45\Delta53$ from the same marked chromosomes (Figure III.12A and Figure III.12B). The crosses made to generate clones are described in Figure III.24. Adult flies were scored for the same type of abnormalities seen in the first clonal analysis experiment. None of the phenotypic effects previously ascribed to $\Delta53$ in the first clonal analysis experiment were observed in this control. This adds evidence of a clonal effect but it does not exclude an effect of the markers on the $\Delta53$ chromosome.

To rule out the possibility that the effects were due to the markers on the mutant chromosome, e.g. Sb^{63b} , a second clonal analysis experiment was done with the markers reversed. I recombined the deficiency from the $G45\Delta53$ line to the FRT chromosome carrying the FRT and the yellow⁺ cassettes (Figure II.5) (Materials and Methods). Using this method, I could also look at the behavior of a yellow marked twin clone to directly test the hypothesis of non cell-autonomous effects on the wild type cells neighboring the $\Delta53$ clone.

The phenotypic effects were of the same types as before. Thirty flies (60 eyes) from the target class were scored for the presence of marked ommatidia. Clones consisting of white ommatidia (mutant clone) next to red ommatidia (twin clone) were detected in 15/60 eyes. Out of this group, 10/15 showed disorganized ommatidia only in the mutant clone, and 5/15 had no phenotypic effect. Every white $\Delta53$ clone was next to a larger red twin clone. These phenotypic effects did not differ from the one seen previously. Internal control flies did not show any of these phenotypic effects associated with the presence of marked ommatidia. The frequency of disorganized ommatidia in the control flies was presented before (Table III.3) and was 2% (2/90 eyes). Two flies out of 30 examined had an ocellus defect. This is a similar frequency to that found in the first clonal analysis experiment. The controls did not show any ocellus abnormality in 103 flies scored.

The same types of thoracic abnormalities were observed as in the first clonal analysis experiment. Extra macrochaetae were used as parameters to measure the effects on the thorax. Thirty thoraxes were scored under the dissecting microscope. The number of thoracic bristles scored in the same thoracic locations was 12 as in the first clonal analysis experiment. Table III.9 gives the data. A contingency χ^2 test showed that duplicated bristles in the thorax are statistically associated with a marked bristle ($\chi^2=59.69$; $P < 0.005$) as in the first experiment.

Table III.9. Distribution of marked and duplicated bristles in thoraces of flies of the second clonal analysis experiment

	Sb/+ bristle	Marked ^a bristle	Total
Normal bristles	343	11	354
Ectopic bristles (duplication)	2	4	6
Total	345	15	360

Calculation $[(2 \times 11) - (343 \times 4)]^2 \times 360 / 345 \times 15 \times 354 \times 6 = \text{Chi}^2 = 59.69; P < 0.005.$

^a Either Sb/Sb or Sb⁺/Sb⁺

The statistical test indicates that the probability that the marked duplicated bristles occurred by chance alone is very low. Duplicated bristles were either Sb/Sb (wild type) or Sb⁺/Sb⁺ ($\Delta 53$). I interpret both results as the effect of $\Delta 53$ clones acting non-autonomously on neighboring cells. Therefore, duplicated bristles are most likely caused by the deletion at 100E in homozygosis. The controls did not show any association between the marked bristles and duplications in 103 thoraces scored. Only three thoraces showed one duplicated Sb/+ bristle.

Wings from the target class flies of the second clonal analysis experiment were mounted and observed under the compound microscope. Thirty one wings were scored for the presence of outgrowths and ectopic marginal bristles as seen previously in the first experiment. Outgrowths were seen only ventrally in the first posterior cell, at about the same distance from the margin as in the first clonal experiment (no further from the margin than 15% of the total length of the longest elliptic diameter). Bristles found at the tip of the outgrowth kept the identity of the closest margin. Ectopic patches were found dorsally along the first vein, on the marginal cell, on the distal part of the second vein (Figure III.25). Ventrally, they were found on the first vein, in the submarginal cell, on the third vein, on the fourth vein and in the second posterior cell (Figure III.26, Figure III.27).

These ectopic structures were located in similar places as compared to the previous experiment. In addition, they showed a similar morphology and retained their compartment identities (Figure III.26, Figure III.25, Figure III.27). The frequency and type of dorsal and ventral effects are summarized in Table III.10. Twin clones (yellow bristles) were present in many of the dorsal ectopic patches (17 out of 22 patches included at least one yellow bristle, Table III.11). The average frequency of yellow medial triple row bristles (twin clones in this case) in the ectopic dorsal patches was higher than the average frequency of the yellow medial triple row bristles (mutant clones in this case) in the first clonal experiment (32% compared to 12% in Table III.11 and Table III.6, bottom of last column). A summary of the data is given in Table III.11. To determine whether the frequency of labeled bristles in the ectopic dorsal patches was greater than in the normal margin a statistical analysis was performed as before. These results are summarized in Table III.13.

A t-test appropriate for data with unequal variances was performed. Table III.12 gives the results. The difference of 36% versus 5% is highly significant ($p < 0.05$). This result confirms a causal connection between the clones and the formation of ectopic margin. Secondly, the morphology of the dorsal ectopic patches and the fact that they contain on average three times as many yellow mutant bristles as in the first clonal analysis experiment (Figure III.25), confirms a non-cell-autonomous effect of the mutant clones since yellow twin clones are also affected. Thirdly, a possible explanation for the higher frequency of marked twin clone cells in the ectopic patches would be a clonal effect of $\Delta 53$ on cell proliferation.

<u>y w P[ry⁺; hs-flp]1</u>	<u>TM3, Sb</u>	×	<u>y w</u>	<u>P[ry⁺; hs-neo; FRTJ82B P[mini-w⁺; hs-πM]87E, Sb^{63b}</u>
<u>y w P[ry⁺; hs-flp]1</u>	<u>DrMio</u>		<u>Y</u>	<u>P[ry⁺; hs-neo; FRTJ82B P[mini-w⁺; hs-πM]87E, Sb^{63b}</u>

yellow, white eyes, Stubble
bristles, eyes with reduced number
of ommatidia.

yellow, orange eyes, StubbleStubble males.

Select yellow, orange eyes, reduced number of ommatidia, Stubble males.

<u>y w P[ry⁺; hs-flp]1</u>	<u>P[ry⁺; hs-neo; FRTJ82B P[mini-w⁺; hs-πM]87E, Sb^{63b}</u>	×	<u>y w</u>	<u>P[ry⁺; hs-neo; FRTJ82B, P[ry⁺; y⁺]96E G45A53</u>
<u>Y</u>	<u>DrMio</u>		<u>y w</u>	<u>TM6B, Hu</u>

Collect eggs for 24 hrs at 25°C, incubate for 24 hrs at 25°C
Heat-shock larvae for 1 hr at 38°C to induce mitotic clones.

white eyes, Humeral virgin females.
This clone is marked as red ommatidia, yellow
Stubble/Stubble
bristles in the body and yellow sensory bristles in the wing.

P[mini-w⁺; hs-πM]87E, Sb^{63b}
P[mini-w⁺; hs-πM]87E, Sb^{63b}

<u>y w P[ry⁺; hs-flp]1</u>	<u>P[ry⁺; hs-neo; FRTJ82B, P[mini-w⁺; hs-πM]87E, Sb^{63b}</u>
<u>y w</u>	<u>P[ry⁺; hs-neo; FRTJ82B, P[ry⁺; y⁺]96E G45A53</u>

This clone is marked as white
ommatidia, Stubble⁺ in the body.
Wings are not marked.

P[ry⁺; y⁺]96E G45A53
P[ry⁺; y⁺]96E G45A53

Score for orange eyes, yellow⁺, Stubble adult females.

Figure III.24 Crossing scheme used to generate clones in the second clonal analysis experiment
Flies were placed in vials as in Figure III.13 and the progeny of first instar larvae were heat-shocked as
described in Figure III.13. Adult flies that carried both FRT chromosomes were recognized by their orange
eye, yellow⁺ and Stubble bristle phenotype.

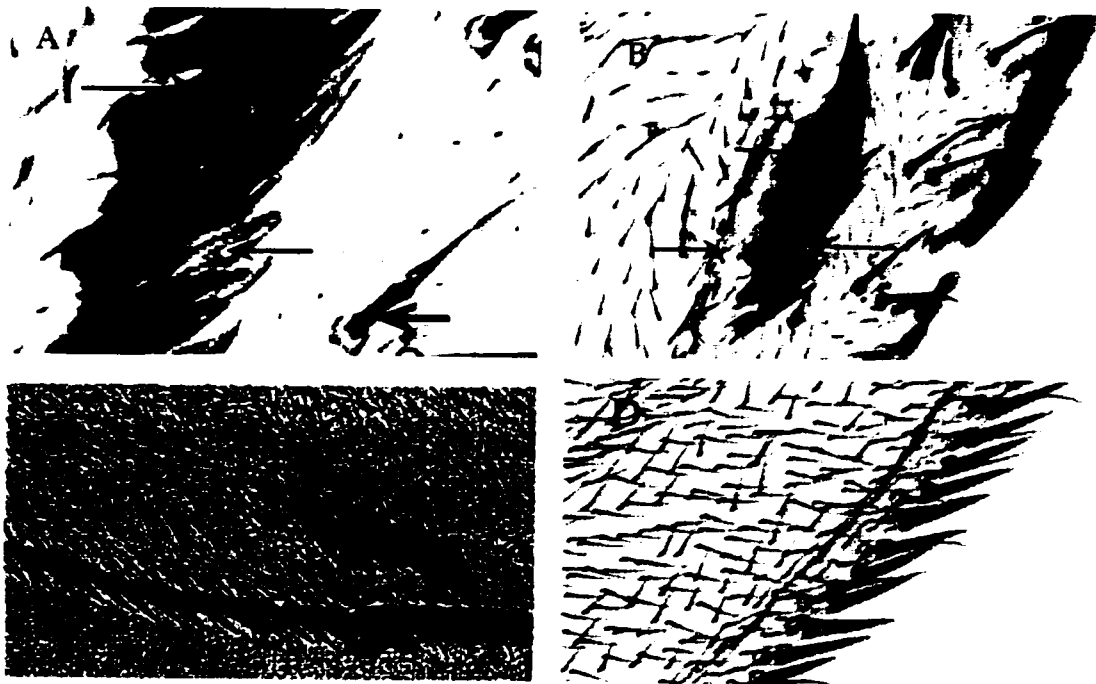


Figure III.25. Triple row abnormalities in the second clonal analysis experiment. Wings of an orange-eyed yellow⁺ Stubble flies (target class of the second clonal analysis experiment) (Figure III.24) genotypically $y^w P[ry^+; hs-FLP]/y^w; P[ry^+; hs-neo; FRT]82B, P[mini-w^+; hsPiM]87E, Sb^{63b}/P[ry^+; hs-neo; FRT]82B, P[ry^+; y^+]96E G45\Delta 53$, in which mitotic clones were induced.

A. Arrows (3) mark the position of the yellow (twin clone, left arrow and middle arrow) and presumably a mix of wild type and mutant bristles ($\Delta 53$ clones). Notice the increased size of the yellow twin clone relative to $\Delta 53$ clones in the previous experiment (see Figure III.21 for comparison), (right arrow marks the position of an ectopic dorsal bristle). B. Same patch as in A, left arrow points at the position of the thickened vein. Middle arrow marks the position of the presumed mutant and wild type bristles. Right arrow marks the position of the twin (yellow). C. Ectopic dorsal triple row bristle (arrows) are generally seen flanking the ectopic patch of medial triple row bristles. D. A yellow twin clone in the normal margin showing the wild type morphology.



Figure III.26. Double row abnormalities in wings of the second clonal analysis experiment.

Wings of orange-eyed flies of the second clonal analysis experiment (Figure III.24) genotypically $y\ w\ P[ry^+; hs-flp]/y\ w; P[ry^+; hs-neo; FRT]82B\ P[mini-w^+; hsPiM]87E\ Sb^{63b} / P[ry^+; hs-neo; FRT]82B\ P[ry^+; y^+]96E\ G45\Delta 53$, in which mitotic clones were induced.

A. A dorsal abnormality. Big arrow shows long socketed ectopic dorsal double row bristles; the same type of bristle is shown on the normal margin for comparison (small arrow). B. A closer view of a double row ectopic patch. Arrows (2) mark the position of socketed bristles.



Figure III.27. Ventral outgrowth in a wing of a fly from the second clonal analysis experiment.

Wing of an orange-eyed yellow⁺ Stubble fly (target class of the second clonal analysis experiment) (Figure III.24) genotypically $y\ w\ P[r\ y^+; hs-flp]/y\ w; P[r\ y^+; hs-neo; FRT]82B, P[mini-w^+; hsPiM]87E, Sb^{63b}/P[r\ y^+; hs-neo; FRT]82B, P[r\ y^+; y^+]96E\ G45\Delta53$, in which mitotic clones were induced. The outgrowth is marked by three arrows. Arrow (small arrowhead) marks the position of ectopic posterior row bristles in the outgrowth. Arrowhead marks the position of the anterior posterior boundary.

The significantly larger fraction of labeled twin clone cells in the ectopic margin relative to labeled $\Delta 53$ mutant cells in the first experiment may be explained by slower growth of the $\Delta 53$ clones than the $\Delta 53^+$ twin clones as was seen in the eye. The internal control flies (Figure II.6; Figure III.25D) showed no wing abnormalities associated with marked bristles in 206 wings scored. Only one blister was found and it was not associated with marked bristles.

In this experiment, I showed that two distinct clonal effects of $\Delta 53$ are the most probable explanation for the effects seen in the eyes, thorax and wings. In the eye, ten out of 15 white mutant clones showed disorganized ommatidia, and none of the red twins showed this phenotype. Therefore, this phenotype is a cell-autonomous effect of $\Delta 53$. In the thorax, marked mutant or twin clones are strongly associated with bristle duplications (Table III.9). In wings, twin clones (yellow bristles) were much more often found in the ectopic margin than in the normal margin. Therefore, the cause of this phenotype must include a non-autonomous effect of $\Delta 53$ clones on adjacent wild type cells. It can also be concluded that the primary, autonomous clonal phenotypic effect is not likely to be explained by an effect of the Sb marker, or by the P[mini-w⁺; hs- π M] cassette because the G45 $\Delta 53$ deficiency segregated away from these markers yet the phenotypic effect is still present at similar frequency as in the first experiment (Table III.13). However, I cannot rule out the possibility that these effects might be caused by an interaction between the G45 $\Delta 53$ and the P[ry⁺; y⁺] cassette, since they segregated together in this experiment.

Table III.10. Number of ectopic patches in 31 wings of the second clonal analysis experiment								
Triple row bristles			Double row bristles		Posterior row bristles		Outgrowths in ventral compartment	
Dorsal	Medial	Ventral	Dorsal	Ventral	Dorsal	Ventral	First post.	fourth vein
19	19	5	0	2	0	2	2	0

Table III.11 Distribution of marked and unmarked medial triple row bristles in ectopic dorsal anterior patches and in the dorsal anterior margin of wings of the second clonal analysis experiment						
wing number	Yellow bristles in normal margin	%yellow bristles in normal margin	Number of ectopic patches per wing	Yellow bristles in ectopic position	Yellow* in ectopic position	%yellow bristles in each ectopic patch
1	10	11	0	0	n/a	n/a
2	2	2	0	0	n/a	n/a
3	4	4	0	0	n/a	n/a
4	0	0	1	0	6	0
5	7	8	1	0	4	0
6	0	0	1	0	7	0
7	6	7	1	8	11	42
8	14	15	0	0	n/a	n/a
9	4	4	1	15	9	62
10	0	0	0	0	n/a	n/a
11	3	3	1	1	3	25
12	2	2	3	3	2	60
				6	2	75
				7	6	54
13	6	7	1	4	0	100
14	2	2	0	0	n/a	n/a
15	3	3	0	0	n/a	n/a
16	6	6	0	0	n/a	n/a
17	8	9	2	2	2	50
				4	4	50
18	0	0	1	0	14	0
19	8	9	2	5	5	50
				3	3	50
20	0	0	1	11	18	38
21	5	5	1	13	25	34
22	0	0	1	4	18	18
23	20	22	0	0	n/a	n/a
24	0	0	0	0	n/a	n/a
25	0	0	1	12	18	40
26	18	20	1	1	14	7
27	2	2	1	4	5	44
28	5	5	0	0	n/a	n/a
29	0	0	0	0	n/a	n/a
30	0	0	1	0	31	0
31	0	0	0	0	n/a	n/a
Average	4 yellow bristles per wing	5% yellow bristles per wing	1 ectopic patch per wing	3 yellow bristles per patch	9 yellow* bristles per patch	36% yellow bristles per patch

Table III.12

t-Test: Two-Sample Assuming Unequal Variances		
	%of yellow bristles in normal margin (see Table III.11, column 3)	%of yellow bristles in each ectopic patch (see Table III.11, column 7)
Mean	$X_1=5$	$X_2=36$
Variance	34	755
Observations	31	22
Hypothesized Mean Difference	$X_1-X_2=0$	
df	22	
t Stat	-5.3	
P(T<=t) one-tail	1.2E-05	
t Critical one-tail	1.7	
P(T<=t) two-tail	2.5E-05	
t Critical two-tail	2	

Table III.13. Comparison of the percentages of yellow medial triple row bristles in ectopic patches and normal margin in wings from the second clonal analysis experiment.

% of yellow medial triple row bristles in ectopic patch			% of yellow medial triple row bristles in the normal margin		
N=22 patches	Average 36	SD 28	N=31 wings	Average 5	SD 6

III.C.3 Third clonal analysis experiment

The first clonal experiment showed that there were several phenotypic effect in the imaginal discs that could be explained by a clonal origin. The second clonal experiment showed that these effects could not be explained by interactions between the Sb^{63b} allele and the $G45\Delta 53$ deficiency nor between the $P[\text{mini-}w^+; \text{hs-}\pi M]$ cassette and $G45\Delta 53$. However, there was still a remote possibility of these effects being caused by an interaction between the $G45\Delta 53$ deficiency and the $P[ry^+; y^+]$ cassette since these two segregated to the same cell in the second clonal analysis experiments.

To confirm an effect of $\Delta 53$ alone in clones I recombined the deletion to an FRT chromosome that carried only the $P[ry^+; \text{hs-neo}; \text{FRT}]$ cassette and repeated the experiment (Figure III.28). A control for this cross is described in Figure III.29. No effects were seen in this control. In order to see whether the effects would be similar to those previously seen, a sample of 28 wings was examined under the compound microscope and the frequency of ectopic structures was recorded. In the dorsal compartment, seven ectopic patches were seen. They were located in the marginal cell. In the ventral compartment, a total of nine ectopic structures were observed. Three of them were outgrowths located close to the A/P boundary. An example of a dorsal triple row patch is shown in Figure III.30. From these results it may be concluded that the induction of ectopic margin is a clonal effect of $\Delta 53$ alone.

III.C.4 Summary and conclusions from the clonal analysis experiments

The strong correlation between the presence of marked bristles and ectopic margin is evidence in favor of a clonal effect hypothesis. The controls for the heat shock treatment ($G45\Delta 53/\text{TM6B}$, Hu heat shocked at 37°C) added evidence in favor of the idea that the phenotypic effect is not a consequence of heat-shocking the chromosome carrying the deficiency but most likely a clonal effect of the mutant.

These results suggest that the ectopic margin phenotype is a clonal effect due to $\Delta 53$ clones. Also, the gene(s) deleted in the $G45\Delta 53$ deficiency line may not be needed for the normal development of bristles because bristles marked with yellow Sb/Sb (mutant clone) were normal in morphology. It is also not required for the formation of the normal wing margin since yellow ($\Delta 53$) bristles were found in the normal margin. It appears to be needed in the wing blade but only peripheral to the central and proximal region of the wing since no effect was found in this area.

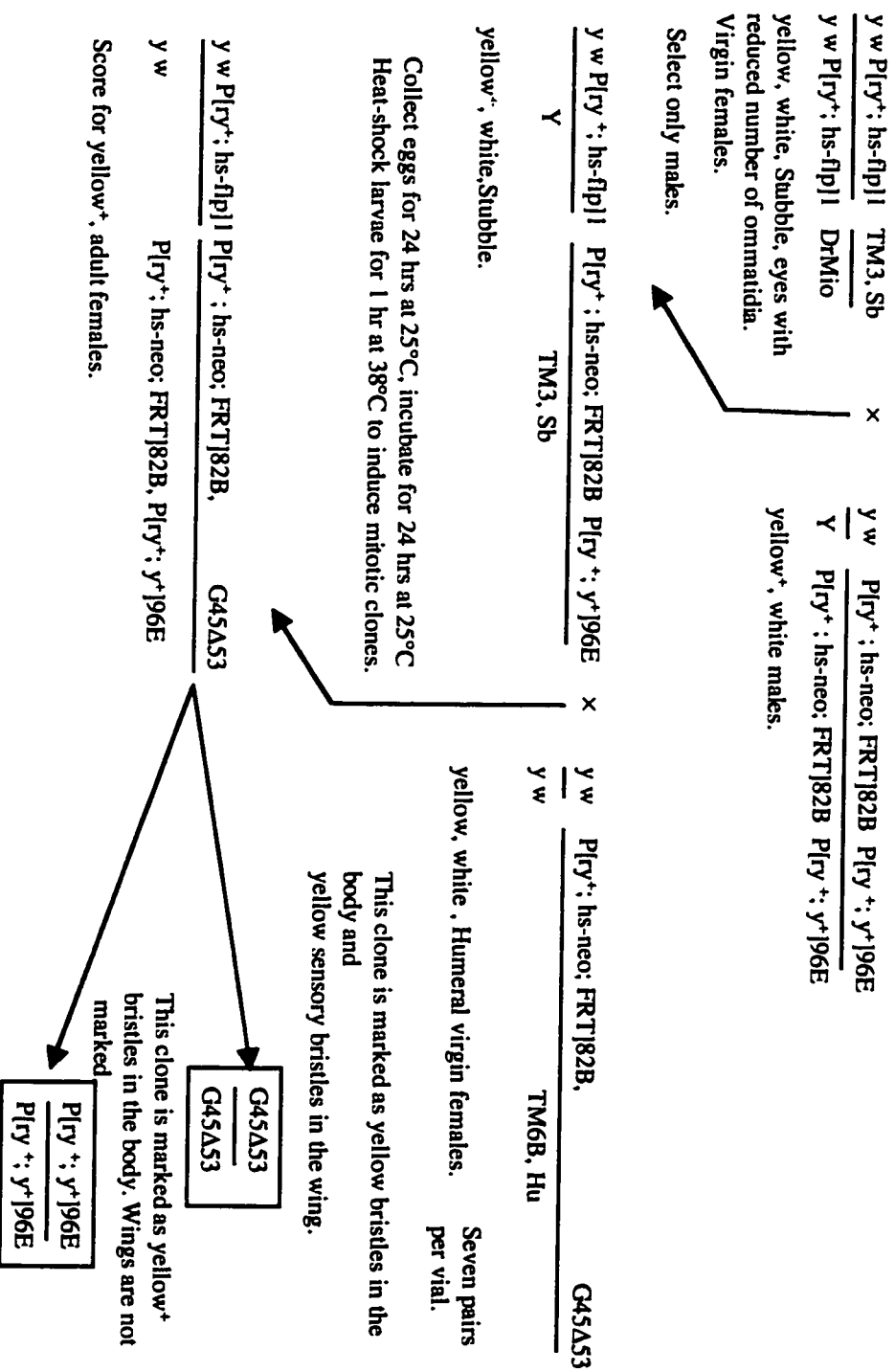


Figure III.28 Crossing scheme used to generate clones in the third clonal analysis experiment. Flies were allowed to lay eggs for 24 h, incubated for 24 h and heat-shocked at 37°C for 1 h when they reached first instar to induce mitotic clones. When larvae developed into adults, we scored only non-Stubble ones. Δ53 clones were marked with yellow.

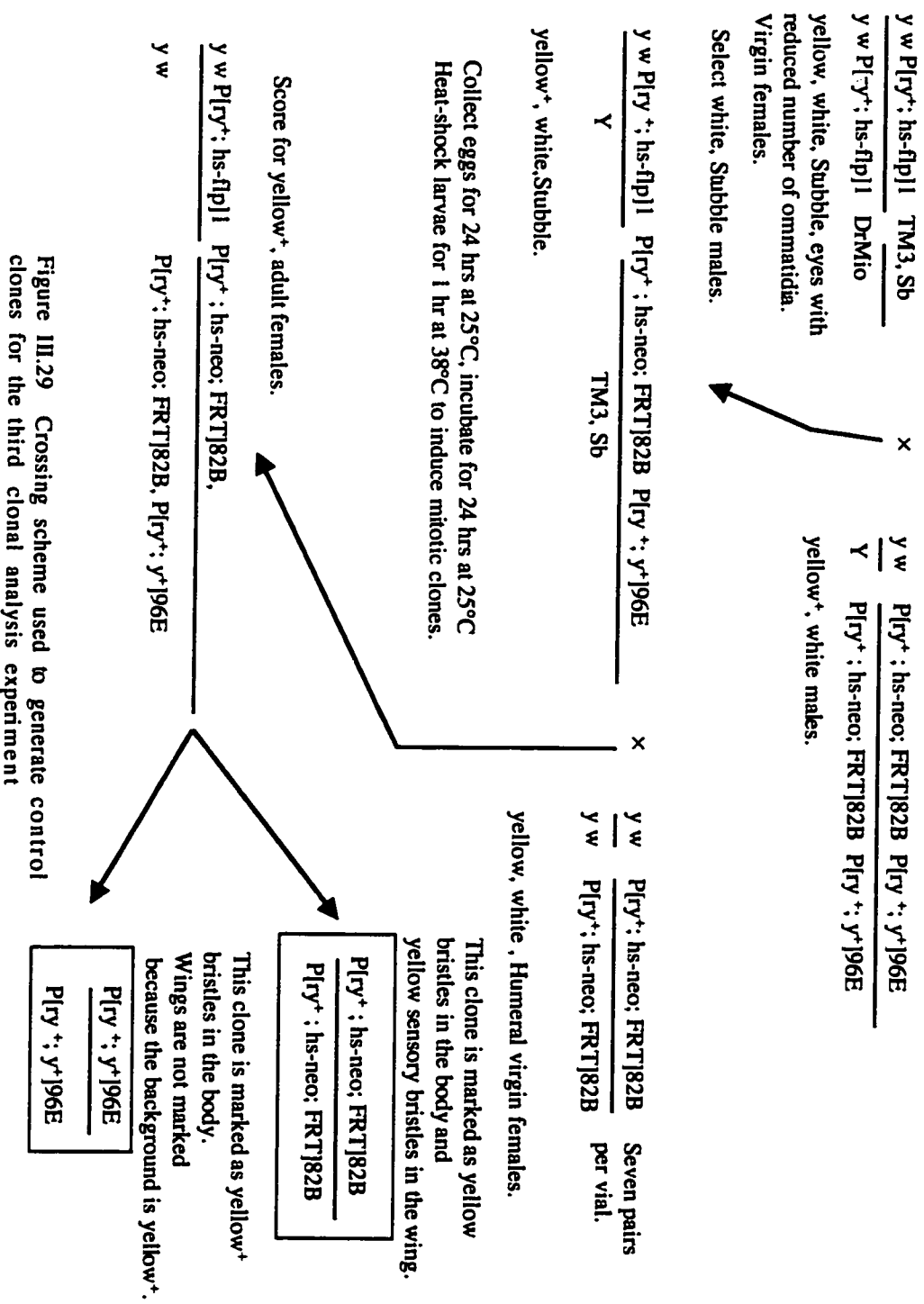


Figure III.29 Crossing scheme used to generate control clones for the third clonal analysis experiment

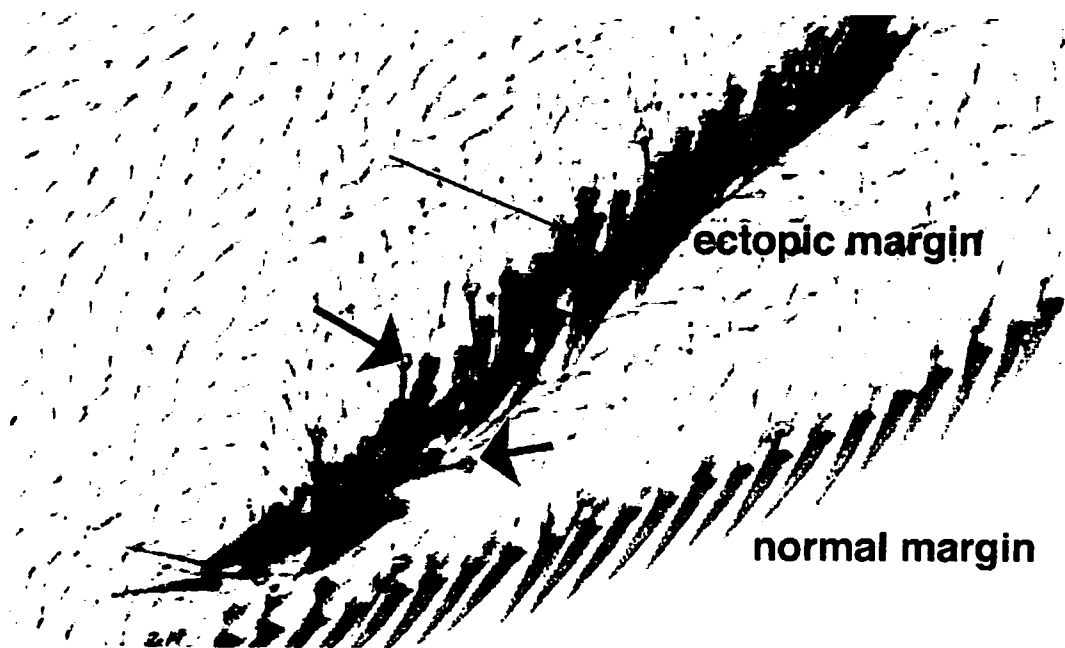


Figure III.30. Dorsal clone in a wing of a fly from the third clonal analysis experiment. Dorsal view of a wing of a white-eyed yellow⁺ fly (target class of the third clonal analysis experiment) (Figure III.28) genotypically $y w$ $P[ry^+; hs-flp]/y w$; $P[ry^+; hs-neo; FRT]82B$ $G45\Delta53/P[ry^+; hs-neo; FRT]82B$, $P[ry^+; y^+]96E$, in which yellow, $\Delta53$ mitotic clones were induced. Long arrow marks yellow bristles (homozygous for $\Delta53$) which are part of the patch.

Short thick arrows mark the position of small triple row dorsal bristles on both sides of the clone. The dorsal medial bristles in the ectopic patch are arranged in a clear mirror-image pattern with two rows of dorsal row bristles flanking the medial row bristles.

Compartment identity is conserved in the clones because bristles seen in ectopic patches are of the same type as the ones found at the margin in the same compartment as the clone. The gene or genes deleted in the G45 Δ 53 deficiency line may be involved in more than one function because several effects observed were observed in various adult structures. Evidence for a clonal effect on ommatidia, ocelli, thoracic bristles, and wing margin is indicated in the results reported. Some gene deleted seems to affect ommatidia in a cell-autonomous way because disorganized ommatidia were only seen in the clones carrying the deletion in homozygosis. Nevertheless, since local cell-cell interactions are known to be involved in the patterning of ommatidia, this conclusion must remain tentative. These data only rule out a long-range effect.

III.D Interaction between Δ 53 and a *wingless* pathway gene, *kiwi*

Given the striking similarity between phenotypic effects produced by clones that misexpress *wg* and clones of Δ 53 (see Discussion), I tested whether Δ 53 interacted somehow with the *wg* pathway. I used a mutant of a gene in that pathway, named *kiwi* (Binari et al., 1997). I used a P-element insertion line which is lethal. This line was generated in this lab, named A64 (line M in Table II.1) and it is allelic to *kiwi* (Sam Scanga, personal communication). I expected to see phenotypic effects in cuticular structures derived from wing imaginal discs since Δ 53 caused effects mainly in wings. A64 females (line M from Table II.1) were crossed to Δ 53 males (line A from Table II.1). This cross was done at 25°C. One hundred progeny flies from the target class, which carries one copy of A64 and one copy of Δ 53, were scored for phenotypic effects.

Thoraces and wing margin (Figure III.31) were the only structures of the adult cuticle that showed a phenotype, 58 thoraces out of 100 were affected, and 3 wings out of 200 wings from the target class showed a phenotype. None of the 200 control sibling flies showed any abnormality. The cross was repeated at 22°C and a reciprocal cross was set up. Flies from the target class (non-balancer) were scored for the same type of phenotypic effects. At 22°C 7 out of 72 flies, and 7 out of 90 flies from the reciprocal cross showed the phenotype previously observed in the thorax. Although the difference in penetrance was high (and probably due to the difference in temperature) the phenotype observed (expressivity) was very similar. The phenotypic effects include a patterning effect in the thorax which I describe as two bristle-free grooves that run in parallel along the A/P axis and a weak effect on the dorsal margin resembling an ectopic outgrowth of the double row bristles.

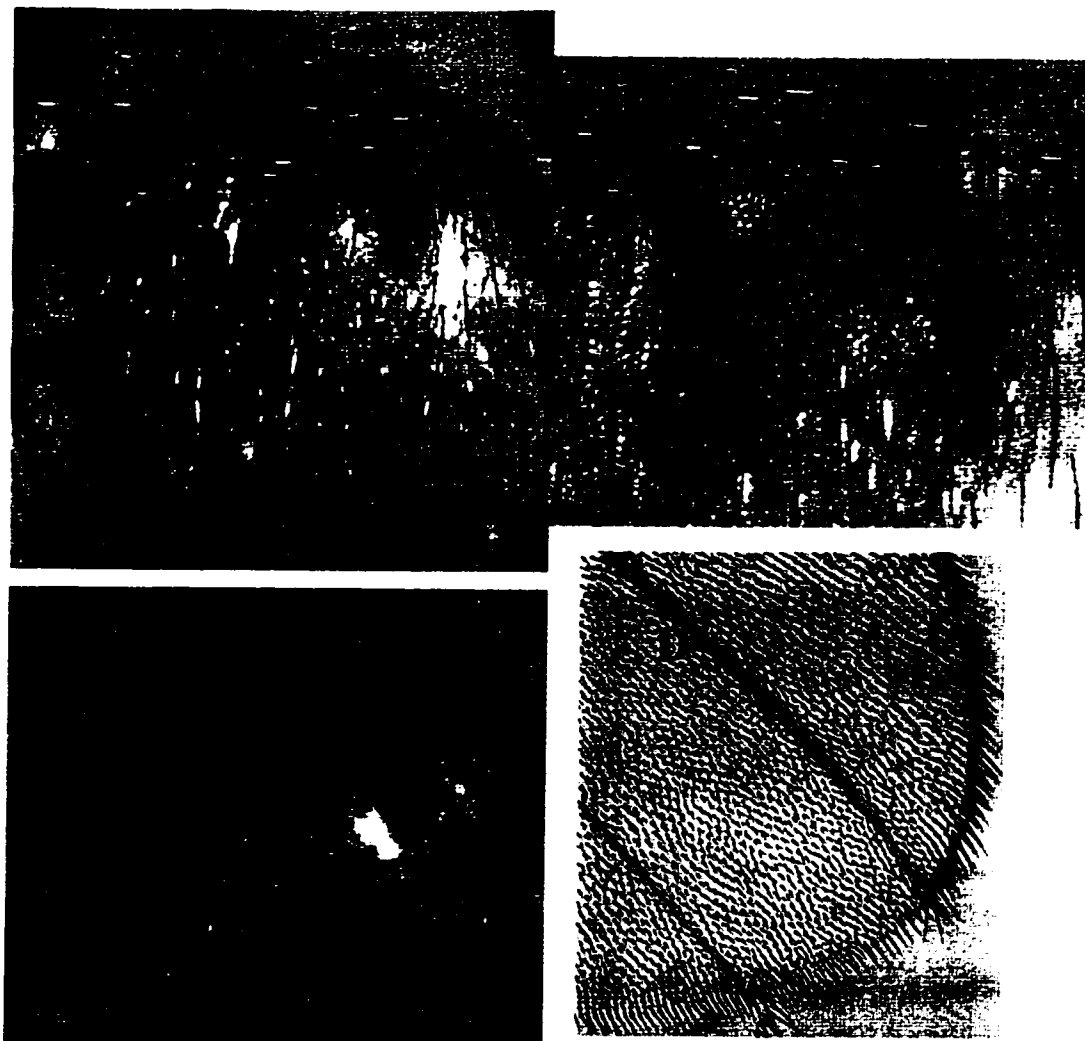


Figure III.31 $G45\Delta53$ interacts with an allele of *kiwi*, A64 showing a thorax and wing margin phenotype. Anterior is up, dorsal view. Thoraces of flies of the target class of a cross between females of line M and males of line A (Table II.1). The genotype of these flies is $G45\Delta53/A64$. Top left picture shows the notum phenotype observed. Arrows in all pictures mark the position of the "wound" phenotype. Top right picture (B) is a higher magnification of A. C. Bottom picture shows the same phenotype in progeny of the reciprocal cross of A and M (see also text). D. The wing margin phenotype. Dorsal view of a wing of a fly of the target class from the same cross. Phenotype was observed in 3 out of 200 wings scored and restricted to the wing margin, between the third and second vein. This phenotypic effect suggests that some function might be affected in the wing that is uncovered by the haploinsufficient effect of A64.

III.E Genetically mapping G45Δ53

In order to find how many complementation groups were present in Δ53 I crossed G45Δ53 to some P-lethal lines that mapped to 100E. *Df(3R)faf^{BP}*, which deletes the entire 100E-F region, is a homozygous lethal deficiency line that includes the *faf* gene (for which null alleles are viable) (Fischer-Vize, 1992). This line must overlap with and share one or more vital genes with G45Δ53 because it does not complement *Df(3R)faf^{BP}* (W. Brook, 1994).

I crossed a P-element insertion line that is lethal (P2167, Bloomington Stock center, Table1) and maps to 100E01-02. Complementation was observed. G45Δ53 was also crossed to a *faf* null (D. Dansereau et al., 1998) to see if Δ53 included *faf* or not. The result of the cross showed that Δ53 complements *faf* because none of the progeny showed the expected fat facets phenotype. Further analysis using *modulo* null, which is the lethal that maps to the most distal position on the 100E-F region shows that Δ53 is indeed located outside the 100E region because it does not complement *modulo* (D. Dansereau, personal communication).

IV. DISCUSSION

A genetic and molecular analysis was undertaken in order to characterize a locus putatively involved in regeneration of imaginal discs. An enhancer-sensitive P-element insertion line from a previous screen (Brook et al., 1993) was selected for this study because its expression on one side of the wound heal in imaginal disc fragments undergoing regeneration suggested a role in cell-signaling. I was also able to make use of a deletion derivative of this line, G45 Δ 53, that was generated by imprecise excision of the P-element in G45PZ (Brook, 1994).

IV.A Genetic organization of the G45 region

Based on segregation of the *rosy*⁺ marker and *in situ* hybridization of a plasmid containing PZ sequences it was shown that the P-element insertion maps to 100E. In addition, a genomic DNA fragment obtained by plasmid rescue, which has a single HindIII site and should come from the region of insertion was shown to map to a unique site in 100E by *in situ* hybridization to polytene chromosomes. No other evident sites of hybridization were detected in this experiment. This flanking DNA (FLR) was also mapped by Southern analysis (Brook, 1994). The result of the experiment showed that the flanking DNA is uncovered in the *Df(3R)faj^{bp}*, which deletes 100E through 100F (Fischer-Vize et al., 1992). The genomic DNA flanking the region of insertion was used to make two single stranded RNA probes transcribed from opposite strands. One of these single stranded RNA probes detected differential transcription in regenerating discs and the other one detected transcription in the eye discs which does not change expression in regeneration conditions (Brook, 1994).

I screened an embryonic cDNA library for cDNAs which cross-hybridized to the genomic DNA flanking the region of insertion. These cDNAs were organized in two non-overlapping contigs. One cDNA from each contig was used as an *in situ* hybridization probe to look for embryonic expression and differential expression in regenerating discs. G45-7 showed a pattern in the embryonic CNS midline similar to the one reported by the G45 line. In imaginal discs it hybridized only to a transcript expressed posterior to the morphogenetic furrow in the eye imaginal disc. This pattern was also similar to the one detected using the T₇ single stranded RNA probe because it did not change in regenerating discs. G45-11, which belongs to the other contig, detects embryonic gene expression in the head region, also reported in G45. In regenerating discs, it detects gene expression in a general pattern similar to the T₃ single strand probe, and there is a weak background staining in controls. This evidence at first suggested there might be two genes reported by G45, one, represented by the cDNA-11 contig, being induced in regeneration. However, sequence information led to a different conclusion.

A partial sequence from the cDNA G45-7 showed that an STS from the clone 65F1, from chromosome X (region 1B) is fully contained within the cDNA, and partially in the FLR. Thus, the T₇ single stranded RNA probe made from the FLR would have an antisense sequence (- strand) complementary to a 50 bp segment of the polydT (+ strand) of G45-7. G45-7 did not hybridize

to any of the three cosmids from 100E-F, but did hybridize to 65F1. This information suggests that G45-7 might represent the gene responsible for the *in vivo* transcription detected by the T₇ single stranded RNA probe, but comes from a segment of the FLR that maps to the X chromosome. G45-11 did not hybridize to 65F1 or to any of the 3 overlapping cosmids spanning 100E-F. Therefore, its validity as a transcript represented in the FLR is dubious. It might represent a weak homology with a gene or genes found elsewhere.

Since G45 is an enhancer-trap line and it should report expression directed by the enhancers affecting nearby genes, it is highly unexpected to find that the G45 line reports expression of a gene located in a different chromosome. A speculative explanation for this unexpected finding is that the P-element, which was originally inserted in the X chromosome (Jacobs, et al., 1989), may have transported regulatory as well as exon sequences of the gene represented by cDNA G45-7 from this site of insertion when it "jumped" to the third chromosome (Brook, 1994). Because of this "jump", chimeric structures may have been created at the site of the G45 insertion and rescued as part of the FLR, which must be chimeric.

This hypothesis could be easily tested by digesting genomic DNA from the original P-element insertion line that maps to the X chromosome if this line were available. The restriction enzymes should be chosen so that the P-element is cut only once (e.g Xba I or Hpa I). This would allow recovery of a band composed of flanking genomic DNA and P-element DNA. Digested DNA can be transferred to a membrane by Southern transfer. If FLR contains sequences from the X, a band of the same length should light up if the FLR, P-element DNA or G45-7 is used as probes on the Southern blot. Evidence in favor of this hypothesis would be the site of the original insertion that should map to 1B in the X chromosome.

If the chimeric hypothesis were correct, then embryonic regulatory proteins could direct transcription of the lacZ gene in a manner corresponding to the gene represented by cDNA G45-7 (CNS mid line in the embryo). This would explain the similarity between G45 embryonic lacZ and G45-7 *in situ* hybridization patterns, although G45-7 came from an X-linked gene.

In imaginal discs, however, the pattern of β -gal expression in wing fragments cultured *in vivo* might reflect the transcription pattern of another endogenous gene, activated by transcription proteins that would bind to regulatory sequences that map to 100E. This gene would be the one activated in the regeneration blastema and might deregulate *wg* or *N* pathways in clones of mutant cells (see below). Thus, $\Delta 53$ may well be a null mutant for that gene. If so, the lethality of $\Delta 53$ should be explained by proposing an embryonic function for that locus which remains to be cloned.

G45 $\Delta 53$ was used to assess the function of genes in the G45 region because it may be a very small deletion since it is not visible when salivary gland polytene chromosomes are observed under the compound microscope. G45 $\Delta 53$ is lethal when homozygous and most likely therefore deletes at least one gene. If the total number of genes estimated in *Drosophila* is 12000 (Miklos and Rubin, 1996), and the total number of polytene chromosome

bands is 5050-5075 (Flybase database) then dividing the estimated number of genes by the total number of bands we obtain 2.4 genes per polytene band on average. An average band from a polytene chromosome has 25 kbp (Spradling et al., 1995) of genomic DNA, and a small band contains about 5 kbp. Since there is no cytologically visible deficiency in $\Delta 53$ the DNA deleted may be less than 5 kbp. This suggests that only one or two genes may be deleted in the deficiency line. I found phenotypic effects of $\Delta 53$ clones in several different parts of the adult cuticle. This suggests that a gene or genes in the region neighboring the insertion must be involved in one or more aspects of patterning, growth or cell differentiation in imaginal discs.

IV.B Function of genes in the G45 region

IV.B.1 Phenotypes seen in the clonal analysis experiments

Phenotypic effects were observed in different adult structures after somatic recombination in $\Delta 53$ heterozygotes. Eyes showed disorganized ommatidia, the ocellus was missing or defective, the palp organ was missing or defective, and in the thorax, duplicated macrochaeta and missing microchaeta were observed. Wings showed ectopic patches of marginal bristles and distal outgrowths. The lack of a trichome marker on the right arm of the third chromosome that would allow us to map the precise limits of clones in the wing blade means that many clones that were probably induced in the wing blade were not detected. However, we could see marked bristles whenever a clone intersected the normal or ectopic margin. Three pieces of evidence suggest that these effects are caused by $\Delta 53$ clones. Firstly, all the phenotypic effects described were seen in the target class and not in controls. Secondly, marked bristles were seen in the ectopic patches in wings, in duplicated thoracic macrochaeta, and in the proximity of the ocellar and palp region. In the eyes, the mutant clones were unambiguously marked and were nearly always seen in association with disorganized ommatidia. Thirdly, statistical analysis showed a significant association between the clones and the phenotypes.

How can the clonal phenotypes be explained? The genes involved in normal margin induction may help explain the wing clone phenotype. Early in development, the wing is divided by the anterior/posterior compartment boundary (García-Bellido et al., 1973). Later, a new compartment subdivides the wing disc into dorsal and ventral (D/V) compartments. The D/V compartment boundary is important here because it plays a role in wing margin specification.

Margin specification is a complex process in which cell-cell interactions across the D/V boundary lead to the localized activation of the *N* receptor (*N*) and *wg* expression. *WG* in turn is necessary for the activation of the expression of proneural and other wing margin genes (Williams et al., 1994; Axelrod et al., 1996). The *N* and *Wnt* gene families have been linked to cell-cell signaling mechanisms in mammals, which if disrupted cause malignant transformations (Robins, 1992; McMahon, 1992; Nusse and Varmus, 1992).

The cascade of events leading to specification of cells giving rise to the margin starts with the activation of *ap* (Figure IV.i). This gene functions as a selector gene for the specification of the dorsal fate in wing imaginal discs. It encodes a LIM-domain homeobox transcription factor (Diaz-Benjumea and Cohen, 1993). Its expression is necessary for the restriction of cells to the dorsal compartment. *ap* activates *fringe* (*fng*), (Irvine and Wieschaus, 1994) and *Serrate* (*Ser*) expression in the dorsal compartment. *fng* encodes a protein (FNG) that is thought to be secreted. Its expression coincides with the *ap* expression domain, which is the dorsal compartment of the wing imaginal disc. FNG modulates N interaction with its ligands, *Delta* (*Dl*) and *Ser* gene products (DL and SER, respectively) (Panin et al., 1997). SER is a transmembrane protein expressed only in the dorsal compartment. It is cleaved to produce a ligand for N, which it activates in the ventral compartment (Speicher et al., 1994). DL signals reciprocally, activating N dorsally (Panin et al., 1997). *N* encodes a receptor with a single transmembrane domain. *N* is required for the expression of *wg* at the dorso/ventral margin in the wing imaginal disc (Rulifson and Blair, 1995) and for lateral inhibition in bristle specification in the thorax (Simpson, 1990; Cabrera, 1990). This may be significant in relation to the duplicated bristle phenotype of $\Delta 53$ clones in the notum. Panin et al., (1997) proposed a model that integrates the roles of these components of the D/V organizer in the wing margin (Figure IV.IB). By coexpression studies, it was shown that a positive feedback loop between SER and DL is responsible for maintaining their expression. At the same time, FNG acts by repressing the positive feedback loop in the dorsal compartment, thereby restricting the positive loop to the D/V boundary. Genetic analysis has shown that N and WG induce bristles at the wing margin (Diaz-Benjumea and Cohen, 1995).

The *wg* gene is an essential component in the regulation of wing development because it encodes a protein that mediates the activity of the D/V organizer (Figure IV.1). WG is a secreted glycoprotein expressed on both sides of the D/V boundary under the control of activated N receptor, which coincides with the presumptive wing margin. It has been implicated in the determination of the bristle fate probably because it controls the *achaete-scute* complex (*As-C*) (Cubas et al., 1991; Couso et al., 1994; Couso and Martinez-Arias 1994), which contains proneural genes required for marginal bristle differentiation. Loss of *wg* expression during the end of the third instar causes a loss of bristles phenotype. In addition, components of the *wg* signal transduction pathway have been shown to generate bristles. *armadillo* (*arm*) is a maternal-effect segment polarity gene (Peifer et al., 1991) which was isolated based on its similarity to the *wg* embryonic phenotype.

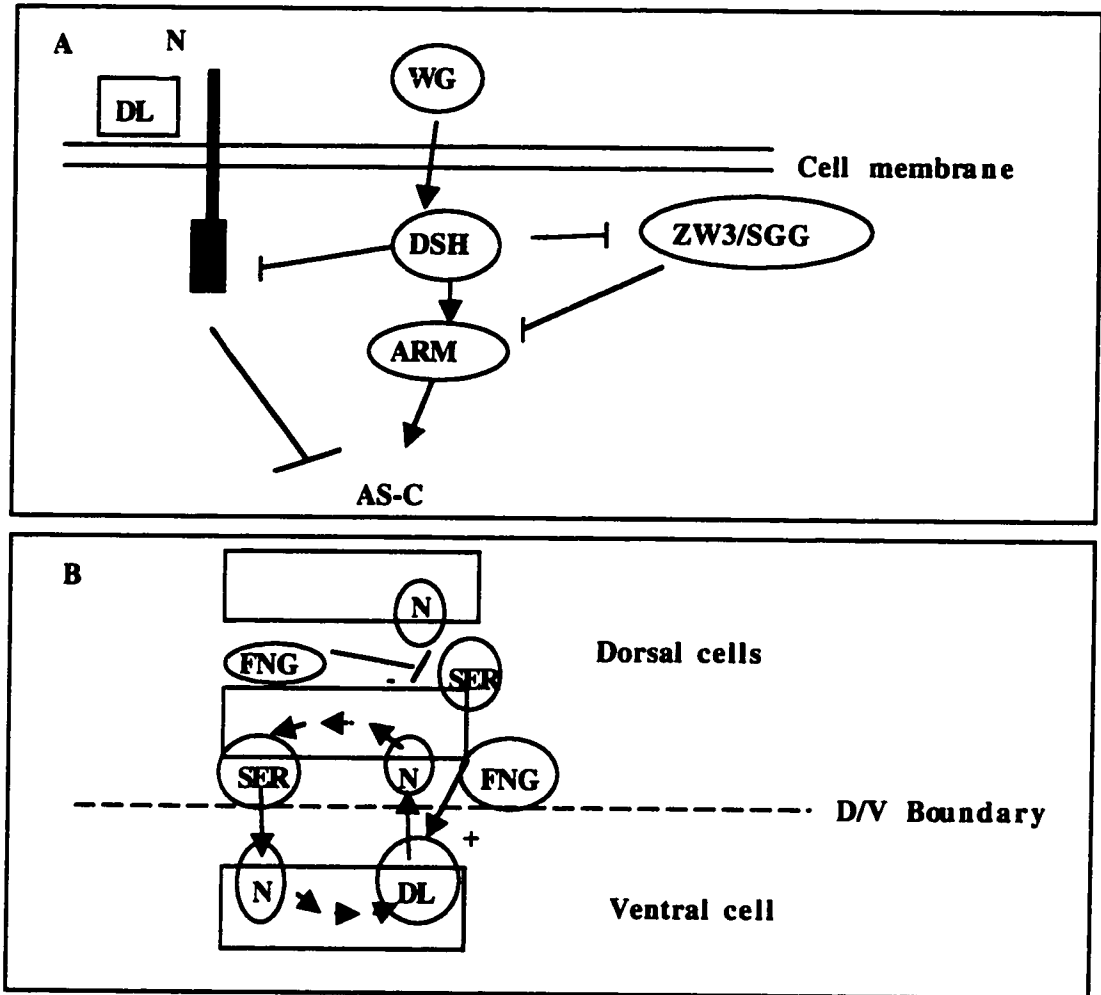


Figure IV.1 Components of the Dorso/ventral pathway. A. Model proposed by Axelrod et al., (1996) to explain N-WG interaction. DL is a ligand of N that binds to this receptor, activating it. WG antagonizes N by activating *dishevelled* (*dsh*) product (DSH) which presumably binds to the COOH terminal end of the cytoplasmic domain of N. DSH also *antagonizes Zeste-white3/shaggy* (*Zw3/sgg*), and regulates *arm* product (ARM) localization, which activates AS-C, thereby specifying Sensillum Mother Cell (SMC) development. N antagonizes AS-C proteins by repressing their transcription in an unknown way. B. Signaling at the D/V boundary. Model proposed by Panin et al., (1997) to explain the role of the different components of the D/V wing margin formation. *Ser* and *fng* are expressed in dorsal cells during early wing development. FNG is an essential factor in determining the activation of N by DL in dorsal cells. This activation promotes the transcription of factors that produce SER. SER signals from dorsal to ventral cells, which activates N. FNG prevents the activation of N by SER in the dorsal compartment. This mechanism permits the positioning of the N activation (by means of the SER-DL feedback) to the D/V boundary, thereby establishing an organizer center for the margin cells.

It encodes a catenin-like junction protein, and it is a target for *wg* because cells exposed to WG accumulate ARM (Riggleman et al., 1990). Another component of the *wg* signal transduction pathway is *dishevelled* (*dsh*). This gene encodes a protein (DSH) that functions cell-autonomously and responds to WG signalling since null mutants of *dsh* have phenotypes which are identical to null *wg* mutants throughout development (Klingensmith et al., 1994). *Zeste-white3/shaggy* (*Zw3/sgg*), encodes a serine-threonine kinase (ZW3/SGG) that is involved in lateral inhibition downstream of N (Blair, 1992b). ZW3/SGG represses the components of the AS-C. Epistatic interactions determined that *dsh* is upstream of *Zw3/sgg*, whereas *arm* is downstream (Siegfried et al., 1994).

WG activates the proneural genes in the wing margin, whereas N acts by repressing a neural fate. By overexpressing *dsh* (with a GAL4 driver, see Glossary) Axelrod et al., (1996) showed that DSH can inhibit the lateral inhibition. This caused an increase for microchaeta on the thorax. An increase in bristle density is also seen in the wing margin when *dsh* is ectopically expressed. This is consistent with the idea that lateral inhibition (see below) by N was blocked. Axelrod et al., (1996) proposed a model to integrate the roles of the main components of the wing margin signal transduction pathway (Figure IV.1A). This model proposes that WG is secreted (e.g. at the D/V boundary in wing imaginal disc) and reaches the target cells where it leads to activation of *dsh*. This activation results in the repression of *Zw3/sgg*, which derepresses the AS-C expression. This allows the development of the bristle fate in the wing margin.

Because of the similarity between phenotypic effects caused by $\Delta 53$ clones and the ones caused by wing margin specification genes described above, it is instructive to compare my results with these genes in clones. One such gene is *ap*, the selector gene for the dorsal compartment of the wing imaginal disc. In the dorsal compartment *ap*⁻ clones (Diaz-Benjumea and Cohen 1993) create a juxtaposition of dorsal cells expressing *ap* and mutant cells that do not express *ap*. Because of an interaction between these cells, an ectopic margin is formed at the boundary of the clone. *ap*⁻ cells at the edge of the clone produce ventral marginal bristles, and wild type cells that surround the clone produce dorsal marginal bristles.

fng⁻ clones induced in the dorsal compartment of the wing also create ectopic wing margin along the clone borders (Irvine and Wieschaus, 1994), but the ectopic margin consists only of dorsal marginal bristles, organized in a mirror image-duplication and composed of a row of wild type and a row of mutant cells. The clone boundary bisects the ectopic margin with dorsal and medial triple row bristles both inside and outside the clone. Neither *ap* nor *fng* clones have any effect in ventral wing, because these genes are not expressed in the ventral compartment. *Dorsal wing* (Tiong et al., 1995) is another locus involved in margin formation. *Dorsal wing* loss of function mutants cause a dorsal-to-ventral transformation of the wing margin but have no effects in the wing blade. SER is an N ligand normally expressed in the dorsal compartment. *Ser*⁻ clones in the wing imaginal disc delete the margin but it produces outgrowths when ectopically expressed ventrally (Speicher et al., 1994). DL is another N ligand expressed in the ventral

compartment that similarly activates *N* in dorsal cells only. Its effect in clones misexpressing *Dl* is complementary to *SER*.

The ectopic structures caused by $\Delta 53$ clones are different from all the clones described above because they induce ectopic margin both in ventral and dorsal compartments, and in each case produce ectopic marginal bristles that keep their compartment identity. However, when the constitutively active ligand-independent intracellular *N* construct is expressed in clones in wing imaginal discs, it causes ectopic expression of *wg* (Diaz-Benjumea and Cohen, 1995). This ectopic expression causes ectopic margin and outgrowths, which resemble the effect of ectopic expression of *wg*. However, cells expressing the constitutive intracellular *N* construct do not differentiate bristles. This is consistent with the proposed role of *N* as an epidermal cell fate determinant and inhibitor of neural cell fate (Simpson, 1990). The ectopic margin induced by *N*-expressing cells is composed only of wild type bristles (yellow⁺), which could be explained by the deregulation of *wg* and signaling to neighboring cells.

This phenotype is most similar to that seen in $\Delta 53$ clones except that unlike clones of cells overexpressing *N* intracellular construct, clones of cells homozygous for $\Delta 53$ are able to differentiate normal bristles. Therefore, $\Delta 53$ probably does not act via the overexpression of *N*. This suggests it might act one step downstream by deregulating the expression of *wg* itself.

Clones with reduced *wg* expression at the margin in the late third larval instar do not form bristles. Clones of *wg*-expressing cells induced in late third instar wing imaginal discs produce ectopic marginal structures in the wing pouch (Diaz-Benjumea and Cohen 1995). This indicates that *WG* has the ability to induce a margin cell-fate by itself (Diaz-Benjumea, 1993). If *wg* clones are induced in the dorsal compartment, the ectopic margin has only dorsal bristle types. If clones are induced ventrally, then only ventral bristles are produced. This is similar to the $\Delta 53$ clone effects. Precursors of sensory bristles are specified in wild type cells next to the *wg*-expressing cells. This is consistent with a non-autonomous effect expected from a secreted molecule. In addition, clones of *wg*-expressing cells cause outgrowths from the surface of the wing blade. This is strikingly similar to the effects we have reported with the $\Delta 53$ deletion.

A very important observation is that the outgrowths reported in this thesis are all found in distal positions and between the third and the fourth veins. In terms of Meinhardt's ideas of cooperation of compartments (1983; see also Campbell and Tomlinson, 1995) these outgrowths could represent the induction of a new proximal-distal axis. The new P/D axis would be formed at, or close to the intersection of A/P compartment border, which happens to be located between the third and fourth veins.

Other genes in the *wg* signal transduction pathway also produce phenotypes similar to the ones found with $\Delta 53$ clones when overexpressed. Concerning margin structures, *dsh* causes extra marginal bristles by activation of the *AS-C* complex (Axelrod et al., 1996). Clones of *dsh*⁺ (Klingensmith et al., 1994) cause a patterning defect in the distribution of marginal bristles in the wing. The patterning defect in clones of *dsh*⁺

include extra hair-secreting cells that displace the neighboring wild type bristles. In addition, clones of *arm*⁻ (Peifer et al., 1991) showed as well an autonomous effect in the wing margin. This is also the case for another component, *Zw3/sgg*, clones of which activate *AS-C* and produce ectopic bristles. This contrasts with the evident non-autonomous effect of *wg* and $\Delta 53$ clones and suggests that the locus deleted in $\Delta 53$ may be acting upstream of *wg*. If $\Delta 53$ were a negative regulator of one of the members of the *wg* pathway downstream of *wg*, its effect would more likely be cell-autonomous.

In the thoracic discs, *AS-C* expression determines the site where a large bristle (macrochaeta) will develop (Romani et al., 1989). The mechanism by which this occurs is not simple. A cluster of initially equipotential proneural cells expressing *scute*, singles out a neural precursor by a mechanism involving cell-cell interactions. *N*, its ligand *DL*, *DSH*, *ZW3/SGG* and *WG* all participate in this mechanism. A model was proposed by Simpson (Simpson, 1990) in which initially, all the cells in the cluster signal and receive equally. By chance, one of the cells (signaler) produces more signals than its neighbors (receivers) and this causes a reduction of signal coming from the neighboring cells (lateral inhibition). Cells that decrease their signal in response to the inhibitory signal become epidermal cells in the adult and do not produce bristles. Cells that signal become bristle mother cells and produce bristle in the adult epidermis. Simpson's model proposes that *DL* is the signal produced by the signaler and *N*, the receptor activated in response to *DL*. Consistent with this model is the fact that *N* loss of function mutants form extra bristles in the notum and the phenotypes of clones with altered relative dosage of *N* and *DL* (Heitzler and Simpson 1991). So, mutant cells defective in the receptor mechanism cannot be inhibited and adopt a neural fate producing extra bristles in the adult.

New information links the *DL-N* signaling pathway in the notum to *wg* and genes of the *AS-C* (Axelrod et al., 1996; Cabrera, 1990). In this model *wg* interacts with the *N* signaling pathway by activating *dsh* (Figure IV.1A). *DSH* suppresses lateral inhibition in the notum by acting negatively on *N* because overexpression of *dsh* in the notum cause an increase in density of macrochaete. As explained above, *dsh* also antagonizes *Zw3/sgg* (Noordermeer et al., 1994), thereby derepressing *AS-C* expression. This results in a production of extra bristles in the notum when *dsh* is overexpressed. I found a strikingly similar effect in the thoracic macrochaetae that is consistent with ectopic expression of *wg*. Its misexpression may explain the extra bristle phenotype seen as a non-autonomous effect of $\Delta 53$ clones.

The *Drosophila* eye contains approximately 800 ommatidia, which are almost identical (Heberlein and Moses, 1995). Each ommatidium is composed of eight photoreceptor neurons (R1-R8), a number of pigment cells and a single bristle. Ommatidial patterning and differentiation starts in the third larval instar in the eye imaginal disc. The direction of ommatidial assembly is determined by the passage of traveling wave of cell interactions called the morphogenetic furrow. As it progresses, the morphogenetic furrow leaves behind a sequence of stages in the assembly of the ommatidia. At a later stage the ommatidia rotate 90° as they assemble to give rise to the adult eye retinal organization, in which ommatidia are arranged in a mirror-

image symmetry established by an equator that divides the eye dorso-ventrally (Chanut and Heberlein 1995).

Genes affecting progression of the morphogenetic furrow affect the ommatidial patterning and produce a roughened eye (Heberlein et. al., 1993). The *fat facets* (*faf*) gene maps to 100E, and spans 83 kbp of genomic DNA. *faf-lacZ* fusion reports expression anterior to the morphogenetic furrow in eye disc, and in ovary, testes and gut. Null mutants in this gene are viable when homozygous and show a disorganized ommatidia phenotype. *faf^{bp}* (Fisher-Vize et al., 1992), used to genetically map the deficiency G45 Δ 53, is a deletion that includes this locus. Δ 53 and *faf^{bp}* must share at least one vital locus since viable heterozygous carrying Δ 53 and *faf^{bp}* were never recovered from crosses between the two balanced stocks (Brook, 1994).

Here I found that Δ 53 clones in the eye show a disorganized ommatidia phenotype, which might be due to a deficiency for *faf* (red ommatidia in the first experiment and white ommatidia in the second experiment). However, a complementation test with a *faf* point mutant and G45 Δ 53 showed no disorganized ommatidia (D. Dansereau, personal communication; Dansereau et al., 1998). This is evidence that *faf* is not included in the Δ 53 deletion.

The size of the clone with marked ommatidia was always smaller than the size of the twin clone indicating an additional effect on growth of the clone. Since all the *faf* mutants reported so far have not shown any growth phenotype, this would be further evidence that the gene or genes deleted in Δ 53 do not just include *faf*. In addition, G45 does not report β -gal expression in imaginal discs under normal conditions as would be expected if *faf* were the gene reported. In addition, the molecular data showed expression posterior to the morphogenetic furrow in eye discs, a pattern different from *faf* (Figure III.5). If Δ 53 does not include *faf*, the eye phenotype may be due to a different eye gene, or perhaps to some gene that deregulates *wg* signal transduction pathway in the eye.

The wild type adult head capsule is formed mainly from the eye-antennal imaginal discs. The head vertex in particular is formed by the fusion of the left and right eye discs (Royet and Finkelstein, 1996). The phenotypic effect we have found using Δ 53 is a partial or total loss of a lateral ocellus (Figure III.15). This is a strikingly similar effect to the one observed in mitotic clones induced during the second larval instar that expressed *wg* ectopically. As we argued above the low density of bristles does not allow for clear identification of the size and border of the clone. Neither is it possible to assess whether the effect is cell autonomous because of the lack of reliable markers in the head epidermis. In view of the other phenotypes described above, the similarity of the *wg* ectopic expression phenotype strongly suggests the effect of Δ 53 clones could be via ectopic expression of *wg*.

IV.B.2 Non-autonomy versus cell-autonomy

Δ 53 appears to show an autonomous effect in ommatidia since mutant clones were usually abnormal and accompanied always by wild type twin

clones (Figure III.14). However, a short range non-autonomous effect cannot be ruled out because the development of the retina relies on many local cell-cell interactions which might account for the abnormal phenotype within the mutant clones.

In adult wings, we have found evidence for a non-autonomous effect since patches of ectopic bristles are composed of marked and twin bristles. In the thorax, marked ectopic bristles from both mutant and twin clones implies that the effect must also be non-autonomous. This is consistent with the proposed model of $\Delta 53$ effects based on ectopic expression of *wg*.

IV.B.3 Growth effects

An EMS-induced embryonic lethal, allelic to $\Delta 53$, was recently found (D. Dansereau, personal communication). A clonal analysis experiment (using the same conditions described in Materials and Methods) was performed using the EMS-induced allele to compare the phenotype produced with previous data generated with $\Delta 53$. Mutant clones in the eyes were found to be of a smaller size than the twin ones. If clones are induced in the wing imaginal discs, they cause the wing blade to be smaller than the wild type size. The results suggest that one of the genes deleted in $\Delta 53$ affects growth. This may explain why yellow marked $\Delta 53$ bristles in dorsal anterior ectopic patches in the first clonal analysis experiment are found in lower frequency than yellow dorsal marginal bristles (twin clones) in ectopic patches in the second clonal analysis experiment. This information rules out the growth gene as the gene that may cause overexpression of *wg* because no ectopic margin was induced. Therefore, a second gene within $\Delta 53$ might be the patterning gene.

The frequency of ectopic structures in the wing varied depending on the position. Most of the ectopic patches were found in the first vein, marginal cell and second vein. Almost all of the outgrowths were found close to or on the anterior/posterior boundary, as expected in the case of *wg* expression (Vincent and Lawrence, 1994). This is consistent with the hypothesis that in order to induce a proximal-distal axis it is necessary to express *wg* and *dpp* in the same position (Vincent and Lawrence, 1994; Campbell and Tomlinson, 1995). *dpp* is expressed in anterior cells adjacent to the anterior-posterior compartment boundary. In addition, all the phenotypic effects were restricted to an area of the wing that could be described as a belt around the margin (Figure III.19). This may be explained by proposing the existence of an additional factor necessary to create a "competent area". This factor would be necessary to induce *wg* ectopic expression in that area. This might be related to the submarginal zone to which the effects of *fng* clones are restricted (Irvine and Wieschaus, 1994).

The following genetic model can be proposed to account for the presence of ectopic wing margin phenotype and associated marked bristles. A gene (or genes) that inhibits margin formation outside the normal wing margin may be deleted or inactivated in the deletion line $G45\Delta 53$. Consequently, clones that do not inherit a copy of the wild type gene are not able to repress margin fate outside the normal margin. The gene deleted would not be required when the clone is induced. Therefore, the clone can

initially grow to a certain size, interact with a large number of neighbors causing a non-autonomous effect that would explain the large number of non-mutant cells in the ectopic patch. Later in development many cells in the clone would die leaving just a few marked cells, or none at all. This would cause wild type cells from opposite side of the clone to become juxtaposed, and create the ectopic margin. This would explain how the mirror symmetry seen in some of the large ectopic patches could arise.

This model is favored here because the ectopic patches carry marked bristles more often than the normal margin. Wing outgrowths, extra marginal bristles in the wing margin, extra bristles in the thorax and the reduced ocellus size suggests that a deregulation of the *wg* pathway may be the primary cause of this phenotype (Vincent and Lawrence, 1994). This hypothesis would be consistent with a non-autonomous effect of a morphogen like WG. Since components downstream of the receptors for a morphogen are expected to show cell-autonomy, the non-autonomy of the $\Delta 53$ clones would advocate in favor of the idea that the gene or genes deleted by $\Delta 53$ is upstream of WG-receptor activation.

V. CONCLUSION

This study has shown that the 2.3 kbp DNA fragment (FLR), initially thought to contain exon sequences from the chromosome 3R, has a chimeric origin, and contains sequences from the X chromosome. I have found evidence that the embryonic cDNAs that cross-hybridize to FLR (G45-7 and G45-11) do not map to 100E. It is likely that the G45-7 cDNA represents the transcript expressed in the eye imaginal discs. This transcript could be the one detected by the T₇ single stranded RNA probe (Brook, 1994). The cDNA G45-11 is probably a transcript with similarity to the FLR. This analysis should be useful in the interpretation of the data obtained from the P-element construct, since it may lead to false interpretation of lacZ expression patterns.

I have also found evidence for the existence of a new locus involved in imaginal disc pattern formation. Analysis by phenotypic comparison, a tool successfully used in mutagenesis screens to find new components of the *wg* pathway, indicates that the locus involved in patterning may encode a new member of the *wg* pathway.

Several questions remain open. First, is the locus deleted in $\Delta 53$ encoding a diffusible secreted factor? Cloning of the gene causing the wing phenotypic effects observed would help elucidate this issue. Second, is this locus indeed involved in the *wg* pathway? Epistatic interactions with other alleles of members of the *wg* signal transduction pathway will help define if the locus does interact and will help determine its position in the pathway. Finally, if G45 reports endogenous expression of the *wg*-pathway gene in the regeneration blastema in imaginal disc fragments, it will be interesting to work out its role in the process of regeneration, in which the *wg* gene is an important player.

VI. BIBLIOGRAPHY

- Abbott, L. C., Karpen G. H., and Schubiger, G. 1981. Compartmental restriction and blastema formation during pattern regulation in *Drosophila* imaginal leg discs. *Dev. Biol.*, 87: 64-75.
- Anderson, K. V., Jurgens, G., and Nüsslein-Volhard, C. 1985. The establishment of dorso-ventral polarity in the *Drosophila* embryo: genetic studies on the role of the *Toll* gene product. *Cell*, 42: 779-789.
- Axelrod, J., Matsuno, K., Artavanis-Tsakonas, S., and Perrimon, N. 1996. Interaction between Wingless and Notch signaling pathways mediated by Dishevelled. *Science*, 271: 1826.
- Baker, N. E. 1987. Molecular cloning of sequences from *wingless*, a segment polarity gene in *Drosophila*: the spatial distribution of a transcript in embryos. *EMBO J.*, 6: 1765-1773.
- Basler, K., and Struhl, G. 1994. Compartment boundaries and the control of *Drosophila* limb patterning by Hedgehog protein. *Nature*, 368: 208-214.
- Bate, M., and Martinez-Arias, A. 1991. The embryonic origin of imaginal discs in *Drosophila*. *Development*, 112: 755-761.
- Baumgartner, S., and Noll, M. 1991. Network of interactions among pair-rule genes regulating *paired* expression during primordial segmentation of *Drosophila*. *Mech. Dev.*, 33: 1-18.
- Binari, R. C., Staveley, B. E., Johnson, W. A., Godavarti, R., Sasisekharan, R. and Manoukian, A. S. 1997. Genetic evidence that heparin-like glycosaminoglycans are involved in *wingless* signaling. *Development*, 124: 2623-2632.
- Blair, S. S. 1992a. *engrailed* expression in the anterior lineage compartment of the developing wing blade of *Drosophila*. *Development*, 115: 21-34.
- Blair, S. S. 1992b. *shaggy* (*zeste-white 3*) and the formation of supernumerary bristle precursors in the developing wing blade of *Drosophila*. *Dev. Biol.*, 152: 263-278.
- Blair, S. S. 1995. Compartments and appendage development in *Drosophila*. *BioEssays*, 17: 4, 299-309.
- Borck, K., Beggs, J. D., Brammar, W. J., Hopkins, A. S., and Murray, N. E. 1976. The construction in vitro of transducing derivatives of phage λ . *Mol. Gen. Genet.*, 146: 199-207.
- Brook, W. J. PhD thesis, University of Alberta, 1994.

- Brook, W. J., Diaz-Benjumea, F. J., and Cohen, S. M. 1996. Organizing spatial pattern in limb development. *Annu. Rev. Cell Dev. Biol.*, 12: 161-180.
- Brook, W. J., Ostafichuk, L. M., Piorecky, J., Wilkinson, M. D., Hodgetts, D. J., and Russell, M. A. 1993. Gene expression during imaginal disc regeneration detected using enhancer-sensitive P-elements. *Development*, 117: 1287-1297.
- Bryant, P. J. 1993. The Polar Coordinate model goes molecular. *Science*, 259: 471-472.
- Bryant, S. V., French, V., and Bryant, P. J. 1981. Distal regeneration and symmetry. *Science*, 212: 993-1002.
- Bryant, P. J. 1975. Pattern formation in the imaginal wing disc of *Drosophila melanogaster*: fate map, regeneration and duplication. *J. Exp. Zool.*, 193: 49-77.
- Bryant, P. J., Adler, P. N., Duranceau, C., Fain, M. J., Glenn, S., Hsei, B., James, A. A., Littlefield, C. L., Reinhardt, C. A., Strub, S., and Schneiderman, H. A. 1978. Regulative interactions between cells from different imaginal discs of *Drosophila melanogaster*. *Science*, 201: 928-930.
- Cabrera, C. V. 1990. Lateral inhibition and cell fate during neurogenesis in *Drosophila*: the interactions between scute, Notch and Delta. *Development*, 109: 733-742.
- Campbell, G., and Tomlinson, A. 1995. Initiation of the proximodistal axis in insect legs. *Development*, 121: 619-628.
- Capdevila, J., and Guerrero, I. 1994. Targeted expression of the signaling molecule decapentaplegic induces pattern duplications and growth alterations in *Drosophila* wings. *EMBO J.*, 13: 4459-4468.
- Capdevila, J., Estrada, M. P., Sanchez-Herrero, E., and Guerrero, I. 1994. The *Drosophila* segment polarity gene *patched* interacts with *decapentaplegic* in wing development. *EMBO J.*, 13: 71-82.
- Carroll, S. B., DiNardo, S., O'Farrell, P. H., White, R. A. H., and Scott, M. P. 1988. Temporal and spatial relationships between segmentation and homeotic gene expression in *Drosophila* embryos: distribution of the *fushi tarazu*, *engrailed*, *Sex combs reduced*, *Antennapedia*, and *Ultrabithorax* proteins. *Genes and Dev.*, 2:350-360.
- Chan, L. N., and Gehring, W. 1971. Determination of blastoderm cells in *Drosophila melanogaster*. *PNAS USA*, 68: 2217-2221.
- Chanut, F., and Heberlein, U. 1995. Role of the morphogenetic furrow in establishing polarity in the *Drosophila* eye. *Development*, 121: 4085-4094.
- Cohen, B., Simcox, A. A., and Cohen, S. M. 1993. Allocation of the thoracic imaginal primordia in the *Drosophila* embryo. *Development*, 117: 597-608.

- Cohen, S. M. 1990. Specification of limb development in the *Drosophila* embryo by positional cues from segmentation genes. *Nature*, 343: 173-177.
- Cohen, S. M. 1993. Imaginal disc development. In Martinez-Arias, A., & M. Bate (Eds.), "Development of *Drosophila* " New York: Cold Spring Harbor Press.
- Couso, J. P., Bishop, S., and Martinez Arias, A. 1994. The *wingless* signaling pathway and the patterning of the wing margin in *Drosophila*. *Development*, 120: 621-636.
- Couso, J. P., and Gonz  les-Gait  n, M. 1993. Embryonic limb development in *Drosophila*. *Trends in Genetics*, 9: (11) 371-373.
- Couso, J. P., and Martinez-Arias, A. 1994. Notch is required for *wingless* signaling in the epidermis of *Drosophila*. *Cell*, 79: 259-272.
- Crick, F. H. C., and Lawrence, P. A. 1975. Compartments and polyclones in insect development. *Science*, 189: 340-347.
- Cubas, P., de Celis, J. F., Campuzano, S., and Modollet, J. 1991. Proneural clusters of *achaete-scute* expression and the generation of sensory organs in the *Drosophila* imaginal wing disc. *Genes and Development*, 5: 996-1008.
- Dansereau, D., Russell, M., and Finkielsztain, A. 1998. Ectopic wing margin formation in clones of an enhancer trap derivative in *Drosophila*. Canadian Federation of Biological Societies, 41st Annual Meeting, June 17-20, Abstract 146.
- Desplan, C., Theis, J., and O'Farrell, P. H. 1985. The *Drosophila* developmental gene, *engrailed*, encodes a sequence-specific DNA binding activity. *Nature*, 318: 630-635.
- Diaz-Benjumea, F. J., and Cohen, S. M. 1995. Serrate signals through Notch to establish a *wingless*-dependent organizer at the dorsal/ventral compartment boundary of the *Drosophila* wing. *Development*, 121: 4215-4225.
- Diaz-Benjumea, F. J., and Cohen, S. M. 1993. Interaction between dorsal and ventral cells in the imaginal disc directs wing development in *Drosophila*. *Cell*, 75: 741-752.
- Driever, W., and N  sslein-Volhard, C. 1988. The bicoid protein determines position in the *Drosophila* embryo in a concentration-dependent manner. *Cell*, 54: 95-104.
- Driever, W., Thoma, G., and N  sslein-Volhard, C. 1989. Determination of spatial domains of zygotic gene expression in the *Drosophila* embryo by the affinity of binding sites for the bicoid morphogen. *Nature*, 340: 363-367.

- Fischer-Vize, J. A., Rubin, G. M., and Lehman, R. 1992. The *fat facet* gene is required for *Drosophila* eye and embryo development. *Development*, 116: 985-1000.
- French, V. 1976. Leg regeneration in the cockroach, *Blatella germanica* II. Regeneration forms a non-congruent tibial graft host junction. *J. Embryol. Exp. Morph.*, 35: 267-301.
- French, V., Bryant, P. J., and Bryant, S. V. 1976. Pattern regulation in epimorphic fields. *Science*, 193: 969-981.
- Garcia-Bellido, A., Morata, G., and Ripoll, P. 1973. Developmental compartmentalization in the wing disk of *Drosophila*. *Nature New Biol.*, 245: 251-253.
- Garcia-Bellido, A. 1975. Genetic control of wing disc development in *Drosophila*. In "Cell Patterning", Ciba Foundation Symposium, 29: 161-182.
- Garcia-Bellido, A., and Nöthiger, R. 1976. Maintenance of determination by cells of imaginal discs of *Drosophila* after dissociation and culture *in vivo*. *Roux's Archives of Developmental Biology*, 180: 189-206.
- Garcia-Bellido, A., Ripoll, P., and Morata, G. 1976. Developmental compartmentalization in the dorsal mesothoracic disc of *Drosophila*. *Dev. Biol.*, 48: 132-147.
- Ghysen A., and Kerridge S., in "*Drosophila*, A laboratory manual" by M. Ashburner, 1989.
- Girton, J. R., and Russell, M. A. 1981. An analysis of compartmentalization in pattern duplications induced in a temperature-sensitive cell-lethal mutant of *Drosophila melanogaster*. *Dev. Biol.*, 85: 55-64.
- Golic, K. G., and Lindquist, S. 1989. The FLP recombinase catalyzes site-specific recombination in the *Drosophila* genome. *Cell*, 59: 499-509.
- Harding, K., Rushlow, C., Doyle, H. J., Hoey, T., and Levine, M. 1986. Cross-regulatory interactions among pair-rule genes in *Drosophila*. *Science*, 233: 953-959.
- Haynie, J. L., and Bryant, P. J. 1976. Intercalary regeneration in imaginal wing discs of *Drosophila melanogaster*. *Nature*, 259: 659-662.
- Heberlein, U., and Moses, K. 1995. Mechanisms of *Drosophila* retinal morphogenesis: The virtues of being progressive. *Cell*, 81: 987-990.
- Heberlein, U., Wolff, T., and Rubin, G. M. 1993. The TGF β homolog *dpp* and the segment polarity gene *hedgehog* are required for propagation of a morphogenetic wave in the *Drosophila* retina. *Cell*, 75: 913-926.
- Heitzler, P., and Simpson, P. 1991. The choice of cell fate in the epidermis of *Drosophila*. *Cell*, 64: 1083-1092.

- Huynh, T. V., Young, R. A., and Davis, R. W. 1985. Constructing and screening cDNA libraries in lambda gt10 and lambda gt11. In "DNA cloning: A practical approach" (ed. D., M., Glover) vol. 1, p. 49. IRL Press, Oxford.
- Ingham, P. W. 1988. The molecular genetics of embryonic pattern formation in *Drosophila*. *Nature*, 335: 25-34.
- Inoue, H., Nojima, H., and Okayama, H. 1990. High efficiency transformation of *Escherichia coli* with plasmids. *Gene*, 0378-1119, 23-28.
- Irvine, K. D., and Wieschaus, E. 1994. Fringe, a boundary-specific signaling molecule, mediates interactions between dorsal and ventral cells during *Drosophila* wing development. *Cell*, 79: 595-606.
- Jäckle, H., Tautz, D., Schuh, R., Seifert, E., and Lehmann, R. 1986. Cross-regulatory interactions among the gap genes of *Drosophila*. *Nature*, 324: 668-670.
- Jacobs, J. R., Hiromi, Y., Patel, N. H., and Goodman, C. S. 1989. Lineage, migration, and morphogenesis in the *Drosophila* CNS as revealed by a molecular lineage marker. *Neuron*, 2: 1625-1631.
- Karn, J., Brenner, S., Barnett L., and Cesareni, G. 1980. Novel bacteriophage λ cloning vector. *PNAS USA*, 77: 5172-5176.
- Karpen, G. H., and Schubiger, G. 1971. Extensive regulatory capabilities of a *Drosophila* imaginal disc blastema. *Nature*, 294: 744-747.
- Kilchherr, F., Baumgartner, S., Bopp, D., Frei, E., and Noll, M. 1986. Isolation of the *paired* gene of *Drosophila* and its spatial expression during early embryogenesis. *Nature*, 321: 493-499.
- Klingensmith, J., Nusse, R., and Perrimon, N. 1994. The *Drosophila* segment polarity gene *dishevelled* encodes a novel protein required for response to the *wingless* signal. *Genes and Dev.*, 8: 118-130.
- Kuroiwa, A., Hafen, E., and Gehring, W. J. 1984. Cloning and transcriptional analysis of the segmentation gene *fushi tarazu* of *Drosophila*. *Cell*, 37: 825-831.
- Lawrence, P. A., and Morata, G. 1976. Compartments in the wing of *Drosophila*: a study of the *engrailed* gene. *Dev. Biol.*, 50: 321-337.
- Lawrence, P. A., and Morata, G. 1977. The early development of the mesothoracic compartments in *Drosophila*. *Dev. Biol.*, 56: 40-51.
- Lawrence, P. A., and Morata, G. 1994. Homeobox genes: their function in *Drosophila* segmentation and pattern formation. *Cell*, 78: 181-189.
- Lawrence, P. A., and Struhl, G. 1996. Morphogens, Compartments, and Pattern: Lessons from *Drosophila*?. *Cell*, 85: 951-961.

- Lewis, E. B. 1978. A gene complex controlling segmentation in *Drosophila*. *Nature*, 276: 565-570.
- Lindsley, D. L., and Zimm, G. G. 1992. The genome of *Drosophila melanogaster*. San Diego, USA: Academic Press.
- Madueño, E., Papagiannakis, G., Rimmington, G., Saunders, R. D. C., Savakis, C., Siden-Kiamos, I., Skavdis, G., Spanos, L., Trenear, J., Adam, P., Ashburner, M., Benos, P., Bolshakov, B. N., Coulson, D., Glover, D. M., Herrmann, S., Kafatos, F. C., Louis, C., Majerus, T., and Modolell, J. 1995. A physical map of the X chromosome of *Drosophila melanogaster* cosmid contigs and sequence tagged sites. *Genetics*, 139: 1631-1647.
- Martinez-Arias, A., and M. Bate. 1993. (Eds.), "The development of *Drosophila melanogaster*". New York: Cold Spring Harbor Press.
- McMahon, A. P. 1992. The Wnt family of developmental regulators. *Trends Genet.*, 8: 236-242.
- Meinhardt, H. 1980. Cooperation of compartments for the generation of positional information. *Z. Naturforsch.* 35c: 1086-1091.
- Meinhardt, H. 1982. The role of compartmentalization in the activation of particular control genes and in the generation of proximo-distal positional information in appendages. *Amer. Zool.* 22: 209-220.
- Meinhardt, H. 1983. Cell determination boundaries as organizing regions for secondary embryonic fields. *Dev. Biol.*, 96: 375-385.
- Meinhardt, H. 1985. Mechanisms of pattern formation during development of higher organisms: a hierarchical solution of a complex problem. *Ber. Bunsenges. Phys. Chem.*, 89: 691-699
- Miklos, G. L. G., and Rubin, G. M. 1996. The role of the genome project in determining gene function: insights from model organisms. *Cell*, 86: 521-529.
- Morata, G. and Lawrence, P. A. 1975. Control of compartment development by the *engrailed* gene in *Drosophila*. *Nature*, 255:614-617.
- Noordermeer, J., Klingensmith, J., and Perrimon, N. 1994. *dishevelled* and *armadillo* act in the Wingless signaling pathway in *Drosophila*. *Nature*, 367: 80-83.
- Nusse, R., and Varmus, H. E. 1992. Wnt genes. *Cell*, 69: 1073-1087.
- Nüsslein-Volhard, C., and Wieschaus, E. 1980. Mutations affecting segment number and polarity in *Drosophila*. *Nature*, 287: 795-801.
- O'Kane, C., and Gehring, W. J. 1987. Detection *in situ* of genomic regulatory elements in *Drosophila*. *PNAS USA*, 84: 9123-9127.

- Panin, V. M., Papayannopoulos, V., Wilson, R., and Irvine, K. D. 1997. Fringe modulates Notch-ligand interactions. *Nature*, 387: 908-912.
- Peifer, M., Rauskolb, C., Williams, M., Riggleman, B., and Wieschaus, E. 1991. The segment polarity gene *armadillo* interacts with the Wingless signaling pathway in both embryonic and adult pattern formation. *Development*, 111: 1029-1043.
- Reinhardt, C. A., Hodgking, N. M., and Bryant, P. J. 1977. Wound healing in the imaginal discs of *Drosophila* I. Scanning electron microscopy of normal and healing wing discs. *Devel. Biol.*, 60: 238-257.
- Reinhardt, C. A., and Bryant, P. J. 1981. Wound healing in the imaginal discs of *Drosophila* II. Transmission electron microscopy of normal and healing wing discs. *J. Exp. Zool.*, 216: 45-61
- Riggleman, R., Schedl, P., and Wieschaus, E. 1990. Spatial expression of the *Drosophila* segment polarity gene *armadillo* is post-transcriptionally regulated by *wingless*. *Cell*, 63: 549-560.
- Rijsewijk, F., Schuermann, M., Wagenaar, E., Parren, P., Weigel, D., and Nusse, R. 1987. The *Drosophila* homolog of the mouse mammary oncogene *int-1* is identical to the segment polarity gene *wingless*. *Cell*, 50: 649-657.
- Romani, S., Campuzano, S., Macagno, E. R., and Modollet, J. 1989. Expression of *achaete* and *scute* genes in *Drosophila* imaginal discs and their function in sensory organ development. *Genes and Development*, 3: 997-1007.
- Royet, J., and Finkelstein, R. 1996. *hedgehog*, *wingless* and *orthodenticle* specify adult head development in *Drosophila*. *Development*, 122: 1849-1858
- Rulifson, E. J., and Blair, S. S. 1995. *Notch* regulates *wingless* expression and is not required for reception of the paracrine *wingless* signal during wing margin neurogenesis in *Drosophila*. *Development*, 121: 2813-2824.
- Russell, M. A. 1974. Pattern formation in the imaginal discs of a temperature sensitive cell lethal mutant of *Drosophila melanogaster*. *Dev. Biol.*, 40: 24-39.
- Russell, M. A. 1983. Positional information in imaginal discs: A Cartesian coordinate model, in : "Mathematical essays on growth and emergence of form". Ed. P. Antonelli, the University of Alberta press, pp. 169-183.
- Sambrook, J., Fritsch, E. F., and Maniatis, T. 1989. "Molecular Cloning: A laboratory manual". Cold Spring Harbor, N.Y.: Cold Spring Harbor Laboratory.
- Schubiger, G. 1968. Anlageplan, determinationszustand und transdeterminationsleistungen der männlichen Vorderbeinscheibe

- von *Drosophila melanogaster*. Roux's Archives of Developmental Biology, 160: 9-40.
- Schubiger, G. 1971. Regeneration, Duplication and Transdetermination in Fragments of the leg discs of *Drosophila melanogaster*. Dev. Biol., 26: 277-295.
- Schubiger, G., and Schubiger, M. 1978. Distal transformation in *Drosophila* leg imaginal discs fragments. Dev. Biol., 67: 286-296.
- Siden-Kiamos, R., Saunders, D. C., Spanos, L., Majerus, T., Treanear, J., Savajis, C., Louis, C., Glover, D. M., Ashburner, M., and Kafatos, F. C. 1990. Towards a physical map of the *Drosophila melanogaster* genome: mapping of cosmid clones within defined genomic divisions. Nucleic Acids Research, 18: 6261-6270.
- Siegfried, E., Wilder, E. L., and Perrimon, N. 1994. Components of *wingless* signaling in *Drosophila*. Nature, 367: 76-79.
- Simcox, A. A., and Sang, J. H. 1983. When does determination occur in *Drosophila* embryos? Dev. Biol. 97: 212-221.
- Simcox, A. A., Roberts, I. J. H., Hersperger, E., Gribbin, M. C, Shearn, A., and Whittle, J. R. S. 1989. Imaginal discs can be recovered from cultured embryos mutant for the segment-polarity genes *engrailed*, *naked* and *patched* but not from *wingless*. Development, 107: 715-722.
- Simpson, P. 1990. Notch and the choice of cell fate in *Drosophila* neuroepithelium. Trends in Genetics, 6: 343-345.
- Speicher, S. A., Thomas, U., Hinz, U., and Knust, E. 1994. The *Serrate* locus of *Drosophila* and its role in morphogenesis of the wing imaginal discs: control of cell proliferation. Development, 120: 535-544.
- Spemann, H., and Mangold, H. 1924. Induction of embryonic primordia by implantation of organizers from a different species. In B. H. Willier and J. M. Oppenheimer (eds.), "Foundations of Experimental Embryology". Hafner, New York, 144-184.
- Spradling, A. C., Stern, D. M., Kiss, I., Roote, J., Lavery, T., and Rubin, G. M. 1995. Gene disruptions using P transposable elements: An integral component of the *Drosophila* genome project. PNAS USA, 92: 10824-10830.
- Steele, G. D., and Torrie, J. H. 1960. "Principles and Procedures of Statistics", McGraw-Hill Book Company, Inc.
- Struhl, G., Struhl, K., and Macdonald, P. M. 1989. The gradient morphogen Bicoid is a concentration-dependent transcriptional activator. Cell 57, 1259-1273.
- Tabata, T., and Kornberg, T. B. 1994. Hedgehog is a signaling protein with a key role in patterning *Drosophila* imaginal discs. Cell, 76: 89-102.

- Tabata, T., Eaton S., and Kornberg T. B. 1992. The *Drosophila hedgehog* gene is expressed specifically in posterior compartment cells and is a target of *engrailed* regulation. *Genes and Dev.*, 6: 2635-2645.
- Tautz, D. 1988. Regulation of the *Drosophila* segmentation gene *hunchback* by two maternal morphogenetic centres. *Nature*, 332: 281-284.
- Tautz, D., Lehmann, R., Schnurch, H., Schuh, R., Seifert, E., Kienlin, A., Jones, K., and Jäckle, H. 1987. Finger protein of novel structure encoded by *hunchback*, a second member of the gap class of *Drosophila* segmentation. *Nature*, 327:383-389.
- Tiong, S. Y. K., Nash, D., and Bender, W. 1995. *Dorsal wing*, a locus that affects dorsoventral wing patterning in *Drosophila*. *Development*, 121: 1649-1656.
- Turing, A. M. 1952. The chemical basis of morphogenesis. *Phil. Trans. Roy. Soc., B*: 237: 37.
- Vincent, J., and Lawrence, P. A. 1994. *Drosophila wingless* sustains *engrailed* expression only in adjoining cells: evidence from mosaic embryos. *Cell*, 77: 909-915.
- Vincent, J., and Lawrence, P. A. 1994. Developmental genetics: it takes three to distalize. *Nature*, 372: 132-133.
- Wieschaus, E., and Gehring, W. J. 1976. Clonal analysis of primordial disc cells in the early embryos of *Drosophila melanogaster*. *Devel. Biol.*, 50: 249-263.
- Whitlock, K. E. 1993. Development of *Drosophila* wing sensory neurons in mutants with missing or modified cell surface molecules. *Development*, 117: 1251-1260.
- Williams, J. A., Paddock, S. W., Vorwerk, K., and Carroll, S. B. 1994. Organization of wing formation and induction of a wing-patterning gene at the dorsal/ventral compartment boundary. *Nature*, 368: 299-305.
- Wilson, C., Pearson, K. R., Bellen, H. J., O'Kane, C. J., Grossniklaus, U., and Gehring, W. J. 1989. P-element mediated enhancer detection: an efficient method for isolating and characterizing developmentally regulated genes in *Drosophila* wing disc into discrete subregions. *Development*, 117: 1301-1313.
- Wolpert, L. 1969. Positional information and the spatial pattern of cellular differentiation. *J. Theoret. Biol.*, 25: 1-47.